# Appendix 1

Karel Škoch, Ivana Císařová, Petr Štěpnička: "Phosphinoferrocene Ureas: Synthesis, Structural Characterization, and Catalytic Use in Palladium-Catalyzed Cyanation of Aryl Bromides". *Organometallics*, **2015**, *34*, 1942.

ORGANOMETALLICS

Article

pubs.acs.org/Organometallics

# Phosphinoferrocene Ureas: Synthesis, Structural Characterization, and Catalytic Use in Palladium-Catalyzed Cyanation of Aryl Bromides

Karel Škoch, Ivana Císařová, and Petr Štěpnička*

Department of Inorganic Chemistry, Faculty of Science, Charles University in Prague, Hlavova 2030, 128 40 Prague 2, Czech Republic

Supporting Information

**ABSTRACT:** Phosphinoferrocene ureas $Ph_2PfcCH_2NHCONR_2$, where $NR_2$ = $NH_2$ (**1a**), NHMe (**1b**), $NMe_2$ (**1c**), NHCy (**1d**), and NHPh (**1e**); the analogous thiourea $Ph_2PfcCH_2NHCSNHPh$ (**1f**); and the acetamido derivative $Ph_2PfcCH_2NHCOMe$ (**1g**) (Cy = cyclohexyl, fc = ferrocene-1,1′-diyl) were prepared via three different approaches starting from $Ph_2PfcCH_2NH_2$·HCl (**3**·HCl) or $Ph_2PfcCHO$ (**4**). The reactions of the representative ligand **1e** with $[PdCl_2(cod)]$ (cod = cycloocta-1,5-diene) afforded $[PdCl(\mu\text{-Cl})(\mathbf{1e}\text{-}\kappa P)_2]_2$ or $[PdCl_2(\mathbf{1e}\text{-}\kappa P)_2]_2$ depending on the metal-to-ligand stoichiometry, whereas those with $[PdCl(\eta^3\text{-}C_3H_5)]_2$ and $[PdCl(L^{NC})]_2$ produced the respective bridge cleavage products, $[PdCl(\eta^3\text{-}C_3H_5)(\mathbf{1e}\text{-}\kappa P)]$ and $[PdCl(L^{NC})(\mathbf{1e}\text{-}\kappa P)]$ ($L^{NC}$ = [(2-dimethylamino-κN)methyl]phenyl-κC[1]). Attempts to involve the polar pendant in coordination to the Pd(II) center were unsuccessful, indicating that the phosphinoferrocene ureas **1** bind Pd(II) preferentially as modified phosphines rather than bifunctional donors. When combined with palladium(II) acetate, the ligands give rise to active catalysts for Pd-catalyzed cyanation of aryl bromides with potassium hexacyanoferrate(II). Optimization experiments revealed that the best results are obtained in 50% aqueous dioxane with a catalyst generated from 1 mol % of palladium(II) acetate and 2 mol % of **1e** in the presence of 1 equiv of $Na_2CO_3$ as the base and half molar equivalent of $K_4[Fe(CN)_6]\cdot 3H_2O$. Under such optimized conditions, bromobenzenes bearing electron-donating substituents are cyanated cleanly and rapidly, affording the nitriles in very good to excellent yields. In the case of substrates bearing electron-withdrawing groups, however, the cyanation is complicated by the hydrolysis of the formed nitriles to the respective amides, which reduces the yield of the desired primary product. Amine- and nitro-substituted substrates are cyanated only to a negligible extent, the former due to their metal-scavenging ability.

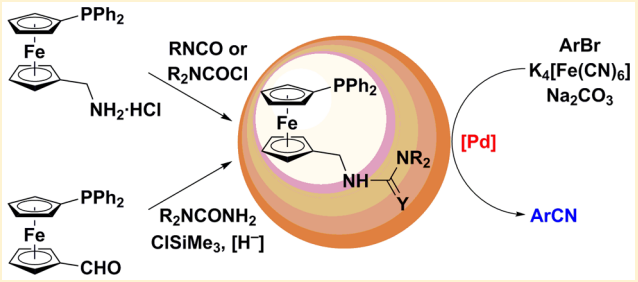


## INTRODUCTION

Modification of phosphines via introduced functional groups has been recognized as an efficient route toward new tailored ligands for coordination chemistry and catalysis. The latter field, in particular, advantageously capitalizes on the modification of pristine phosphine donors. For instance, phosphines modified with highly polar moieties such as sulfonato, carboxyl, or hydroxy groups have been successfully incorporated into catalysts for organic reactions performed in less environmentally demanding aqueous reaction media including pure water, homogeneous aqueous mixtures, and biphase mixtures.[1] The range of polar phosphine derivatives has been recently extended by those bearing urea substituents (**A** and **B** in Scheme 1).[2] The presence of urea pendants in these donors has been shown to be responsible for the formation of supramolecular assemblies via hydrogen bond interactions, which in turn affect their catalytic properties.

In the chemistry of phosphinoferrocene ligands,[3] the urea moiety has been used relatively scarcely, most often as a stable and structurally defined linking group in the preparation of immobilized or water-soluble donors[4] and conjugates of ferrocene with biologically relevant molecules.[5] Genuine applications of urea-functionalized phosphinoferrocene donors appear to be represented only by the preparation of urea- and thiourea-modified BPPFA-type donors (**C** in Scheme 1; BPPFA = 1,1′-bis(diphenylphosphino)-2-(1-dimethylaminoethyl)-ferrocene[6]) and their applications in asymmetric catalytic hydrogenations.[7,8] In addition, our laboratory recently reported the synthesis of phosphinoferrocene carboxamides[9] bearing extended urea-based pendants (**D** in Scheme 1) and their use in Pd-catalyzed cross-coupling of arylboronic acids with acyl chlorides to yield benzophenones.[10] This situation markedly contrasts with the numerous studies devoted to the electrochemical sensing properties of ferrocenyl- and ferrocenylmethyl-substituted ureas.[11]

In this contribution, we report on the preparation, coordination properties, and catalytic performance in the Pd-catalyzed cyanation of aryl bromides of a new type of phosphinoferrocene ureas (**1** in Scheme 1). The urea moiety in these functional hybrid ligands[12] is attached to the ferrocene scaffold via a methylene spacer, which increases conformational

Received: March 10, 2015
Published: May 7, 2015





DOI: 10.1021/acs.organomet.5b00197
Organometallics 2015, 34, 1942−1956

**Scheme 1**

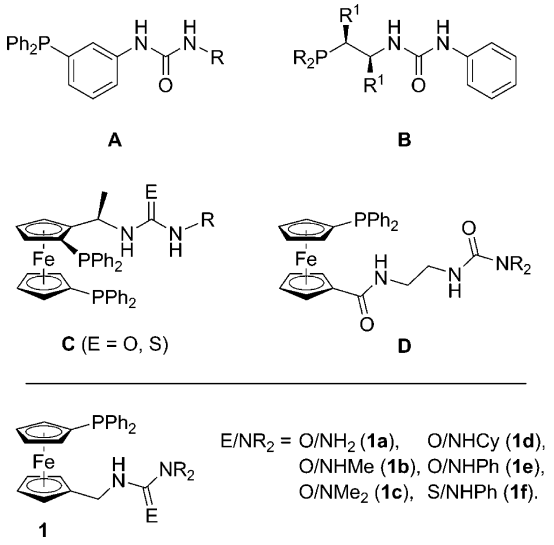


flexibility[13] and enhances the ditopic nature of these polar donors.

## RESULTS AND DISCUSSION

**Synthesis of Phosphinoferrocene Ureas.** Three different methods were employed for the synthesis of phosphinoureas **1**, partly due to their exclusivity with respect to the substituents at the terminal nitrogen atoms as well as for comparison of different preparative routes leading to this type of functionally modified, polar phosphinoferrocene donors. The first, perhaps inevitable approach, method A, was based on the conventional and widely applicable addition of amines across isocyanates. The amine **3** required for this reaction was prepared by hydride reduction of the known oxime **2** (Scheme 2),[14] which is in turn

**Scheme 2. Preparation of 3·HCl**

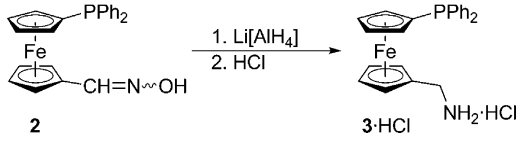


accessible from 1′-(diphenylphosphino)ferrocene-1-carbaldehyde (**4**).[15] The amine was advantageously isolated in the form of stable and easy-to-handle hydrochloride (**3**·HCl), which separates in reasonable yield from the solution of the crude product upon addition of methanolic HCl. Contamination of **3**·HCl with the corresponding phosphine oxide, which is otherwise difficult to separate (e.g., by chromatography), does not exceed 5% in this case.

Gratifyingly, the reaction of amine **3** generated *in situ* from the hydrochloride and triethylamine proceeded in the anticipated manner, leading to 1,3-disubstituted ureas **1d** and **1e** in very good isolated yields (Scheme 3). Not surprisingly, this method could be successfully adopted for the synthesis of thiourea **1f** (yield: 94%). However, when applied to the preparation of *N*-ferrocenylmethyl urea **1a** by the action of sodium cyanate on the amine, method A furnished a relatively lower yield (37%) of the desired urea derivative, presumably because of a low equilibrium concentration of HNCO as the active reagent[16] in the presence of excess triethylamine.

**Scheme 3. Synthesis of Phosphinoferrocene Ureas from *in Situ* Generated Amine 3**

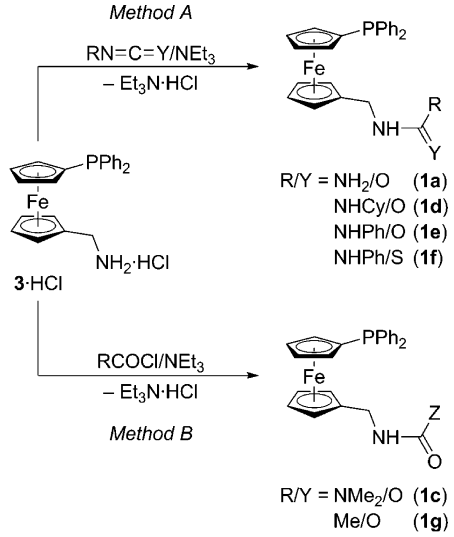


Nevertheless, because most of the starting amine hydrochloride remained unreacted and could be isolated (57% of the starting amine was recovered), the yield of **1a** with respect to unconsumed **3**·HCl was very satisfactory (86%). It should be noted that compound **1a** is typically contaminated by traces of the respective phosphine oxide (**1aO**), which cannot be efficiently removed by chromatography or crystallization.

The second approach, method B, employed for the preparation of trisubstituted urea **1c** and the acetamido (i.e., non-urea) derivative **1g**, which was included in the series of prospective ligands for comparison, was also rather straightforward, making use of the reactions of amine **3** with the corresponding acyl or carbamoyl chlorides (Scheme 3). As in the previous case, free amine **3** was liberated *in situ* from its hydrochloride by the action of triethylamine, which was used in excess to also serve as a scavenger of the formed HCl. Even these reactions proceeded satisfactorily and afforded the aforementioned products in isolated yields exceeding 90%.

The last alternative (method C, Scheme 4) relied on the direct reaction of aldehyde **4** with the respective urea by

**Scheme 4. Preparation of Phosphinoferrocene Ureas by Reductive Alkylation**

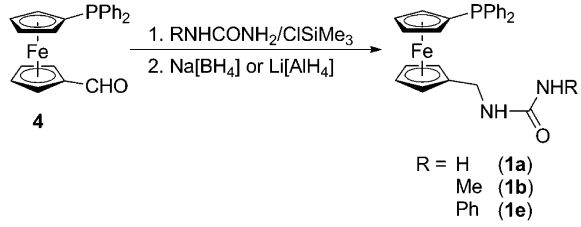


condensation and reduction of the presumed imine intermediates (reductive alkylation).[17] This method was tested mainly because it could possibly eliminate the two steps required to convert **4** to **3**. Thus, the reaction of **4** with *N*-phenylurea performed in the presence of chlorotrimethylsilane as the condensation agent and subsequent reduction with $Li[AlH_4]$ led to **1e** in a good 82% yield. The choice of the reducing agent proved to be crucial since a similar reaction with $Na[BH_4]$ and simultaneous addition of acetic acid afforded a



DOI: 10.1021/acs.organomet.5b00197
*Organometallics* 2015, 34, 1942−1956

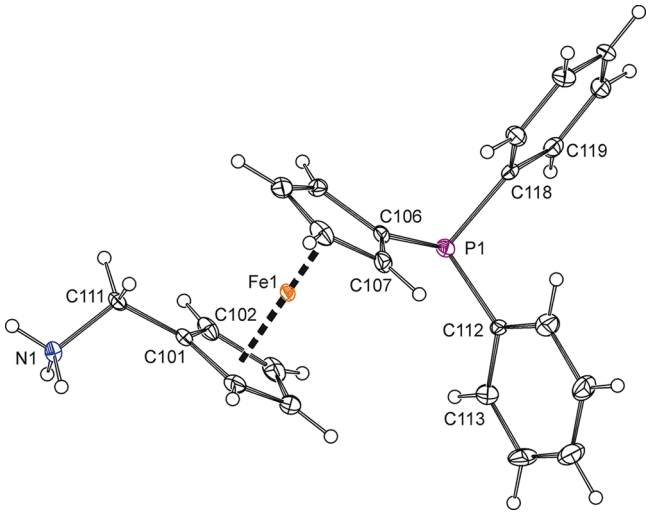


**Figure 1.** PLATON plot of cation 1 in the structure of **3**·HCl showing atom labeling and displacement ellipsoids at the 30% probability level. Note: Atom numbering in molecule 2 is strictly analogous.

product containing considerable amounts (approximately 30%) of the respective borane adduct, **1e**·$BH_3$ ($\delta_P$ 16.5). On the other hand, method C proved unsuitable for the preparation of **1a** because it mainly led to [1′-(diphenylphosphino)-ferrocenyl]methanol[15] (68% of this alcohol and only ca. 9% of **1a** were isolated with Li[$AlH_4$]) or yielded the desired product **1a** contaminated with the respective phosphine oxide and borane adduct, only the latter of which could be efficiently removed by crystallization (reaction with Na[$BH_4$]; chromatography proved to be inefficient in separating **1a**, **1aO**, and **1a**·$BH_3$).

On the other hand, method C becomes particularly important when no isocyanate or carbamoyl chloride required for the conventional additions or condensations is available or at least reasonably accessible. In the present case, method C was employed for the synthesis of *N*-methylurea **1b**. Thus, "reductive alkylation" of **4** with *N*-methylurea in the presence of $ClSiMe_3$ in THF−$CH_3CO_2H$ followed by reduction by Na[$BH_4$] provided **1b** in a 73% yield with less than 5% contaminants (phosphine oxide and borane adduct; further purification could be achieved through recrystallization). Similar reaction in the presence of Li[$AlH_4$] as a more energetic reducing agent afforded a cleaner product but in a lower yield because a considerable part of the starting aldehyde was reduced directly to the corresponding alcohol (isolated yields of **1b** and the alcohol were 30% and 49%, respectively).

All newly prepared compounds were characterized by multinuclear NMR and IR spectroscopy, electrospray ionization (ESI) mass spectrometry, and elemental analysis. In their $^1$H NMR spectra, the compounds showed signals typical of the phosphinoferrocenyl moiety, namely, a set of virtual multiplets (three triplets and one quartet) attributable to the unsymmetrically 1,1′-disubstituted ferrocene moiety bearing one phosphine substituent and a multiplet due to protons at the $PPh_2$ group. Corresponding signals were found in the $^{13}$C NMR spectra. Signals of the methylene linkers in **1a**−**e** and **1g** were observed at $\delta_H$ around 4.0 and $\delta_C$ 38−39, whereas those of **1f** appeared shifted to lower fields ($\delta_H$ 4.34, $\delta_C$ 44.25). $^{13}$C NMR resonances of the C═O units, another characteristic feature in the NMR spectra, were observed at $\delta_C$ ca. 155−159 for ureas **1a**−**e**, at $\delta_C$ 180.16 for thiourea **1f**, and at $\delta_C$ 169.73 for the *N*-acetyl derivative **1g**. Finally, the $^{31}$P NMR signals of **3**·HCl and **1a**−**g** were found within the narrow range of $\delta_P$ −16 to −18 ppm.

The ESI mass spectra of ureas **1** displayed pseudomolecular ions of the type $[M + X]^+$, where X = H, Na, and K. In contrast, the mass spectrum of **3**·HCl showed a strong signal attributable to the [1′-(diphenylphosphino)ferrocenyl]methylium cation, $Ph_2PfcCH_2^+$, analogous to the stabilized $[FcCH_2]^+$ fragment (Fc = ferrocenyl) typically appearing in the mass spectra of ferrocenylmethyl derivatives.[18]

In addition to characterization by various solution techniques, the crystal structures of **3**·HCl, **1a**, **1e**, and **1f** were determined by single-crystal X-ray diffraction analysis. Compound **3**·HCl (Figure 1 and Table 1) crystallizes with the symmetry of the monoclinic space group $P2_1/n$ and two molecules per asymmetric unit. The two independent molecules differ only marginally, mainly in the mutual orientation of the cyclopentadienyl rings (see $\tau$ angles in Table 1 and the overlap in the Supporting Information, Figure S1), and their geometric parameters are unexceptional. Hence, the reason for their "multiplication" most likely lies in the complexity of the hydrogen-bonded array in the crystal state.

Individual ions constituting the crystal structure of **3**·HCl assemble via charge-assisted N−H···Cl hydrogen bonds (N···Cl = 3.054(4)−3.143(4) Å), forming infinite columnar assemblies oriented parallel to the crystallographic *b*-axis. The bulky nonpolar phosphinoferrocenyl moieties are directed away from the "central" polar domains and thus decorate the hydrogen-bonded stacks on their exterior (Figure 2).

**Table 1. Selected Geometric Data for the Two Independent Cations in the Crystal Structure of 3·HCl (in Å and deg)[a]**

| parameter | molecule 1 | parameter | molecule 2 |
|---|---|---|---|
| Fe−Cg1 | 1.654(2) | Fe−Cg1 | 1.655(2) |
| Fe−Cg2 | 1.651(2) | Fe−Cg2 | 1.650(2) |
| ∠Cp1,Cp2 | 1.0(3) | ∠Cp1,Cp2 | 1.5(3) |
| $\tau$ | −156.8(4) | $\tau$ | −171.3(4) |
| P1−C106 | 1.825(5) | P2−C206 | 1.821(5) |
| P1−C112 | 1.846(5) | P2−C212 | 1.836(5) |
| P1−C118 | 1.840(5) | P2−C218 | 1.844(5) |
| N1−C111 | 1.482(6) | N2−C211 | 1.497(6) |
| C101−C111−N1 | 112.5(4) | C201−C211−N2 | 111.4(4) |

[a]Definitions: Cp1 and Cp2 are the azoniamethyl- [C(101−105) and C(201−205) in molecules 1 and 2] and phosphine-substituted [C(106−110) and C(206−210) in molecules 1 and 2] cyclopentadienyl rings, respectively. Cg1 and Cg2 are their respective centroids. $\tau$ represents the torsion angle C*n*01−Cg1−Cg2−C*n*06, where *n* = 1 and 2 for molecules 1 and 2, respectively.



DOI: 10.1021/acs.organomet.5b00197
*Organometallics* 2015, 34, 1942−1956

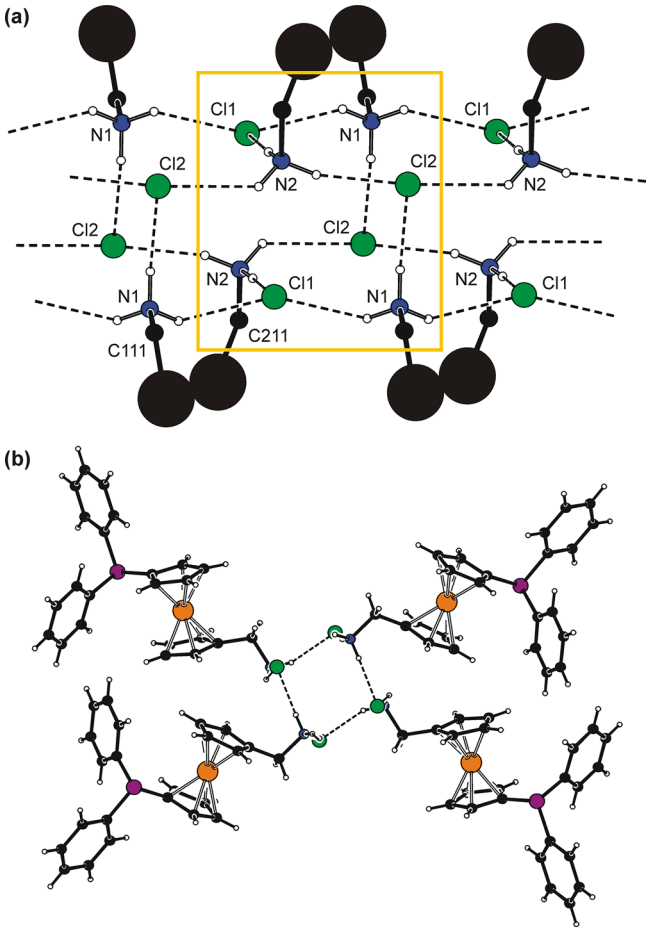


**Figure 2.** (a) Section of the hydrogen-bonded array in the structure of **3**·HCl. For convenience, the repeating unit is enclosed within a yellow box. Only the NH hydrogens are shown, and the bulky phosphinoferrocenyl moieties have been replaced with black circles to avoid complicating the figure. (b) Projection of a single columnar stack along the *b*-axis.

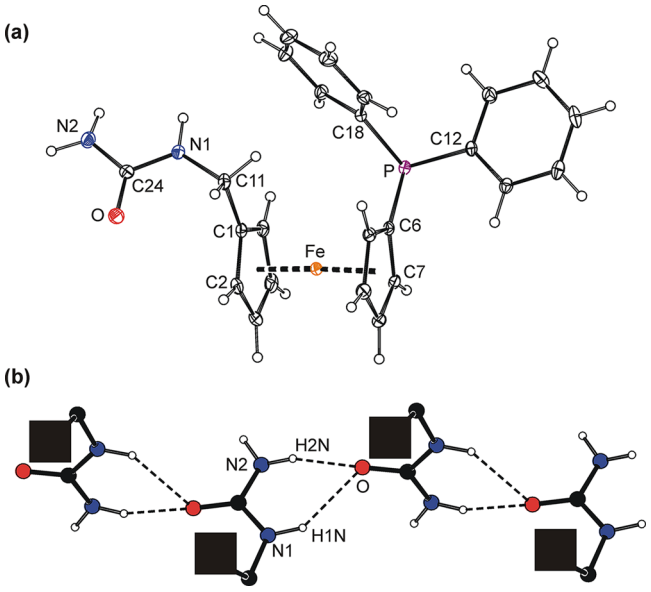


**Figure 3.** (a) PLATON plot of the molecular structure of **1a**. Displacement ellipsoids enclose the 30% probability level. (b) Section of the hydrogen-bonded chains in the structure of **1a**. For clarity, only the NH hydrogens are shown, and the phosphinoferrocenyl moieties have been replaced with black squares.

**Table 2. Selected Geometric Parameters for 1a, 1e, and 1f (in Å and deg)**

| parameter[a] | **1a** (Y = O) | **1e** (Y = O) | **1f** (Y = S) |
|---|---|---|---|
| Fe−Cg1 | 1.646(1) | 1.6458(9) | 1.662(2) |
| Fe−Cg2 | 1.639(1) | 1.6402(9) | 1.656(2) |
| ∠Cp1,Cp2 | 4.5(2) | 2.6(1) | 1.8(2) |
| $\tau$ | −68.1(2) | −90.0(1) | 157.7(3) |
| P−C6 | 1.805(2) | 1.815(2) | 1.823(3) |
| P−C12 | 1.836(2) | 1.840(2) | 1.838(4) |
| P−C18 | 1.829(2) | 1.838(2) | 1.838(4) |
| C1−C11 | 1.503(3) | 1.504(3) | 1.505(5) |
| C11−N1 | 1.454(3) | 1.452(3) | 1.452(5) |
| C1−C11−N1 | 113.8(2) | 112.0(2) | 110.3(3) |
| N1−C24 | 1.354(3) | 1.346(2) | 1.344(5) |
| N2−C24 | 1.353(3) | 1.376(2) | 1.343(5) |
| N2−C25 | n.a. | 1.408(3) | 1.434(5) |
| C24−Y | 1.241(2) | 1.238(2) | 1.699(4) |
| N1−C24−N2 | 115.4(2) | 113.2(2) | 117.0(3) |

[a]Definitions: Cp1 and Cp2 are the $CH_2$- [C(1−5)] and phosphine-substituted [C(6−10)] cyclopentadienyl rings, respectively. Cg1 and Cg2 stand for the respective centroids. $\tau$ is the torsion angle C1−Cg1−Cg2−C6. n.a. = not applicable.

The molecular structure of **1a** is depicted in Figure 3, and the selected geometric parameters for all structurally characterized phosphinoureas (i.e., **1a**, **1e**, and **1f**) are compiled in Table 2. Generally, the structural parameters determined for **1a** fall into the typical ranges.[19,20] The individual Fe−C distances vary slightly (2.020(3)−2.068(2) Å), which in turn results in tilting of the cyclopentadienyl ring planes by ca. 5°. The cyclopentadienyl rings assume an approximately synclinal eclipsed (ideal value:[21] 72°) conformation, and the urea pendant is directed below the ferrocene unit and takes part in intermolecular interactions.

The individual molecules of **1a** associate in a manner typical for *N*,*N*′-disubtituted ureas by forming infinite chains through pairs of N−H···O hydrogen bonds between proximal[22] NHCONH moieties, whose oxygen atoms behave as bifurcate hydrogen bond acceptors.[23] These hydrogen bonds thus involve only hydrogen atoms in an *anti* position with respect to the urea oxygen and are significantly asymmetric (N1···O = 3.212(3) Å; N2···O = 2.870(2) Å). The third NH proton available in **1a** (H3N) does not take part in hydrogen bonding with any conventional acceptor. Nonetheless, it is positioned appropriately for an interaction[24] with the "residual" electron density attributable to the lone pair of phosphorus, which manifests itself as the most intense peak in the final difference electron density map (see the Supporting Information, Figure S2).

Although the molecules of **1e** and **1f** (Figure 4 and Table 2) differ "only" by the chalcogen atom in the urea pendant, their structures are considerably dissimilar. The individual distances and angles are quite unexceptional and, for **1e**, compare well with those determined for a calix[4]arene modified by two $FcCH_2NHCONH-$ redox-active pendants (Fc = ferrocenyl).[25] The main difference lies in the molecular conformation and solid-state assemblies the compounds constitute in their crystals.

The cyclopentadienyl rings in the molecules of **1e** and **1f** are tilted by only 2.6(1)° and 1.8(2)°, respectively. They adopt



DOI: 10.1021/acs.organomet.5b00197
*Organometallics* 2015, 34, 1942−1956

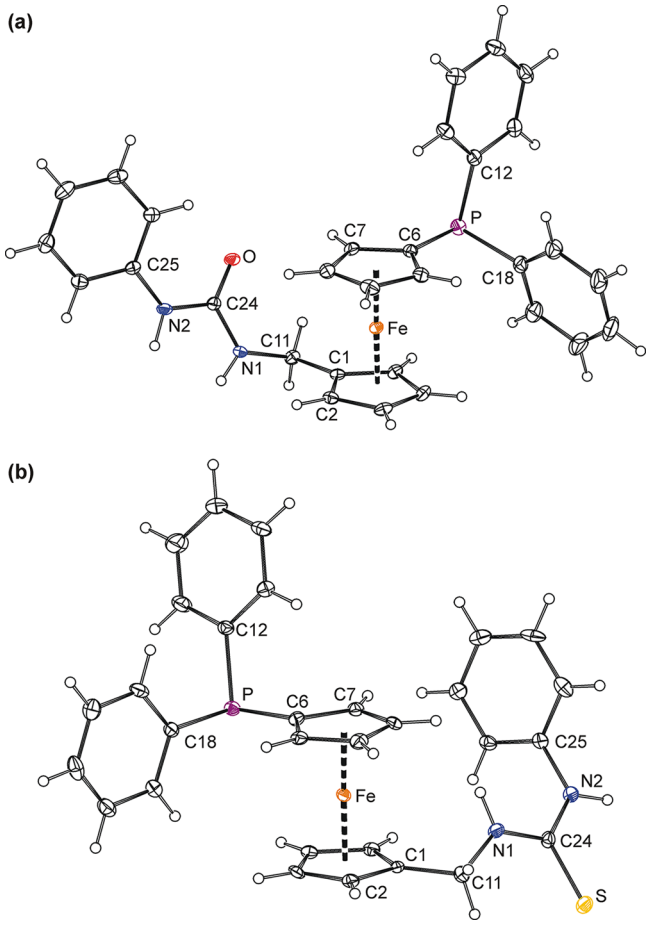


**Figure 4.** PLATON plots of the molecular structures of (a) **1e** and (b) **1f**. Displacement ellipsoids are scaled to the 30% probability level.

different mutual orientations, namely, an intermediate conformation between synclinal eclipsed and anticlinal staggered in **1e** and a conformation close to ideal anticlinal eclipsed in **1f**. Another substantial difference can be observed in the arrangement of the urea pendants. Whereas the urea moiety in **1e** has both hydrocarbyl groups in *syn* positions with respect to the oxygen of the central C═O bond, the substituents at the NHC(S)NH assume *syn* ($CH_2$) and *anti* (Ph) positions. Together with reorientation of the entire urea pendant with respect to the ferrocene units (cf. the C2/5−C1−C11−N1 angles 64.9(3)/−112.1(3)° for **1a**, 17.6(3)/−165.1(2)° for **1e**, and −149.7(4)/34.8(5)° for **1f**), this positioning directs the phenyl ring closer to the ferrocene unit and results in twisting of the terminal phenyl group with respect to the urea moiety, as evidenced by the dihedral angles subtended by the phenyl and the NC(E)N (E = O or S) planes being 24.8(1)° and 63.3(2)° for **1e** and **1f**, respectively. (Note: The values of the C11−N1−C24−N2 angles are higher than 175° in all three structures, thereby ruling out any signification torsion at the connecting urea motifs.)

The different geometries of the urea pendants are clearly associated with differences in the solid-state architecture. Compound **1e** forms the typical one-dimensional chain described by the C(4)[$R^1_2$(6)] descriptors[23a] in graph set notation[26] and observed as the main motif in the crystal structure of **1a** (see the Supporting Information, Figure S3; N1···O = 3.053(2) Å, N2···O = 2.884(2) Å). In contrast, the molecules of **1f** associate into simple centrosymmetric dimers via the relatively softer (weaker) N−H···S interactions (N2···S = 3.335(3) Å) and make use of only one of the available NH protons (N2−H2N, which is *syn* with respect to the sulfur atom; see Figure S4 in the Supporting Information).

**Preparation of Palladium(II) Complexes.** The coordination properties of the phosphinoferrocene ureas were examined in palladium(II) complexes using **1e** as a representative ligand. The experiments confirmed that the compounds behave as modified phosphines rather than as true bifunctional donors. For instance, the reaction of **1e** with [$PdCl_2$(cod)] (cod = cycloocta-1,5-diene) at 1:1 molar ratio provided the dipalladium(II) chloride-bridged complex **5** ($\delta_P$ 33.6;[27] Scheme 5). A similar reaction with two molar equivalents of **1e** with

**Scheme 5. Synthesis of Palladium(II) Complexes 5 and 6**[a]

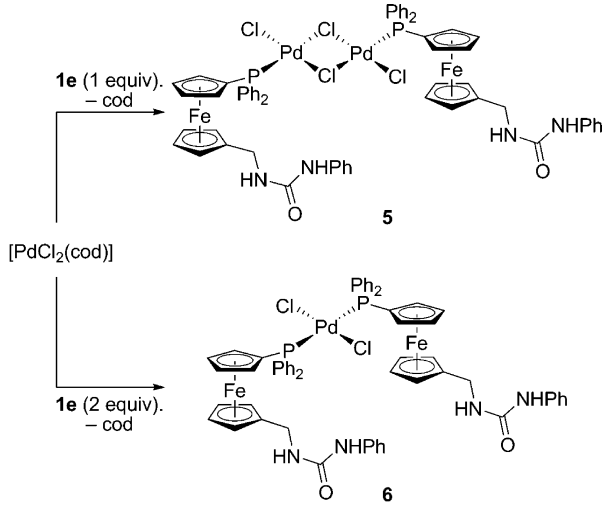


[a]cod = cycloocta-1,5-diene.

respect to Pd proved to be complicated due to unexpected side reactions and required careful optimization to produce the bisphosphine complex **6** ($\delta_P$ 16.5[28]).

The reactions of **1e** with dipalladium precursors [$Pd(L^{NC})(\mu$-$Cl)]_2$ and [$Pd(\eta^3$-$C_3H_5)(\mu$-$Cl)]_2$ also gave rise to the expected "simple" phosphine complexes **7** and **8**, both resulting via cleavage of the chloride bridges in the starting Pd complexes (Scheme 6). Repeated attempts to induce a chelate

**Scheme 6. Synthesis of Palladium(II) Complexes 7 and 8**

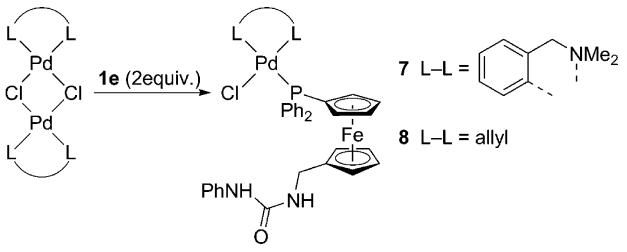


coordination of **1e** by removal of the Pd-bound chloride in **7** by either a soluble Ag(I) or Tl(I) salt (Ag[$SbF_6$] and Tl[$PF_6$]) or via an intramolecular replacement following deprotonation of the NH group(s) with *t*-BuOK were unsuccessful, affording only complicated and easily decomposing reaction mixtures.

Although partly disordered, the molecular structures of **7**·$2CHCl_3$ and **8** could be determined by X-ray diffraction



DOI: 10.1021/acs.organomet.5b00197
*Organometallics* 2015, 34, 1942−1956

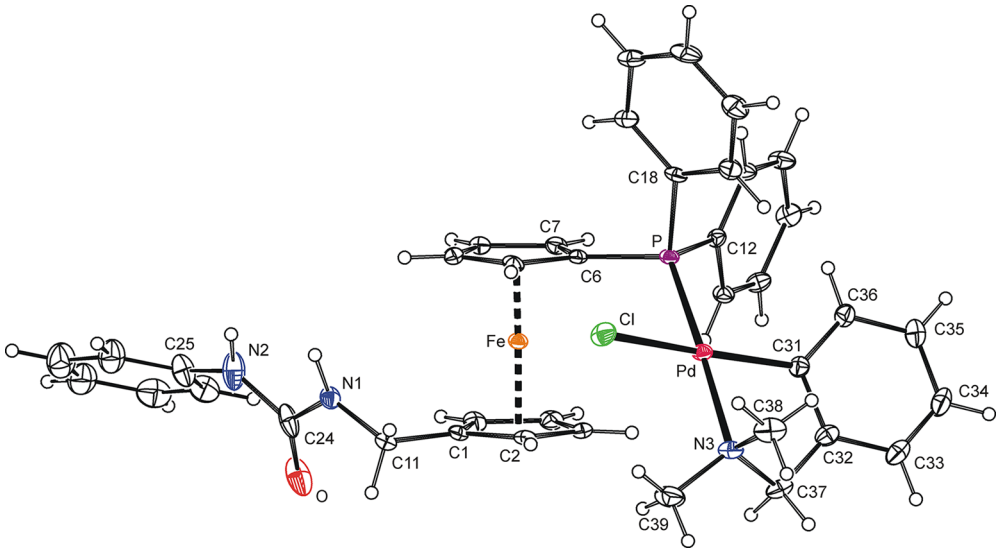


**Figure 5.** PLATON plot of the molecular structure of **7**. The displacement ellipsoids are scaled to the 30% probability level. For clarity, only one orientation of the disordered phenyl group is shown (for a complete drawing, see the Supporting Information). Selected geometric data (in Å and deg): Pd−Cl 2.4160(9), Pd−P 2.2576(8), Pd−N(3) 2.153(3), Pd−C(31) 2.005(4), P−Pd−Cl 91.87(3), Cl−P−N3 90.28(8), N2−Pd−C31 81.9(1), C31−Pd−P 97.1(1).

analysis. The structures are presented in Figures 5 and 6, respectively, along with relevant geometric parameters.

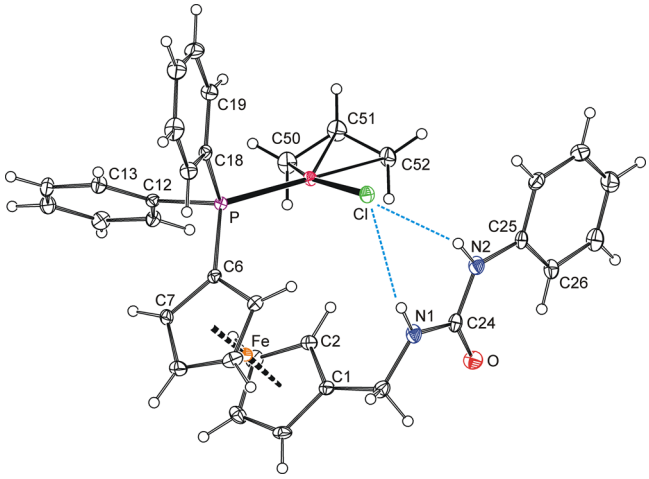


**Figure 6.** PLATON plot of the molecular structure of **8** (30% probability displacement ellipsoids) showing only the dominant orientation of the $\pi$-allyl moiety and the N−H···Cl hydrogen bonds as dashed lines (for a complete structural drawing, see the Supporting Information, Figure S6). Coordination geometry parameters (in Å and deg): Pd−Cl 2.3826(6), Pd−P 2.3013(6), Pd−C50 2.124(5), Pd−C51 2.138(5), Pd−C52 2.221(7), Cl−Pd−P 95.35(2), P−Pd−C50 102.8(1), Cl−Pd−C52 94.6(2).

The structure of solvated **7** corroborates the *trans*-P−N relationship already deduced from the NMR parameters of the $CH_2NMe_2$ moiety, namely, the $^3J_{PC}$ and $^4J_{PH}$ coupling constants.[29] The compound has the expected square-planar coordination environment around the palladium center, which is distorted due to the presence of a small metallacycle (the Pd−C and Pd−N bonds are the shortest among the Pd-donor distances, and the C−Pd−N angle is the most acute interligand angle).[29a,c,e,g] The five-membered palladium ring has an envelope conformation with the nitrogen N3 at the tip position.

Ferrocene cyclopentadienyls in the structure of **7** are tilted by as little as 0.5(2)° (Fe−Cg1 and Fe−Cg2 are 1.646(2) and 1.647(2) Å, respectively) and assume a conformation near anticlinal eclipsed ($\tau$ = 136.3(2)°, cf. ideal value: 144°). The urea moiety is rotated by 68.5(2)° with respect to the plane of the cyclopentadienyl ring C(1−5), forming a pair of N−H···Cl hydrogen bridges toward chloride in a proximal, inversion-related molecule of the complex (see the Supporting Information, Figure S7; N1···Cl = 3.335(3) Å, N2···Cl = 3.351(2) Å).

The $\eta^3$-allyl moiety in the structure of **8** is disordered over two positions that are approximately related by reflection through the plane constituted by the remaining ligands (i.e., the {Pd, Cl, P} plane). The allyl unit intersects the latter plane at an angle of 65.7(6)° (60.5(8)° for the less abundant orientation), and the Pd−C distances gradually increase on going from C50 to C52, following the trend dictated by *trans* influence (P > Cl).[30] Similar structural features have been observed in the structures of analogous ($\eta^3$-allyl)Pd(II) complexes with phosphinoferrocene ligands.[10,31]

Similarly to **7**, the urea protons in **8** form hydrogen bridges to the Pd-bound chloride, although within the same molecule (N1···Cl = 3.408(2) Å, N2···Cl = 3.380(2) Å). However, because the N−H···Cl interactions are intramolecular, the urea moiety is oriented nearly perpendicularly to the plane of its parent cyclopentadienyl ring C(1−5) (dihedral angle: 89.8(1)°; see Figure 6), and the ferrocene unit has a less open conformation ($\tau$ = 99.5(2)°, N.B. the tilting is slightly higher: 3.4(1)°; Fe−Cg1/Cg2 = 1.657(1)/1.649(1) Å).

**Pd-Catalyzed Cyanation of Aryl Bromides.** In view of the presence of the highly polar urea tags in the newly prepared phosphinoferrocene donors, we decided to evaluate their catalytic potential in aqueous, Pd-catalyzed cyanation of aryl bromides leading to synthetically valued benzonitriles,[32] using potassium hexacyanoferrate(II) as an environmentally benign, hydrolytically stable, and water-soluble cyanide source.[33] For the initial screening of the reaction conditions, we chose the cyanation of 4-bromoanisole (**9g**), providing the corresponding nitrile **10g** and amide **11g** as its hydrolytic side-product



DOI: 10.1021/acs.organomet.5b00197
*Organometallics* 2015, 34, 1942−1956

(Scheme 7). This reaction can be easily followed by $^1$H NMR spectroscopy using the signals of the methoxy groups as

**Scheme 7. Model Cyanation Reaction**

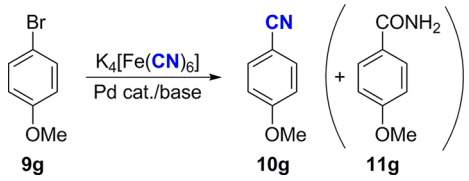


characteristic markers. A catalyst generated *in situ* by mixing palladium(II) acetate with two equivalents of ligand **1e** was used in most of the screening experiments.

Aiming at understanding the effect of aqueous reaction media on the reaction course,[1,34] the possible influence of the solvent was evaluated first. The results presented graphically in Figure 7

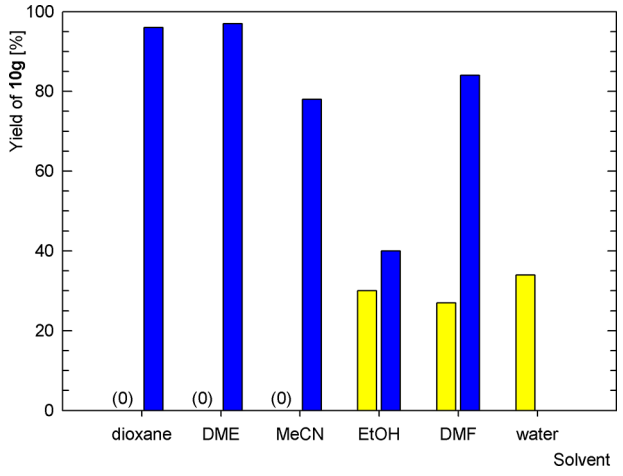


**Figure 7.** Effect of the solvent on the yield of the coupling product **10g**. Pure solvents (yellow bars) are compared with their 1:1 (by volume) aqueous mixtures (blue bars). Conditions: substrate **9g** (1.0 mmol), $K_2CO_3$ (1.0 mmol), and $K_4[Fe(CN)_6]\cdot 3H_2O$ (0.5 mmol) were reacted in the presence of *in situ* generated catalyst (1 mol % Pd, 2 mol % **1e**; see Experimental Section) in the respective solvent (4 mL) at 100 °C for 3 h. NMR yields are given.

demonstrate that the yields of **10g** achieved in an aqueous mixture (solvent–water 1:1 by volume) were better than those obtained in any tested *pure* organic solvent. This observation likely reflects the solubility of the inorganic components in the reaction mixture because the difference in the reaction outcome was most pronounced for ethereal solvents such as (1,4-) dioxane and 1,2-dimethoxyethane (DME) and for acetonitrile, in which the polar reagents would be practically insoluble.

It is also noteworthy that the yield of the coupling product obtained in pure water was lower than that in all other water–organic solvent mixtures tested. Again, this result can be accounted for by the solubility of the reaction components and phase mixing phenomena. We observed that the addition of the mixed solvent typically gave rise to a heterogeneous reaction mixture (two liquid phases). However, this mixture was partly or even fully homogenized upon heating to the reaction temperature (100 °C), which in turn allowed for efficient interaction between the organic substrate, the catalyst, and the highly polar inorganic reagents (i.e., the base and $CN^-$ source).

On the basis of the results of the solvent screening experiments, dioxane was chosen for further reaction tests as an inexpensive aprotic solvent possessing favorable properties, including a reasonably high boiling point and unlimited miscibility with water. More detailed tests showed that changing the water/dioxane ratio also significantly affects the reaction course. For instance, whereas no coupling product was obtained from reactions performed in pure and 80% dioxane (Figure 8), the yield of **10g** suddenly grew to 92% upon

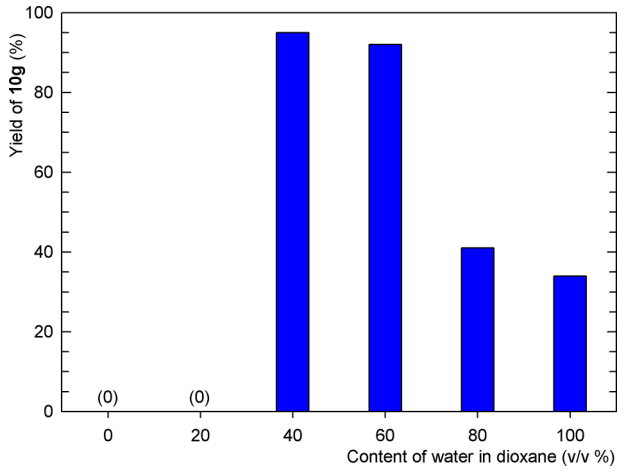


**Figure 8.** Effect of the composition of the water–dioxane mixture on the yield of the coupling product **10g**. For detailed conditions, see caption of Figure 7

increasing the water content to 40 vol %. In accord with our previous results,[35] the best results were obtained in 40:60–60:40 solvent mixtures (cf. 96% yield of **10g** in 50% dioxane). A further increase in the water content to 80% and 100% markedly decreased the yield of the coupling product. Consequently, a 1:1 dioxane–water mixture was employed as the solvent for this particular reaction in all subsequent experiments.

Experiments were also focused on the possible effects of the palladium source and the base. The evaluation of various common palladium precursors at 1 mol % Pd loading (Table 3) has indeed shown that the type of palladium precursor plays an important role. The most satisfactory yields of the coupling

**Table 3. Survey of Various Pd Precursors in the Model Coupling Reaction[a]**

| Pd source | yield of **10g** [%] | Pd source | yield of **10g** [%] |
|---|---|---|---|
| $Pd(OAc)_2$ | 88 | $[PdCl_2(cod)]$ | 89 |
| $Pd(OAc)_2$ | 56[b] | $K_2[PdCl_4]$ | <5[f] |
| $Pd(OAc)_2$ | 29[c] | $[PdCl_2(MeCN)_2]$ | 91 |
| $Pd(OAc)_2$ | 24[d] | $[PdCl(L^{NC})]_2$ | 52[b] |
| $Pd(OAc)_2$ | <5[e] | $[PdCl(\eta^3\text{-}C_3H_5)]_2$ | 18[b] |
| $Pd(O_2CCF_3)_2$ | 92 | $[Pd_2(dba)_3]$ | 30 |

[a]Conditions: substrate **9g** (1.0 mmol), $K_2CO_3$ (1.0 mmol), and $K_4[Fe(CN)_6]\cdot 3H_2O$ (0.5 mmol) were reacted in the presence of *in situ* generated catalyst (1 mol % Pd, 2 mol % **1e**; see Experimental Section) in dioxane–water (1:1, 4 mL) at 100 °C for 3 h. The yield was determined by integration of $^1$H NMR spectra using mesitylene as an internal standard. [b]Pd:**1e** = 1:1. [c]Reaction with 0.5 mol % Pd. [d]Reaction at 80 °C. [e]Reaction at 60 °C. [f]The catalyst was prepared in methanol due to the insolubility of the starting Pd complex in dichloromethane.



DOI: 10.1021/acs.organomet.5b00197
*Organometallics* 2015, 34, 1942–1956

product (around 90%) were obtained with catalysts resulting from simple palladium(II) carboxylates, viz., $Pd(OAc)_2$ and $Pd(O_2CCF_3)_2$, at a Pd:**1e** ratio of 1:2. For practical reasons, the former Pd(II) salt appears particularly attractive because it not only gives rise to a highly active catalyst but is also relatively inexpensive and readily available. Notably, catalysts generated from other Pd(II) precursors as well as from $[Pd_2(dba)_3]$ as an immediate source of Pd(0) performed significantly worse. Similarly, lowering the amount of the ligand to 1 equiv with respect to palladium or decreasing the reaction temperature (100 °C → 80 and 60 °C) considerably reduced the yield of **10g** with the $Pd(OAc)_2$/**1e** catalyst.

The catalytic results achieved with different bases are presented in Table 4. Sodium and potassium carbonate

**Table 4. Survey of Various Bases**[a]

| base | yield of **10g** [%] | base | yield of **10g** [%] |
|---|---|---|---|
| $Li_2CO_3$ | 50 | $NaHCO_3$ | 8 |
| $Na_2CO_3$ | 92 | $Na_3PO_4$ | 49[c] |
| $Na_2CO_3$ | 45[b] | $Na_2HPO_4$ | 8[b] |
| $K_2CO_3$ | 88 | $NaH_2PO_4$ | 0[d] |
| $K_2CO_3$ | 80[b] | NaOAc | <5 |
| $Cs_2CO_3$ | 28 | NaOH | 12[e] |

[a]Conditions: substrate **9g** (1.0 mmol), base (1.0 mmol unless specified otherwise), and $K_4[Fe(CN)_6]\cdot 3H_2O$ (0.5 mmol) were reacted in the presence of *in situ* generated catalyst (1 mol % $Pd(OAc)_2$, 2 mol % **1e**; see Experimental Section) in dioxane−water (1:1, 4 mL) at 100 °C for 3 h. The yield was determined by integration of $^1$H NMR spectra using mesitylene as an internal standard. [b]0.5 mmol of base. [c]0.33 mmol of $Na_3PO_4$. Amide **11g** (<5%) was also detected. [d]***Caution!*** *(Partial) hydrolysis to HCN likely occurs.* [e]Amide **11g** (42%) also formed.

afforded comparable, very good yields (around 90%) when employed in a 1:1 molar ratio with respect to the substrate **9g**. When the amount of these bases was reduced by half (i.e., to one molar equivalent of alkali metal cation per **9g**), the yields of the coupling product decreased, although to different extents, to approximately half in the case of $Na_2CO_3$ and by only 8% with $K_2CO_3$. Both the lighter ($Li_2CO_3$) and the heavier ($Cs_2CO_3$) congeners of these carbonates produced **10g** in lower yields, the former most likely due its relatively poor solubility in the reaction system. Likewise, sodium hydrogen carbonate as well as other bases tested (sodium phosphates, sodium acetate, and sodium hydroxide) did not match the results obtained for either simple carbonate from which the common $Na_2CO_3$ was selected as the most suitable for further reactions because of its good performance and lower molar weight (less material was needed).

To further minimize the amount of inorganic reagents required for the cyanation reaction to proceed with good yields and to limit the amount of waste produced, we have studied the effect of the amount of the cyanide source on the yield of the coupling product. Unfortunately, the results presented in Table 5 indicate that the amount of $K_4[Fe(CN)_6]\cdot 3H_2O$ cannot be reduced further below approximately 0.5 molar equivalents (i.e., 3 equiv of $CN^-$) with respect to **9g** without reducing the yields of the corresponding nitrile in the present case.

Having established the optimal reaction conditions in terms of the reaction solvent, base, and palladium source, we turned to studying the properties of individual phosphinoferrocene ligands (Table 6). The best catalytic results showed catalysts resulting from ligands equipped with urea moieties bearing

**Table 5. Effect of the Amount of $CN^-$ Equivalents on the Yield of Nitrile 10g**[a]

| amount of $K_4[Fe(CN)_6]\cdot 3H_2O$ [mmol] | CN equiv | yield of **10g** [%] |
|---|---|---|
| 1.00 | 6 | 96 |
| 0.50 | 3 | 92 |
| 0.33 | 2 | 65 |
| 0.17 | 1 | 46 |

[a]Conditions: substrate **9g** (1.0 mmol), $Na_2CO_3$ (1.0 mmol), and varying amounts of $K_4[Fe(CN)_6]\cdot 3H_2O$ were reacted in the presence of *in situ* generated catalyst (1 mol % $Pd(OAc)_2$, 2 mol % **1e**; see Experimental Section) in dioxane−water (1:1, 4 mL) at 100 °C for 3 h. The yield was determined by integration of $^1$H NMR spectra using mesitylene as an internal standard.

**Table 6. Catalytic Results Achieved with Different Ligands**[a]

| ligand | yield of **10g** [%] | ligand | yield of **10g** [%] |
|---|---|---|---|
| **1a** | 52 | **1e** | 92 |
| **1b** | 53 | **1f** | 0 |
| **1c** | 55 | **1g** | 40 |
| **1d** | 86 | $FcPPh_2$ | 30 |

[a]Conditions: substrate **9g** (1.0 mmol), $Na_2CO_3$ (1.0 mmol), and $K_4[Fe(CN)_6]\cdot 3H_2O$ (0.5 mmol) were reacted in the presence of *in situ* generated catalyst (1 mol % $Pd(OAc)_2$, 2 mol % ligand; see Experimental Section) in dioxane−water (1:1, 4 mL) at 100 °C for 3 h. The yields were determined by integration of $^1$H NMR spectra using mesitylene as an internal standard.

more bulky and lipophilic substituents (phenyl and cyclohexyl), with phenyl urea **1e** being the most efficient (92% of **10g**). Donors possessing urea substituents with relatively smaller terminal substituents (NHMe and $NMe_2$) as well as the monosubstituted urea **3a** furnished only ca. 50% yields of **10g**, whereas a further reduction of the polar pendants, such in the acetylamino derivative **1g**, caused the yield to decrease even further.

The reaction performed in the absence of any supporting ligand (i.e., employing only $Pd(OAc)_2$ as the catalyst) did not proceed in any appreciable extent under otherwise identical conditions (results not tabulated), suggesting that the supporting phosphine ligand represents a vital component of the catalytic system (unlike many other cross-coupling reactions). In addition, from the dependence of the reaction yield on the structure of the phosphine ligands, it appears likely that the urea moiety is also involved in the catalytic reaction, e.g., by (temporary) coordination of the metal center or through its solubility-tuning properties. The most indicative signs are the dramatically different performance of catalysts based on the analogous phenyl-substituted urea and thiourea ligands (**1e** vs **1f**) and the fact that the catalyst based on $FcPPh_2$ as a P-monodentate donor produced a rather low yield of the coupling product.

As the last step, we studied the scope of the cyanation reaction by altering the structure of the aryl bromide substrate (Scheme 8). The results collected in Table 7 demonstrate that the reaction proceeds satisfactorily with electron-rich, alkylated substrates, despite moderate steric hindrance (see entries 1−5

**Scheme 8. General Scheme of the Cyanation Reaction**

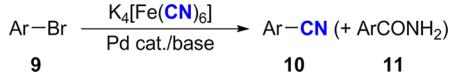




DOI: 10.1021/acs.organomet.5b00197
*Organometallics* 2015, 34, 1942−1956

Table 7. Cyanation of Different Aryl Bromides[a]

| entry | Ar in ArBr (9) | conversion to (yield of)[b] 10 after 3 h [%] | conversion (yield)[b] after 24 h [%] 10 | 11 |
|---|---|---|---|---|
| 1 | 2-$MeC_6H_4$ (**9a**) | 92 (89) | | |
| 2 | 3-$MeC_6H_4$ (**9b**) | 96 (90) | | |
| 3 | 4-$MeC_6H_4$ (**9c**) | 100 (94) | | |
| 4 | 4-*t*-$BuC_6H_4$ (**9d**) | 88 (84) | 91 (84) | n.d. (9) |
| 5 | 2,4,6-$Me_3C_6H_2$ (**9e**) | 48 (n.d.) | 100 (97) | |
| 6 | 4-$PhC_6H_4$ (**9f**) | 100 (96) | | |
| 7 | 4-$MeOC_6H_4$ (**9g**) | 100 (92) | | |
| 8 | 3,4-$(MeO)_2C_6H_3$ (**9h**) | 98 (94) | | |
| 9 | 3,4-$(OCH_2O)C_6H_3$ (**9i**) | 62 (60) | | |
| 10 | 4-$AcC_6H_4$ (**9j**) | 9 (n.d.) | 16 (15) | 84 (82) |
| 11 | 4-$F_3CC_6H_4$ (**9k**) | 18 (n.d.) | 16 (n.d.) | 84 (80) |
| 12 | 4-$ClC_6H_4$ (**9l**) | 25 (n.d.) | 17 (14) | 83 (80) |
| 13 | 4-$O_2NC_6H_4$ (**9m**) | 0 | <5 | |
| 14 | 4-$H_2NC_6H_4$ (**9n**) | 10 (n.d.) | 10 (n.d.) | |
| 15 | 4-$Me_2NC_6H_4$ (**9o**) | 10 (n.d.) | 9 (n.d.) | |
| 16 | 4-$AcNHC_6H_4$ (**9p**) | 60 (55) | 50 (48) | 32 (25)[d] |
| 17 | 4-$HO_2CC_6H_4$ (**9q**) | 93 (84)[c] | | |
| 18 | 1-naphthyl (**9r**) | 18 (n.d.) | 100 (94) | |
| 19 | 2-naphthyl (**9s**) | 99 (94) | | |
| 20 | 1-pyrenyl (**9t**) | | n.d. (79) | |
| 21 | Fc (**9u**) | | 21 (18) | |

[a]Conditions: substrate **9** (1.0 mmol), $Na_2CO_3$ (1.0 mmol), and $K_4[Fe(CN)_6]\cdot 3H_2O$ (0.5 mmol) were reacted in the presence of *in situ* generated catalyst (1 mol % $Pd(OAc)_2$, 2 mol % **1e**; see Experimental Section) in dioxane−water (1:1, 4 mL) at 100 °C for 3 or 24 h. [b]$^1$H NMR conversion (isolated yield in parentheses). These values are averages of two independent runs. n.d. = not determined. [c]2 mmol of $Na_2CO_3$ were used. [d]Nitrile **10n** was also formed (conversion: 18%, isolated yield: 16%).

in Table 7). The introduction of a methoxy group(s) or similar substituents, whose +*M* effect prevails over an −*I* effect, does not hamper the cyanation reaction (entries 7−9). On the other hand, substrates bearing groups with a pronounced electron-withdrawing character react less willingly, and the respective nitriles as the primary products are activated toward hydrolysis to the corresponding amides (see entries 10−12).[36] The crystal structures determined for two such amides, **11j** and **11k**, are discussed in the Supporting Information.

The presence of the nitro group in the *para* position of the benzene ring, exerting strong −*M* and −*I* effects, practically stopped the cyanation reaction, and substrate **9m** thus remained unchanged (entry 13). Aryl bromides bearing amine substituents **9n** and **9o** (entries 14 and 15) also reacted only sluggishly, albeit presumably due to the metal-scavenging effect of their donor substituents. This was corroborated by cyanation of 4-bromoacetanilide (**9p**, entry 16), which furnished nitrile **10p** with 60% conversion (55% isolated yield; entry 16) after 3 h. Extending the reaction time to 24 h did not improve the yield of **10p** (isolated yield: 48%) because of partial hydrolysis to the corresponding amide **11p** (isolated yield: 25%) and removal of the acetyl group resulting in the formation of 4-aminobenzonitrile (**10n**; isolated yield: 16%). The cyanation of 4-bromobenzoic acid (**9q**, entry 16) also represents a notable example because the deprotonation of the carboxyl group under the applied reaction conditions (2 equiv of $Na_2CO_3$ are used) activated the substrate, which was then efficiently converted to the corresponding nitrile without any notable hydrolysis (COOH: −*I* and −*M*; $COO^-$: +*I* and +*M*).

In addition to substituted bromobenzenes, we tested a few other brominated arenes. Thus, 1-bromonaphthalene was fully converted to the respective nitrile **10r** over a period of 24 h, whereas the isomeric 2-bromonaphthalene reacted to a similar extent already within 3 h. The described procedure could also be used to prepare 1-cyanopyrene (**10t**) and cyanoferrocene (**10u**), in which case, however, extended reaction times were required, and the latter product was isolated in only a modest 18% yield. In this case, however, 75% of the starting bromoferrocene was recovered unchanged.

In an attempt to further expand the scope of the reaction, we also varied the halide substituent. Quite expectedly, 4-iodoanisole reacted smoothly under the standard conditions (1 mol % Pd, 3 h), affording **10g** in a 95% isolated yield, but no reaction was observed with the less reactive chloride (i.e., 4-chloroanisole). 4-Bromobenzyl bromide (**9v**) was not cyanated either, being cleanly hydrolyzed under the reaction conditions to 4-bromobenzyl alcohol (**12**; 100% conversion, 90% isolated yield after 24 h).

In is also noteworthy that analysis of the crude reaction mixtures (i.e., prior to workup) typically revealed a characteristic low-field signal in the $^1$H NMR spectrum attributable to a ligand decomposition product ($\delta_H$ ca. 8.7). To identify this reaction product and, consequently, the fate of the phosphine ligand, we prepared phosphine oxide **1eO** by standard hydrogen peroxide oxidation of the model ligand **1e**. Indeed, the NMR signals of authentic **1eO** were identical to those observed in the reaction mixtures, thereby confirming that the ligand undergoes oxidation during the reaction.

## CONCLUSION

This contribution describes the synthesis and catalytic applications of a series of phosphinoferrocene donors modified by various urea moieties, appended via a methylene linker. These compounds were synthesized through three different methods, starting from either the newly prepared phosphinoamine **3** (or rather its stable hydrochloride) or aldehyde **4**. The applicability of these methods was demonstrated to depend on the urea pendant to be incorporated into the newly formed molecule, namely, on the number and type of the substituents at the nitrogen atoms.

As exemplified for the model ligand **1e**, phosphinoferrocene ureas **1** coordinate the Pd(II) ion as typical soft donors (functionally modified phosphines) via their phosphine groups, while the polar urea moieties remain available for the formation of hydrogen-bonded assemblies in the solid state. When combined with a suitable palladium source, these ligands give rise to active catalysts for Pd-catalyzed cyanation of aryl bromides with nontoxic $K_4[Fe(CN)_6]\cdot 3H_2O$ in aqueous reaction media. Under the optimized conditions, the cyanation reaction proceeds with very good to excellent yields for bromoarenes devoid of other substituents and substrates modified by electron-donating groups. In the case of


DOI: 10.1021/acs.organomet.5b00197
*Organometallics* 2015, 34, 1942−1956

electron-poor substrates, the yield of cyanation product (the nitrile) is typically reduced by subsequent hydrolysis upon the action of the base present in the reaction mixture. Substrates with amine substituents also pose some problems, presumably because of their metal-scavenging effect.

## EXPERIMENTAL SECTION

**Materials and Methods.** The syntheses were performed under an argon atmosphere using standard Schlenk techniques. Compounds **2**,[14] **4**,[15] $[PdCl_2(cod)]$,[37] and $[(L^{NC})Pd(\mu\text{-}Cl)]_2$[38] were synthesized according to procedures reported in the literature. Commercial *N,N*-dimethylcarbamoyl chloride was distilled before use. Methanol, dichloromethane, and tetrahydrofuran (HPLC grade) were dried with a PureSolv MD5 solvent purification system (Innovative Technology). Other chemicals and solvents used for crystallizations and during chromatography were used as received without any additional purification.

NMR spectra were recorded at 25 °C on a Varian UNITY Inova 400 spectrometer operating at 399.95, 100.58, and 161.90 MHz for $^1$H, $^{13}$C, and $^{31}$P, respectively. Chemical shifts ($\delta$/ppm) are reported relative to internal tetramethylsilane ($^1$H and $^{13}$C) or to external 85% $H_3PO_4$ ($^{31}$P). In addition to the standard notation of signal multiplicity, vt and vq are used to denote virtual multiplets arising from the protons constituting the AA′BB′ and AA′BB′X spin systems in the methylene- and $PPh_2$-substituted cyclopentadienyl rings, respectively (fc = ferrocene-1,1′-diyl). IR spectra were recorded with a Thermo Nicolet Magna 6700 FTIR spectrometer over the range 400−4000 cm$^{-1}$. Low-resolution ESI mass spectra were obtained with an Esquire 3000 (Bruker) spectrometer. Elemental analyses were determined with a PerkinElmer PE 2400 CHN analyzer. The amount of residual solvents, typically present in amorphous products, was verified by NMR analysis and taken into account during all subsequent experiments.

*Synthesis of 1′-(Diphenylphosphino)-1-(aminomethyl)ferrocene Hydrochloride (**3**·HCl).* Aldoxime **2** (250 mg, 0.61 mmol; mixture of *E*- and *Z*-isomers) was dissolved in dry THF (15 mL), and the solution was added dropwise to solid $Li[AlH_4]$ (115 mg, 3.0 mmol) while stirring and cooling in an ice bath. The reaction mixture was stirred at room temperature for 6 h and then recooled on ice and quenched by sequential addition of water (0.55 mL) and 15% aqueous NaOH (0.15 mL). After stirring for another 30 min, the resulting heterogeneous mixture was filtered through a pad of diatomaceous earth (Celite). The filtrate was diluted with diethyl ether (15 mL), washed with brine (5 mL), dried over magnesium sulfate, and, after removal of the drying agent, treated with methanolic HCl (0.81 mL of a 0.75 M solution, 0.61 mmol). The separated product was filtered off and dried under vacuum to afford hydrochloride **3**·HCl as a yellow solid (168 mg, 64%). Crystals for X-ray diffraction measurements were grown from hot methanol−chloroform.

$^1$H NMR (DMSO-$d_6$): $\delta$ 3.55 (s, 2 H, $CH_2$), 4.06 (vt, $J'$ = 1.9 Hz, 2 H, fc), 4.11 (vq, $J'$ = 1.9 Hz, 2 H, fc), 4.30 (vt, $J'$ = 1.9 Hz, 2 H, fc), 4.50 (vt, $J'$ = 1.8 Hz, 2 H, fc), 7.29−7.41 (m, 10 H, Ph), 8.15 (br s, 3 H, $NH_3^+$). $^{13}$C{$^1$H} NMR (DMSO-$d_6$): $\delta$ 37.73 ($CH_2$), 69.48 (CH of fc), 70.52 (CH of fc), 71.70 (d, $J_{PC}$ = 4 Hz, CH of fc), 73.11 (d, $J_{PC}$ = 15 Hz, CH of fc), 75.99 (d, $^1J_{PC}$ = 7 Hz, *C*-$PPh_2$ of fc), 79.84 (*C*-$CH_2$ of fc), 128.22 (d, $^2J_{PC}$ = 7 Hz, $CH^{ortho}$ of $PPh_2$), 128.58 ($CH^{para}$ of $PPh_2$), 132.94 (d, $^3J_{PC}$ = 20 Hz, $CH^{meta}$ of $PPh_2$), 138.44 (d, $^1J_{PC}$ = 10 Hz, $C^{ipso}$ of $PPh_2$). $^{31}$P{$^1$H} NMR (DMSO-$d_6$): $\delta$ −17.7 (s). IR (Nujol, cm$^{-1}$): $\nu_{max}$ 3068 m, 2635 w, 2559 w, 1594 w, 1562 w, 1309 w, 1241 w 1162 m, 1104 m, 1026 m, 963 w, 911 w, 884 w, 827 s, 817 s, 746 s, 698 s, 633 w, 522 w, 503 s, 483 s, 452 m, 424 w, 412 w. ESI+ MS: *m*/*z* 383 ($[Ph_2PfcCH_2]^+$). Anal. Calcd for $C_{23}H_{23}ClFeNP\cdot0.1CHCl_3$ (447.6): C 61.98, H 5.20, N 3.13. Found: C 61.78, H 5.07, N 3.02 (crystallized sample).

*Synthesis of N-[1′-(Diphenylphosphino)ferrocenyl]urea (**1a**). Method A.* Anhydrous triethylamine (1.0 mL, 7.2 mmol, 16 equiv) was added to a suspension of **3**·HCl (200 mg, 0.46 mol) in dry methanol (15 mL), causing the solid hydrochloride to dissolve the compound. Sodium cyanate (47 mg, 0.6 mmol, 1.5 equiv) dissolved in methanol and water (4 + 4 mL) was added, and the resultant solution was stirred at room temperature overnight. Next, the mixture was diluted with water (10 mL) and extracted with dichloromethane (2 × 10 mL). The organic extracts were combined, washed with brine, dried over anhydrous magnesium sulfate, and evaporated. Subsequent chromatography over silica gel with dichloromethane−methanol (10:1 v/v) led to the development of two orange bands. The first one contained the desired product **1a**, which was isolated by evaporation as an orange, readily crystallizing oil (75 mg, 37%). Evaporation of the second band afforded unreacted free amine (105 mg, 57%). Note: Isolated **1a** is typically contaminated by traces of the corresponding phosphine oxide, which cannot be removed by crystallization. Increasing the amount of NaOCN to 5 equiv did not improve the yield of **1a**.

*Attempted Preparation of **1a** by Method C.* Aldehyde **4** (398 mg, 1.00 mmol) and urea (900 mg, 15 mmol) were mixed with THF (50 mL) and freshly distilled acetic acid (50 mL), and the resultant mixture was cooled in an ice bath. Neat chlorotrimethylsilane (0.16 mL, 1.2 mmol) was added with stirring, and the stirring was continued at room temperature for 3 h, during which time the color of the reaction mixture changed from red to orange. The mixture was recooled in ice, and $Na[BH_4]$ (189 mg, 5.0 mmol) was added in one portion. After the addition, the reaction mixture was stirred at 0 °C for 30 min and then at room temperature for another 2 h, whereupon it turned yellow. The mixture was diluted with saturated aqueous $NaHCO_3$ (60 mL; ***Caution**: gas evolution!*) and extracted with dichloromethane (40 mL). The organic layer was washed with saturated aqueous $NaHCO_3$, water, and brine, dried over magnesium sulfate, and evaporated with chromatography-grade silica gel. Subsequent column chromatography of the crude preadsorbed product over silica gel with dichloromethane−methanol (10:1) and evaporation furnished an orange foam (353 mg), which was analyzed as a mixture of **1a** (approximately 80%), **1aO** (approximately 10%), and **1a**·$BH_3$ (10%). Crystallization from hot ethyl acetate−hexane efficiently removes the borane adduct but not the phosphine oxide. A similar reaction with $Li[AlH_4]$ (5.0 mmol) in THF (no acid added) afforded **1a** in only 9% yield, the majority of the aldehyde being converted to 1′-[(diphenylphoshino)ferrocenyl]methanol (isolated yield: 68%). Crystals used for X-ray diffraction analysis were grown from ethyl acetate−hexane.

$^1$H NMR ($CDCl_3$): $\delta$ 3.97 (d, $^3J_{HH}$ = 4.8 Hz, 2 H, $CH_2$), 3.98 (vt, $J'$ = 1.8 Hz, 2 H, fc), 4.08 (vq, $J'$ = 1.8 Hz, 2 H, fc), 4.13 (vt, $J'$ = 1.9 Hz, 2 H, fc), 4.41 (vt, $J'$ = 1.8 Hz, 2 H, fc), 4.54 (br s, 2 H, $NH_2$), 5.32 (br s, 1 H, NH), 7.31−7.39 (m, 10 H, $PPh_2$). $^{13}$C{$^1$H} NMR ($CDCl_3$): $\delta$ 39.21 ($CH_2$), 68.86 (CH of fc), 69.01 (CH of fc), 71.46 (d, $J_{PC}$ = 3 Hz, CH of fc), 73.27 (d, $J_{PC}$ = 15 Hz, CH of fc), 75.58 (C-P of fc), 86.86 (*C*-$CH_2$ of fc), 128.28 (d, $^2J_{PC}$ = 7 Hz, $CH^{ortho}$ of Ph), 128.81 ($CH^{para}$ of Ph), 133.40 (d, $^3J_{PC}$ = 19 Hz, $CH^{meta}$ of Ph), 138.04 (br s, $C^{ipso}$ of Ph), 158.47 (C═O). $^{31}$P{$^1$H} NMR ($CDCl_3$): $\delta$ −16.1 (s). IR (Nujol, cm$^{-1}$): 3355 br w, 3389 br w, 3322 br w, 3191 br m, 1738 w, 1644 br s, 1601 s, 1431 s, 1329 s, 1311 m, 1269 w, 1232 w, 1202 w, 1162 m, 1123 m, 1096 m, 1069 w, 1029 s, 998 w, 929 w, 888 w, 823 m, 781 w, 742 s, 696 s, 655 w, 571 m, 532 s, 488 s, 460 s, 436 m. ESI+ MS: *m*/*z* 443 ($[M + H]^+$), 465 ($[M + Na]^+$), 481 ($[M + K]^+$). Anal. Calcd for $C_{24}H_{23}FeN_2OP\cdot0.2AcOEt$ (459.9): C 64.77, H 5.39, N 6.09. Found: C 64.62, H 5.25, N 5.94 (sample crystallized from ethyl acetate−hexane).

*Synthesis of N-[1′-(Diphenylphosphino)ferrocenyl]-N′-methylurea (**1b**). Method C.* Aldehyde **4** (398 mg, 1.00 mmol) and *N*-methylurea were dissolved in a mixture of dry THF (30 mL) and acetic acid (60 mL). Chlorotrimethylsilane (0.15 mL, 1.2 mmol) was added, causing an immediate change in color from the initial red to deep orange. After stirring at room temperature for 3 h, the mixture was cooled in an ice bath, and $Na[BH_4]$ (189 mg, 5.00 mmol) was added in one portion (the color of the reaction changed gradually to yellow). The stirring was continued at 0 °C for 30 min and then at room temperature overnight before quenching with water (100 mL, effervescence). The resultant mixture was extracted with dichloromethane (50 and 20 mL), and the combined organic layers were washed twice with saturated aqueous $NaHCO_3$ (***Caution**: gas evolution!*), water, and brine, dried over magnesium sulfate, and


DOI: 10.1021/acs.organomet.5b00197
*Organometallics* 2015, 34, 1942−1956

evaporated. The crude product was purified by column chromatography (silica gel, dichloromethane−methanol, 20:1 v/v). The major band containing the product and some phosphine oxide was evaporated, and the residue was purified again by chromatography over silica gel using ethyl acetate as the eluent to afford **1b** as an orange solid (335 mg, 73%).

A similar reaction with $Li[AlH_4]$ in THF (without added acetic acid) yielded analytically pure **1b** (30%) together with [1′-(diphenylphoshino)ferrocenyl]methanol (49%). The second chromatography was not needed in this case.

$^1$H NMR ($CDCl_3$): $\delta$ 2.80 (s, 3 H, $CH_3$), 3.95 (br s, 2 H, $CH_2$), 3.98 (vt, $J'$ = 1.9 Hz, 2 H, fc), 4.07 (vq, $J'$ = 1.8 Hz, 2 H, fc), 4.12 (vt, $J'$ = 1.8 Hz, 2 H, fc), 4.39 (vt, $J'$ = 1.8 Hz, 2 H, fc), 4.62 (br s, 1 H, NH), 5.01 (br s, 1 H, NH), 7.30−7.38 (m, 10 H, $PPh_2$). $^{13}$C{$^1$H} NMR ($CDCl_3$): $\delta$ 27.26 ($CH_3$), 39.19 ($CH_2$), 69.22 (CH of fc), 68.99 (CH of fc), 71.42 (d, $J$ = 4 Hz, CH of fc), 73.25 ($J$ = 15 Hz, CH of fc), 75.60 (br s, *C*-$CH_2$ of fc), 87.22 (C-P of fc), 128.26 (d, $^2J_{PC}$ = 7 Hz, $CH^{ortho}$ of Ph), 128.76 ($CH^{para}$ of Ph), 133.40 ($^3J_{PC}$ = 19 Hz, $CH^{meta}$ of Ph), 138.20 (br s, $C^{ipso}$ of Ph), 158.71 (C═O). $^{31}$P{$^1$H} NMR ($CDCl_3$): $\delta$ −16.1 (s). IR (Nujol, $cm^{-1}$): $\nu_{max}$ 3326 s, 3294 s, 3137 br m, 3100 m, 3078 m, 3043 m, 1625 s, 1582 s, 1259 m, 1194 w, 1161 m, 1089 w, 1059 w, 1038 m, 1025 m, 998 w, 923 w, 889 w, 831m, 807 s, 776 w, 794 s, 696 s, 667 m, 635 m, 570 w, 529 m, 496 s, 485 s, 453 m, 422 w, 410 w $cm^{-1}$. ESI+ MS: $m/z$ 457 ($[M + H]^+$), 479 ($[M + Na]^+$), 495 ($[M + K]^+$). Anal. Calcd for $C_{25}H_{25}FeN_2OP{\cdot}0.25AcOEt$ (478.3): C 65.28, H 5.69, N 5.86. Found: C 65.19, H 5.44, N 5.91.

*Synthesis of N-[1′-(Diphenylphosphino)ferrocenyl]-N′,N′-dimethylurea (**1c**). Method B.* Anhydrous triethylamine (1.0 mmol, 7.2 mmol) was added to a suspension of **3**·HCl (437 mg, 1.0 mmol) in dry dichloromethane (20 mL). To the resulting clear orange solution was introduced neat *N,N*-dimethylcarbamoyl chloride (0.10 mL, 1.1 mmol), and the resulting mixture was stirred at room temperature overnight. The reaction was terminated by the addition of saturated aqueous $NaHCO_3$ solution (10 min). The organic phase was separated, washed with water and brine, and dried. The product was isolated by flash column chromatography over silica gel with dichloromethane−methanol (20:1 v/v) as the eluent and evaporation under vacuum. Yield of **1c**: 433 mg (92%), yellow solid foam.

$^1$H NMR ($CDCl_3$): $\delta$ 2.91 (s, 6 H, $NMe_2$), 3.99 (br d, $^3J_{HH}$ = 3.8 Hz, 2 H, $CH_2$), 4.01 (vt, $J'$ = 1.8 Hz, 2 H, fc), 4.08 (vq, $J'$ = 1.8 Hz, 2 H, fc), 4.13 (vt, $J'$ = 1.9 Hz, 2 H, fc), 4.36 (vt, $J'$ = 1.8 Hz, 2H, fc), 4.67 (br s, 1 H, NH), 7.29−7.38 (m, 10 H, Ph). $^{13}$C{$^1$H} NMR ($CDCl_3$): $\delta$ 36.37 ($NMe_2$), 37.77 ($CH_2$), 69.06 (CH of fc), 69.15 (CH of fc), 71.33 (d, $J_{PC}$ = 4 Hz, CH of fc), 73.22 (d, $J_{PC}$ = 15 Hz, C-P of fc), 87.14 (*C*-$CH_2$ of fc), 128.18 (d, $^2J_{PC}$ = 7 Hz, $CH^{ortho}$ of Ph), 128.63 ($CH^{para}$ of Ph), 133.41 (d, $^3J_{PC}$ = 20 Hz, $CH^{meta}$ of Ph), 138.58 (d, $^1J_{PC}$ = 8 Hz, $C^{ipso}$ of Ph). 158.11 (C═O). One signal due to ferrocene CH probably overlaps with the solvent resonance. $^{31}$P{$^1$H} NMR ($CDCl_3$): $\delta$ −16.5 (s). IR (Nujol, $cm^{-1}$): 3356 m, 3047 w, 1721 w, 1630 s, 1585 w, 1533 s, 1339 m, 1239 m, 1220 w, 1162 w, 1088 w, 1038 w, 1027 w, 831w, 812 w, 747 m, 699 m, 569 w, 500 m, 486 w, 449 w. ESI+ MS: $m/z$ 471 ($[M + H]^+$), 493 ($[M + Na]^+$), 509 ($[M + K]^+$). Anal. Calcd for $C_{26}H_{27}FeN_2OP{\cdot}0.1CH_2Cl_2$ (478.8): C 65.47, H 5.73, N 3.55. Found: C 65.48, H 5.77, N 5.62.

*Synthesis of N-[1′-(Diphenylphosphino)ferrocenyl]-N′-cyclohexylurea (**1d**). Method A.* Hydrochloride **3**·HCl (219 mg, 0.50 mmol) and triethylamine (1.0 mmol, 7.2 mmol) were mixed in dry dichloromethane (10 mL), producing a clear orange solution, which was cooled on ice. Neat cyclohexyl isocyanate (10 μL, 0.55 mmol) was introduced, and the reaction mixture was stirred at 0 °C for 15 min and then at room temperature overnight. After the reaction was quenched by addition of water (10 mL), the organic layer was separated, and the aqueous residue was extracted with dichloromethane (3 × 10 mL). The combined organic phases were washed with brine, dried over magnesium sulfate, and evaporated under vacuum to afford a crude product, which was purified by chromatography (silica gel, dichloromethane−methanol, 10:1) and then crystallized from hot ethyl acetate−hexane (approximately 1:3) to afford urea **1d** as orange crystals (217 mg, 83%). Crystals suitable for X-ray diffraction analysis were obtained from ethyl acetate−hexane.

$^1$H NMR ($CDCl_3$): $\delta$ 1.06−1.20 (m, 3 H, $CH_2$ of Cy), 1.29−1.41 (m, 2 H, $CH_2$ of Cy), 1.54−1.61 (m, 1 H, $CH_2$ of Cy), 1.64−1.72 (m, 2 H, $CH_2$ of Cy), 1.90−1.98 (m, 2 H, $CH_2$ of Cy), 3.59 (m, 1 H, CH of Cy), 3.95 (d, $^3J_{HH}$ = 4.8 Hz, 2 H, C$H_2$NH), 3.97 (vt, $J'$ = 1.9 Hz, 2 H, fc), 4.06 (vq, $J'$ = 1.7 Hz, 2 H, fc), 4.12 (vt, $J'$ = 1.8 Hz, 2 H, fc), 4.39 (vt, $J'$ = 1.9 Hz, 2 H, fc), 4.64 (br d, $^3J_{HH}$ = 7.7 Hz, 1 H, N*H*Cy), 5.01 (br m, 1 H, $CH_2$N*H*), 7.30−7.39 (m, 10 H, Ph). $^{13}$C{$^1$H} NMR ($CDCl_3$): $\delta$ 24.87 ($CH_2$ of Cy), 25.63 ($CH_2$ of Cy), 33.94 ($CH_2$ of Cy), 38.99 (*C*$H_2$NH), 48.94 (CH of Cy), 68.76 (CH of fc), 69.01 (CH of fc), 71.40 (d, $J_{PC}$ = 4 Hz, CH of fc), 73.19 (d, $J_{PC}$ = 15 Hz, CH of fc), 75.55 (br s, C-P of fc), 87.53 (*C*-$CH_2$ of fc), 128.25 (d, $^2J_{PC}$ = 7 Hz, $CH^{ortho}$ of Ph), 128.75 ($CH^{para}$ of Ph), 133.39 (d, $^3J_{HH}$ = 19 Hz, $CH^{meta}$ of Ph), 138.09 (br d, $^1J_{HH}$ = 6 Hz, $C^{ipso}$ of Ph), 157.37 (C═O). $^{31}$P{$^1$H} NMR ($CDCl_3$): $\delta$ −16.4 (s). IR (Nujol, $cm^{-1}$): 3392 m, 3264 br m, 3049 m, 1740 w, 1620 s, 1598 s, 1497 s, 1310 w, 1272 m, 1254 m, 1233 m, 1160 m, 1084 m, 1049 w, 1033 m, 1025 m, 921 w, 871 w, 842 w, 813 m, 750 s, 745 s, 700 s, 634 m, 528 w, 499 s, 484 s, 461 w, 413 w. ESI+ MS: $m/z$ 525 ($[M + H]^+$), 547 ($[M + Na]^+$), 563 ($[M + K]^+$). Anal. Calcd for $C_{30}H_{33}FeN_2OP$ (524.4): C 68.71, H 6.34, N 5.34. Found: C 68.51, H 6.29, N 5.22.

*Synthesis of N-[1′-(Diphenylphosphino)ferrocenyl]-N′-phenylurea (**1e**). Method A.* Anhydrous triethylamine (2.5 mL, 18 mmol) was added to a suspension of **3**·HCl (437 mg, 1.0 mmol) in dichloromethane (35 mL), whereupon the hydrochloride dissolved to yield a clear orange solution. After cooling in an ice bath, neat phenyl isocyanate (86 μL, 1.1 mmol) was added, and the resulting mixture was stirred at 0 °C for 15 min and then at room temperature overnight. Next, the reaction mixture was diluted with water (20 mL), and the organic layer was separated. The aqueous residue was extracted with dichloromethane (10 mL), and the organic phases were combined, washed with brine, dried over anhydrous magnesium sulfate, and, finally, evaporated under vacuum. The crude product was purified by flash chromatography (silica gel, dichloromethane−methanol, 20:1 v/v). The first intense band was collected and evaporated to afford **1e**, which was further crystallized from hot ethyl acetate−hexane (approximately 1:1). Yield: 458 mg (88%), orange microcrystalline solid.

*Method C.* Aldehyde **4** (199 mg, 0.50 mmol) and *N*-phenylurea (136 mg, 1.0 mmol) were dissolved in anhydrous THF (20 mL), and the solution was cooled on ice. Chlorotrimethylsilane (76 μL, 0.60 mmol) was added with stirring at 0 °C, and the reaction was continued at room temperature for 30 min. The color of the reaction mixture changed from deep red to orange, and a fine precipitate formed. Then, the reaction mixture was cooled again to 0 °C, and $Li[AlH_4]$ (57 mg, 1.5 mmol) was added at once. Instant effervescence and a change in color to yellow were observed upon the addition. After the gas evolution ceased (ca. 5 min), the reaction was terminated by a careful addition of degassed water (0.3 mL) and 3 M NaOH (0.1 mL). The cooling bath was removed, and the resultant mixture was stirred for 20 min at room temperature (to complete hydrolysis) and then filtered through a pad of Celite, eluting with diethyl ether. The yellow filtrate was washed with water (3×) and brine, dried over magnesium sulfate, mixed with chromatography-grade silica gel, and, finally, evaporated under reduced pressure. The preadsorbed crude product was transferred to the top of a chromatographic column packed with silica gel in ethyl acetate−hexane (1:3). Elution with the same solvent mixture removed minor impurities. Changing the solvent to pure ethyl acetate eluted the main yellow band due to **1e**, which was collected and evaporate to furnish pure **1e** as an orange solid (212 mg, 82%).

A similar reaction of **4** (199 mg, 0.50 mmol), *N*-phenylurea (136 mg, 1.0 mmol), and chlorotrimethylsilane (76 μL, 0.6 mmol) in THF (10 mL) and acetic acid (10 mL) with $Na[BH_4]$ (95 mg, 2.5 mmol) as the reducing agent followed by aqueous workup provided 250 mg of a solid product, which contained the desired product **1e** strongly contaminated by the respective borane adduct (**1e**·$BH_3$: approximately 30%) according to NMR analysis.

$^1$H NMR ($CDCl_3$): $\delta$ 3.98 (vt, $J'$ = 1.9 Hz, 2 H, fc), 4.01 (d, $^3J_{HH}$ = 4.9 Hz, 2 H, $CH_2$), 4.04 (vq, $J'$ = 1.8 Hz, 2 H, fc), 4.13 (vt, $J'$ = 1.8 Hz, 2 H, fc), 4.35 (vt, $J'$ = 1.8 Hz, 2 H, fc), 5.53 (br s, 1 H, NH), 6.99 (br s, 1 H, NH), 7.02−7.06 (m, 1 H, Ph), 7.26−7.39 (m, 14 H, NH*Ph* and



DOI: 10.1021/acs.organomet.5b00197
*Organometallics* 2015, 34, 1942−1956

$PPh_2$). $^{13}C\{^1H\}$ NMR ($CDCl_3$): $\delta$ 38.80 ($CH_2$), 68.87 (CH of fc), 69.00 (CH of fc), 71.44 (d, $J_{PC}$ = 3 Hz, CH of fc), 73.17 (d, $J_{PC}$ = 14 Hz, CH of fc), 87.11 (C-$CH_2$ of fc), 120.42 ($CH^{ortho}$ of NHPh), 123.41 ($CH^{para}$ of NHPh), 128.35 (d, $^2J_{PC}$ = 7 Hz, $CH^{ortho}$ of $PPh_2$), 128.91 ($CH^{meta}$ of NHPh), 129.19 ($CH^{para}$ of $PPh_2$), 133.37 (d, $^3J_{PC}$ = 19 Hz, $CH^{meta}$ of $PPh_2$), 137.79 (br, $C^{ipso}$ of $PPh_2$), 138.87 ($C^{ipso}$ of NPh), 155.40 (C═O). Signal due to *C*-P of fc was not observed. $^{31}P\{^1H\}$ NMR ($CDCl_3$): $\delta$ − 16.3 (s). IR (Nujol, $cm^{-1}$): $\nu_{max}$ 3370 br w, 3318 w, 3183 w, 3092 m, 1645 s, 1598 s, 1544 s, 1324 m, 1310 s, 1250 s, 1189 w, 1159 m, 1089 w, 1051 w, 1025 w, 997 w, 912 w, 862 w, 839 s, 815 m, 756 s, 748 s, 698 s, 514 m, 493 s, 482 s, 451 m, 430 w. ESI+ MS: *m*/*z* 519 ($[M + H]^+$), 542 ($[M + Na]^+$), 557 ($[M + K]^+$). Anal. Calcd for $C_{30}H_{27}FeN_2OP$ (518.4): C 69.51, H 5.25, N 5.41. Found: C 69.30, H 5.08, N 5.29.

*Preparation of N-[1′-(Diphenylphosphino)ferrocenyl]-N′-phenylthiourea (**1f**). Method A.* Hydrochloride **3**·HCl (437 mg, 1.0 mmol) and dry triethylamine (2.5 mL, 18 mmol) were mixed in dry dichloromethane (30 mL), and the resulting clear solution was cooled on ice. Phenyl isothiocyanate (0.13 mL, 1.1 mmol) was added, and the mixture was stirred at 0 °C for 15 min and then at room temperature overnight. The reaction was terminated by addition of water (20 mL), the organic phase was separated, and the aqueous residue was extracted with dichloromethane (approximately10 mL). The combined dichloromethane layer was washed with brine, dried with magnesium sulfate, and evaporated under vacuum. The crude product was purified by flash chromatography (silica gel, dichloromethane−methanol 50:1 v/v) and further crystallized from hot ethyl acetate−hexane (1:1) to yield stoichiometric solvate **1f**·AcOEt as yellow-orange crystals (483 mg, 77%). Crystals of unsolvated **1f** used for X-ray diffraction analysis were grown from ethyl acetate−hexane.

$^1H$ NMR ($CDCl_3$): $\delta$ 3.88 (vq, $\acute{J}$ = 1.8 Hz, 2 H, fc), 4.01 (vt, $\acute{J}$ = 1.9 Hz, 2 H, fc), 4.04 (vt, $\acute{J}$ = 1.8 Hz, 2 H, fc), 4.07 (vt, $\acute{J}$ = 1.8, 2 H, fc), 4.34 (d, $^3J_{HH}$ = 4.9 Hz, 2 H, $CH_2$), 6.27 (br s, 1 H, $CH_2NH$), (101 MHz): $\delta$ 44.25 ($CH_2$), 68.53 (CH of fc), 69.45 (CH of fc), 71.02 (d, *J* = 4 Hz, CH of fc), 73.08 (d, *J* = 14 Hz, CH of fc), 85.09 (*C*-$CH_2$ of fc), 125.77 ($CH^{ortho}$ of NHPh), 127.62 ($CH^{para}$ of NHPh), 128.19 (d, $^2J_{PC}$ = 7 Hz, $CH^{ortho}$ of $PPh_2$), 128.67 ($CH^{meta}$ of NHPh), 130.25 ($CH^{para}$ of $PPh_2$), 133.40 (d, $^3J_{PC}$ = 20 Hz, $CH^{meta}$ of $PPh_2$), 136.06 ($C^{ipso}$ of NHPh), 138.54 (d, $^1J_{PC}$ = 9 Hz, $C^{ipso}$ of $PPh_2$), 180.16 (C═S). The signal due to *C*-P of fc was not observed. $^{31}P\{^1H\}$ NMR ($CDCl_3$): $\delta$ − 16.7 (s). IR (Nujol, $cm^{-1}$): 3371 w, 3356 m, 3154 br m, 1734 w 1588 w, 1515 s, 1316 m, 1300 m, 1261 m, 1240 m, 1192 w, 1163 m, 1092 w, 1050 w, 1026 m, 970 w, 960 w, 844 w, 833 m, 754 s, 746 s, 699 w, 532 w, 493 m, 480 m, 458 w. ESI+ MS: *m*/*z* 535 ($[M + H]^+$), 557 ($[M + Na]^+$), 573 ($[M + K]^+$). Anal. Calcd for $C_{30}H_{27}FeN_2PS$·AcOEt (622.5) C 65.59, H 5.67, N 4.50. Found: C 66.00, H 5.42, N 4.50.

*Preparation of 1′-(Diphenylphosphino)-1-[(acetylamino)methyl]ferrocene (**1g**). Method B.* Freshly distilled acetyl chloride (45 μL, 0.63 mmol) was added to a solution of amine **3** generated *in situ* by mixing **3**·HCl (250 mg, 0.57 mmol) and triethylamine (0.7 mL, 5 mmol) in dry dichloromethane (10 mL). The reaction mixture was stirred at room temperature overnight before quenching with 3 M HCl (5 mL). The organic phase was separated and washed successively with 3 M HCl, 0.1 M NaOH, water, and brine (5 mL each), dried over magnesium sulfate, and evaporated. The crude product was purified by column chromatography over silica gel using dichloromethane−methanol (5:1, v/v) as the eluent. Following evaporation under vacuum, the product was isolated as a viscous, orange-brown oil (231 mg, 91%).

$^1H$ NMR ($CDCl_3$): $\delta$ 2.03 (s, 3 H, $CH_3$), 4.00−4.03 (m, 4 H, 2× fc + $CH_2$), 4.07 (vq, *J*′ = 1.8 Hz, 2 H, fc), 4.11 (vt, *J*′ = 1.8 Hz, 2 H, fc), 4.38 (vt, *J*′ = 1.8 Hz, 2 H, fc), 6.02 (br s, 1 H, NH), 7.30−7.39 (m, 10 H, Ph). $^{13}C\{^1H\}$ NMR ($CDCl_3$): $\delta$ 22.23 ($CH_3$), 38.51 ($CH_2$), 69.14 (CH of fc), 69.24 (CH of fc), 71.50 (d, $J_{PC}$ = 4 Hz, 75.35 (br s, C-$PPh_2$ of fc), 71.53 (CH of fc), 73.34 (d, $J_{PC}$ = 14 Hz, CH of fc), 85.79 (*C*-$CH_2$ of fc), 128.29 (d, $^3J_{PC}$ = 7 Hz, $CH^{meta}$ of $PPh_2$), 128.91 ($CH^{para}$ of $PPh_2$), 133.40 (d, $^2J_{PC}$ = 19 Hz, $CH^{ortho}$ of $PPh_2$), 137.82 (br s, $C^{ipso}$ of $PPh_2$), 169.73 (C═O). $^{31}P\{^1H\}$ NMR ($CDCl_3$): $\delta$ −16.3 (s). IR (Nujol, $cm^{-1}$): 3279 br m, 1721 w, 1645 s, 1585 m, 1552 s, 1288 s, 1265 m, 1230 w, 1202 m, 1161 m, 1122 w, 1077 m, 1053 w, 1033 s, 1024 s, 929 w, 887 w, 864 w, 831 s, 738 s, 694 s, 634 w, 592 m, 569 w, 513 s, 484 s, 474 s, 453 m, 434 m, 413 w. ESI+ MS: *m*/*z* 462 ($[M + H]^+$), 464 ($[M + Na]^+$), 480 ($[M + K]^+$). Anal. Calcd for $C_{25}H_{24}FeNOP$ (441.3): C 68.04, H 5.48, N 3.17. Found: C 67.76, H 5.36, N 2.90.

*Synthesis of Phosphine Oxide **1eO**.* Compound **1e** (40 mg, 77 μmol) was dissolved in acetone (6 mL), and the solution was cooled on ice. Concentrated hydrogen peroxide (0.1 mL 30%) was added, and the resulting mixture was stirred at 0 °C for 20 min. Then, the reaction mixture was diluted with water (ca. 6 mL), and its volume was reduced to half by evaporation under vacuum, whereupon the product separated as a yellow solid. The latter was extracted into dichloromethane, and the extract was dried briefly over anhydrous magnesium sulfate and passed through a short silica gel column using dichloromethane−methanol (10:1) as the eluent. Subsequent evaporation afforded phosphine oxide **1eO** as a yellow-orange, glassy solid. Yield: 40 mg, 97%.

$^1H$ NMR ($CDCl_3$): $\delta$ 3.93 (vt, *J*′ = 1.9 Hz, 2 H, fc), 4.08 (d, $^3J_{HH}$ = 3.7 Hz, 2 H, $CH_2$), 4.32 (vq, *J*′ = 1.8 Hz, 2 H, fc), 4.38 (vt, *J*′ = 1.9 Hz, 2 H, fc), 4.57 (vq, *J*′ = 1.8 Hz, 2 H, fc), 6.93 (tt, *J*′ = 7.4, 1.2 Hz, 1 H, NPh), 7.22−7.28 (m, 2 H, NPh), 7.45−7.72 (m, 13 H, Ph and NH), 8.73 (br s, 1 H, NH). $^{13}C\{^1H\}$ NMR ($CDCl_3$): $\delta$ 37.96 ($CH_2$), 68.33 (CH of fc), 68.78 (CH of fc), 72.20 (d, $J_{PC}$ = 10 Hz, CH of fc), 72.30 (d, $^1J_{PC}$ = 117 Hz, $C^{ipso}$-P of fc), 72.69 (d, $J_{PC}$ = 13 Hz, CH of fc), 89.21 (*C*-$CH_2$ of fc), 118.10 ($CH^{ortho}$ of NHPh), 121.17 ($CH^{para}$ of NHPh), 128.52 (d, $^2J_{PC}$ = 12 Hz, $CH^{ortho}$ of $PPh_2$), 128.69 ($CH^{meta}$ of NPh), 131.24 (d, $^3J_{PC}$ = 10 Hz, $CH^{meta}$ of $PPh_2$), 132.08 (d, $^4J_{PC}$ = 3 Hz, $CH^{para}$ of $PPh_2$), 132.94 (d, $^1J_{PC}$ = 108 Hz, $C^{ipso}$ of $PPh_2$), 140.72 ($C^{ipso}$ of NHPh), 156.47 (C═O). $^{31}P\{^1H\}$ NMR ($CDCl_3$): $\delta$ 32.8 (s). ESI+ MS: *m*/*z* 535 ($[M + H]^+$), 557 ($[M + Na]^+$), 573 ($[M + K]^+$). IR (Nujol, $cm^{-1}$): $\nu_{max}$ 3329 br m, 3228 w, 3082 w, 1707 s, 1600 m, 1541 s, 1500 s, 1325 m, 1279 w, 1227 m, 1216 m, 1197 s, 1186 m, 1176 m, 1161 s, 1101 m, 1038 m, 997 w, 896 w, 871 w, 843 w, 754 s, 705 s, 696 s, 633 w, 571 s, 532 m, 507 m, 496 s, 483 m, 443 m. Anal. Calcd for $C_{30}H_{27}FeN_2O_2P$·0.05$CHCl_3$ (540.5): C 66.80, H 5.05, N 5.18. Found: C 66.59, H 5.03, N 4.99.

*Preparation of [PdCl(**1e**-κP)(μ-Cl)]$_2$ (**5**).* A solution of phosphine **1e** (50 mg, 96 μmol) in dichloromethane (5 mL) was added to a solution of $[PdCl_2(cod)]$ (27.5 mg, 96 μmol) in the same solvent (1 mL). The dark reaction mixture was stirred for 1 h and then filtered through a syringe filter (0.45 μm) into pentane (40 mL). The mixture was stored at −18 °C overnight before the precipitated product was filtered off, washed with pentane, and dried under vacuum. Yield of **5**: 66 mg (quant.), grayish solid.

$^1H$ NMR ($CDCl_3$): $\delta$ 4.23, 4.53, 4.54, 4.64, and 4.93 (5× br s, 2 H, fc and $CH_2$); 6.26 (br s, 1 H, $NHCH_2$), 6.95−7.00 (m, 1 H, Ph), 7.17−7.28 (m, 6 H, Ph), 7.35−7.41 (m, 3 H, Ph), 7.44−7.7.51 (m, 5 H, Ph), 7.94 (br s, 1 H, N*H*Ph). $^{13}C\{^1H\}$ NMR ($CDCl_3$): $\delta$ 38.83 ($CH_2$), 67.80 (d, $^1J_{PC}$ = 68 Hz, C-P of fc), 70.00 (CH of fc), 70.99 (CH of fc), 73.32 (d, $J_{PC}$ = 9 Hz, CH of fc), 75.82 (d, $J_{PC}$ = 11 Hz, CH of fc), 89.30 (*C*-$CH_2$ of fc), 118.72 (CH of NHPh), 122.00 ($CH^{para}$ of NHPh), 128.58 (d, $^1J_{PC}$ = 63 Hz, C-P of $PPh_2$), 128.15 (d, $J_{PC}$ = 13 Hz, CH of $PPh_2$), 128.85 ($CH^{para}$ of $PPh_2$), 131.78 (CH of NHPh), 133.45 (d, $J_{PC}$ = 11 Hz, CH of $PPh_2$), 139.76 ($C^{ipso}$ of NHPh), 155.99 (C═O). $^{31}P\{^1H\}$ NMR ($CDCl_3$): $\delta$ 33.6 (s). ESI+ MS: *m*/*z* 623 ($[Pd(\mathbf{1e} - H)]^+$), 659 ($[Pd(\mathbf{1e})Cl]^+$). IR (Nujol, $cm^{-1}$): $\nu_{max}$ 3350 br m, 3055 w, 1655 s, 1597 s, 1548 s, 1498 s, 1311 m, 1236 m, 1166 m, 1099 m, 1059 w, 1030 m, 999 w, 921 w, 896 w, 835 m, 748 s, 712 m, 692 s, 620 w, 548 m, 542 s, 478 s, 447 m. Anal. Calcd for $C_{60}H_{54}Cl_4Fe_2N_4O_2P_2Pd_2$ (1391.4): C 51.79, H 3.91, N 4.03. Found: C 51.66, H 3.86, N 3.85.

*Preparation of [PdCl$_2$(**1e**-κP)$_2$] (**6**).* A dichloromethane solution of $[PdCl_2(cod)]$ (28.3 mg, 29 μmol in 2 mL) was added to a solution of phosphine **1e** (30 mg, 58 μmol) in the same solvent (3 mL). The resulting red solution was stirred for 15 min, concentrated to approximately one-half its original volume by evaporation under vacuum, and precipitated by addition of pentane (20 mL). The separated solid was filtered off, washed with pentane, and dried under vacuum. Yield of **6**: 34 mg (96%), red solid. Note: The crude products


DOI: 10.1021/acs.organomet.5b00197
*Organometallics* 2015, 34, 1942−1956

contained traces of an unidentified impurity (different from **5**, **1e**, and **1eO**), which could be removed by precipitation of the concentrated reaction mixture with pentane.

$^1$H NMR ($CDCl_3$): $\delta$ 4.04 (d, $^3J_{HH}$ = 4.3 Hz, 2 H, $CH_2$), 4.37 (br s, 2 H, fc), 4.40 (br s, 2 H, fc), 4.47 (br s, 2 H, fc), 4.54 (br s, 2 H, fc), 5.63 (br s, 1 H, $CH_2NH$), 6.94–6.98 (m, 1 H, Ph), 7.15–7.23 (m, 5 H, Ph), 7.30–7.38 (m, 5 H, Ph), 7.55–7.62 (m, 4 H, 3× CH of Ph + NHPh). $^{13}$C{$^1$H} NMR ($CDCl_3$): $\delta$ 38.81 ($CH_2$), 69.34 (CH of fc), 70.41 (CH of fc), 71.70 (apparent t, $J'$ = 27 Hz, C-P of fc), 72.29 (apparent t, $J'$ = 4 Hz, CH of fc), 75.86 (apparent t, $J'$ = 5 Hz, CH of fc), 88.41 (C-$CH_2$ of fc), 119.94 (CH of NHPh), 122.86 ($CH^{para}$ of NHPh), 127.87 (apparent t, $J_{PC}$ = 5 Hz, CH of $PPh_2$), 128.90 (CH of NHPh), 130.56 ($CH^{para}$ of $PPh_2$), 130.77 (apparent t, $^1J_{PC}$ = 25 Hz, $C^{ipso}$-P of $PPh_2$), 134.04 (apparent t, $J_{PC}$ = 6 Hz, CH of $PPh_2$), 139.02 ($C^{ipso}$ of NHPh) 155.62 (C═O). $^{31}$P{$^1$H} NMR ($CDCl_3$): $\delta$ 16.4 (s). ESI+ MS: $m/z$ 519 ([**1e** + H]$^+$), 623 ([Pd(**1e** − H)]$^+$). ESI− MS: $m/z$ 659 ([PdCl(**1e** − 2H)]$^-$), 740 ([Pd(**1e**)$Cl_3$]$^-$), 1247 ([Pd(**1e**)$_2Cl_2$ + Cl]$^-$). IR (Nujol, cm$^{-1}$): $\nu_{max}$ 3343 br m, 3053 w, 1652 s, 1598 s, 1552 s, 1498 s, 1311 m, 1236 m, 1164 m, 1099 m, 1058 w, 1029 m, 999 w, 920 w, 895 w, 833 m, 746 s, 692 s, 539 w, 509 m, 446 w. Anal. Calcd for $C_{60}H_{54}Cl_2Fe_2N_4O_2P_2Pd$ (1214.0): C 59.36, H 4.48, N 4.62. Found: C 59.09, H 4.65, N 4.44.

*Preparation of [PdCl($C_6H_4CH_2NMe_2$-$\kappa^2C^1$,N)(**1e**-$\kappa$P)] (**7**).* A solution of ligand **1e** (50 mg, 96 $\mu$mol) dissolved in dichloromethane (6 mL) was added to [PdCl($L^{NC}$)]$_2$ dissolved in the same solvent (2 mL). The reaction mixture was stirred for 60 min and then evaporated under vacuum to afford **7** as a yellow solid. Yield: 76 mg (quant.). Crystals suitable for X-ray diffraction analysis were obtained upon layering a chloroform solution of the complex with hexane and slow crystallization by liquid-phase diffusion.

$^1$H NMR ($CDCl_3$): $\delta$ 2.81 (d, $^4J_{PH}$ = 2.8 Hz, 6 H, $NMe_2$), 4.12 (d, $^3J_{HH}$ = 2.2 Hz, 2 H, $C_5H_4CH_2$), 4.18 (d, $^4J_{PH}$ = 4.8 Hz, 2 H, $Me_2NCH_2$), 4.29 (vt, $J'$ = 1.9 Hz, 2 H, fc), 4.41 (td, $J'$ = 1.9, 1.0 Hz, 2 H, fc), 4.49 (vq, $J'$ = 1.9 Hz, 2 H, fc), 4.58 (vt, $J'$ = 1.8 Hz, 2 H, fc), 6.24 (ddd, $J$ = 7.7 Hz, 6.5 Hz, 1.0 Hz, 1 H, $C_6H_4$), 6.38 (m, 2 H, 1H of $C_6H_4$ and $CH_2NH$), 6.83 (td, $J$ = 7.4, 1.1 Hz, 1 H, $C_6H_4$), 6.94 (tt, $J$ = 7.4, 1.1 Hz, 1 H, NHPh), 7.01 (dd, $J$ = 7.4, 1.5 Hz, 1 H, $C_6H_4$), 7.21–7.25 (m, 2 H, Ph), 7.29–7.35 (m, 4 H, Ph), 7.39–7.44 (m, 2 H, Ph), 7.49–7.55 (m, 6 H, Ph), 8.23 (s, 1 H, NHPh). $^{13}$C{$^1$H} NMR ($CDCl_3$): $\delta$ 38.79 ($C_5H_4CH_2$), 50.14 (d, $^3J_{PC}$ = 3 Hz, $N(CH_3)_2$), 68.87 (CH of fc), 69.91 (CH of fc), 72.32 (d, $J_{PC}$ = 7 Hz, CH of fc), 73.38 (d, $^1J_{PC}$ = 3 Hz, C-$PPh_2$ of fc), 73.73 (d, $^3J_{PC}$ = 60 Hz, $Me_2NCH_2$), 75.89 (d, $J_{PC}$ = 9 Hz, CH of fc), 89.05 (C-$CH_2$ of fc), 118.49 (CH of NHPh), 121.83 ($CH^{para}$ of NHPh), 122.58 (CH of $C_6H_4$), 123.94 (CH of $C_6H_4$), 125.04 (d, $J_{PC}$ = 6 Hz, CH of $C_6H_4$), 128.01 (d, $^4J_{PC}$ = 11 Hz, $CH^{para}$ of $PPh_2$), 128.77 (CH of NHPh), 130.68 (d, $J_{PC}$ = 2 Hz, CH of $C_6H_4$), 131.35 (d, $^2J_{PC}$ = 50 Hz, CH of $PPh_2$), 134.33 (d, $^3J_{PC}$ = 12 Hz, CH of $PPh_2$), 138.71 (d, $^1J_{PC}$ = 11 Hz, $C^{ipso}$ of $PPh_2$), 139.95 ($C^{ipso}$ of NHPh), 147.85 (d, $^2J_{PC}$ = 2 Hz, C-Pd of $C_6H_4$), 151.91 (C-$CH_2$ of $C_6H_4$), 155.85 (C═O). $^{31}$P{$^1$H} NMR ($CDCl_3$): $\delta$ 33.9 (s). IR (Nujol, cm$^{-1}$): $\nu_{max}$ 3379 w, 3344 w, 3314 w, 3280 m, 1698 s, 1601 m, 1579 w, 1548 s, 1499 s, 1318 m, 1233 m, 1210 m, 1162 w, 1097 w, 1032 w, 991 w, 839 w, 814 w, 738 m, 693 m, 654 w, 542 m, 522 w, 496 w, 462 w, 443 w. ESI+ MS: $m/z$ 758 ([M − Cl]$^+$). Anal. Calcd for $C_{39}H_{39}ClFeN_3OPPd$ (794.4): C 58.96, H 4.95, N 5.29. Found: C 58.81, H 4.90, N 5.05.

*[PdCl($\eta^3$-$C_3H_5$)(**1e**-$\kappa$P)] (**8**).* A solution of ligand **1e** (50 mg, 96 $\mu$mol) in dichloromethane (6 mL) was added to a solution of [PdCl($\eta^3$-$C_3H_5$)]$_2$ (17.5 mg, 48 $\mu$mol) in the same solvent (2 mL). The resulting solution was stirred for 60 min and then evaporated under vacuum to afford **8** as a glassy solid, which slowly crystallized. Yield of **8**·0.2$CH_2Cl_2$: 69 mg (quant.). Crystals suitable for X-ray diffraction measurements were grown from ethyl acetate–hexane.

$^1$H NMR ($CDCl_3$): $\delta$ 2.83 (d, $J$ = 12.2 Hz, 1 H, $CH_2$-allyl *trans*-Cl), 3.12 (d, $J$ = 6.4 Hz, 1 H, $CH_2$-allyl *trans*-Cl), 3.74 (dd, $J$ = 13.8, 9.8 Hz, 1 H, $CH_2$-allyl *trans*-P), 3.84 (m, 1 H, fc), 3.86 (m, 1 H, fc), 4.11 (dd, $J_{HH}$ = 15.4, 5.1 Hz, 1 H, $CH_2NH$), 4.21 (dd, $J_{HH}$ = 15.4, 5.8 Hz, 1 H, $CH_2NH$), 4.27 (br s, 1 H, fc), 4.38 (br s, 1 H, fc), 4.46–4.52 (m, 3 H, fc), 4.63 (br s, 1 H, fc), 4.71 (td, $J$ = 7.2, 1.7 Hz, 1 H, $CH_2$-allyl *trans*-P), 5.57 (ddd, $J$ = 18.9, 13.9, and 7.6 Hz, 1H, CH-allyl), 6.34 (t, $^3J_{HH}$ = 5.4 Hz, 1 H, $CH_2NH$), 6.96 (m, 1 H, NPh), 7.24–7.29 (m, 2 H, NHPh), 7.35–7.55 (m, 10 H, $PPh_2$), 7.57–7.61 (m, 2 H, NPh), 8.45 (s, 1 H, NHPh). $^{13}$C{$^1$H} NMR ($CDCl_3$): $\delta$ 38.33 ($CH_2NH$), 61.12 (d, $^2J_{PC}$ = 2 Hz,$CH_2$-allyl *trans*-Cl), 67.80 (CH of fc), 67.91 (CH of fc), 69.08 (CH of fc), 69.22 (CH of fc), 71.92 (d, $J_{PC}$ = 7 Hz, CH of fc), 72.18 (d, $J_{PC}$ = 7 Hz, CH of fc), 73.45 (d, $^1J_{PC}$ = 48 Hz, C-P of fc), 74.38 (d, $J_{PC}$ = 11 Hz, CH of fc), 74.78 (d, $J_{PC}$ = 13 Hz, CH of fc), 81.16 (d, $^2J_{PC}$ = 31 Hz, $CH_2$-allyl *trans*-*P*), 89.49 (*C*-$CH_2$ of fc), 118.34 (CH-allyl *meso*; partly overlapped), 118.38 (CH of NHPh), 121.68 ($CH^{para}$ of NHPh), 128.36 (d, $J_{PC}$ = 10 Hz, CH of $PPh_2$), 128.80 (CH of NHPh), 130.32 (d, $^4J_{PC}$ = 2 Hz, $CH^{para}$ of $PPh_2$), 132.94 (d, $J_{PC}$ = 11 Hz, CH of $PPh_2$), 134.54 (dd, $J$ = 45 Hz, 3 Hz, $C^{ipso}$ of $PPh_2$), 140.23 ($C^{ipso}$ of NHPh), 155.95 (C═O). $^{31}$P{$^1$H} NMR ($CDCl_3$): $\delta$ 16.4 (s). IR (Nujol, cm$^{-1}$): $\nu_{max}$ 3359 w, 3317 w, 3269 w, 3088 w, 3071 w, 1688 s, 1595 m, 1544 s, 1310 m, 1269 w, 1233 m, 1167 w, 1097 w, 1054 w, 1024 w, 846 w, 824 w, 758 m, 744 m, 696 m, 626 w, 614 w, 517 m, 503 w, 495 m, 462 w, 444 m. ESI+ MS: $m/z$ 665 ([M − Cl]$^+$). Anal. Calcd for $C_{33}H_{32}ClFeN_2OPPd$·0.1$CH_2Cl_2$ (709.8): C 56.01, H 4.57, N 3.95. Found: C 55.99, H 4.41, N 3.88.

*Pd-Catalyzed Cyanation of Aryl Bromides. General Procedure.* A dry Schlenk tube was charged with the respective ligand (0.02 mmol) and palladium complex (0.01 mmol). These solid educts were dissolved in dichloromethane (2 mL), and the resulting solution was stirred for 5 min before being evaporated under vacuum. Aryl bromide (**8**, 1.0 mmol), $K_4[Fe(CN)_6]\cdot 3H_2O$ (212 mg, 0.50 mmol), and anhydrous sodium carbonate (106 mg, 1.0 mmol) were introduced successively, and the reaction vessel was flushed with argon and sealed with a rubber septum. Dioxane and degassed water (2 mL each) were added, and the Schlenk tube was transferred to an oil bath preheated to 100 °C, in which the reaction mixture was stirred for 3 or 24 h.

Next, the reaction mixture was cooled to room temperature and diluted with ethyl acetate and water (5 mL each). The organic layer was separated, and the aqueous residue was extracted with ethyl acetate (3× 5 mL). The organic layers were combined, washed with brine, dried over anhydrous magnesium sulfate, and evaporated to afford crude products, which were analyzed by NMR spectroscopy. Pure products were isolated by column chromatography over silica gel using ethyl acetate–hexane mixtures as the eluents (see the Supporting Information). Details regarding the screening experiments are presented in the text and tables above. Mesitylene (1.0 mmol) was added to the reaction mixture as an internal standard for $^1$H NMR analysis after the aqueous workup.

**X-ray Crystallography.** Diffraction data ($\pm h$ $\pm k$ $\pm l$, $\theta_{max}$ = 26.0–27.5°, completeness ≥99.5%) were collected at 150(2) K with a Nonius Kappa CCD diffractometer equipped with an Apex II image plate detector and Cryostream Cooler (Oxford Cryosystems) using graphite-monochromatized Mo K$\alpha$ radiation ($\lambda$ = 0.710 73 Å). The data were processed and corrected for absorption by methods included in the diffractometer software. Parameters of the data collection, structure solution, and refinement are available in the Supporting Information (Table S1).

The structures were solved by direct methods (SHELXS97[39]) and refined by full-matrix least-squares routines based on $F^2$ (SHELXL97[39]). Unless specified otherwise, the non-hydrogen atoms were refined with anisotropic displacement parameters. The urea and amide hydrogen atoms (NH) were typically located on the difference electron density maps and refined as riding atoms with $U_{iso}$(H) = 1.2$U_{eq}$(N). Hydrogens residing on the carbon atoms as well as the $NH_3$ protons in the structure of **3**·HCl were included in their calculated positions and refined similarly with $U_{iso}$(H) set to 1.5$U_{eq}$(C) for the methyl groups and to 1.2$U_{eq}$(C) for all other $CH_n$ moieties and the $NH_3$ hydrogens. Further details regarding the structure refinement are as follows.

The terminal phenyl group in the structure of **7**·2$CHCl_3$ is disordered and was modeled over two positions. Carbon atoms in the less abundant component (20%) were refined isotropically, and the hydrogen residing at the nitrogen N2 was placed into its calculated position. Furthermore, the solvent molecules in the structure of **7**·2$CHCl_3$ were heavily disordered in structure voids and were thus modeled by PLATON/SQUEEZE.[40] Finally, the $\eta^3$-allyl moiety in the


DOI: 10.1021/acs.organomet.5b00197
*Organometallics* 2015, 34, 1942–1956

crystal structure of **8** was disordered over two positions related approximately by rotation along the axis connecting the center of gravity of the allyl moiety and the Pd center, similarly to other [PdCl($\eta^3$-$C_3H_5$)(L)]) complexes with **D**-type ligands (see Scheme 1).[10] The refined occupancies of the contributing orientations were ca. 60:40.

All geometric calculations were carried out, and the diagrams were obtained with the recent version of the PLATON program.[41] The numerical values were rounded with respect to their estimated deviations (ESDs) given to one decimal place. Parameters pertaining to atoms in constrained positions (mostly hydrogens) are presented without ESDs.

## ■ ASSOCIATED CONTENT

### Supporting Information

Supporting Information for this article comprises additional structural drawings and description of the crystal structure of **11j** and **11k**, a tabular summary of relevant crystallographic data (Table S1), characterization data for the catalytic products (**10**, **11**, and **12**), and copies of the NMR spectra for the newly prepared compounds. The Supporting Information is available free of charge on the ACS Publications website at DOI: 10.1021/acs.organomet.5b00197.

## ■ AUTHOR INFORMATION

### Corresponding Author

*E-mail: stepnic@natur.cuni.cz.

### Notes

The authors declare no competing financial interest.

## ■ ACKNOWLEDGMENTS

The results reported in this paper were obtained with financial support from the Czech Science Foundation (project no. 13-08890S) and the Grant Agency of Charles University in Prague (project no. 108213). This article is dedicated to Professor Tamotsu Takahashi in honor of his 60th birthday.

## ■ REFERENCES

(1) (a) Herrmann, W. A.; Kohlpaintner, C. W. *Angew. Chem., Int. Ed. Engl.* **1993**, *32*, 1524−1544. (b) Joó, F. *Aqueous Organometallic Catalysis*; Kluwer: Dordrecht, 2001. (c) Pinault, N.; Bruce, D. W. *Coord. Chem. Rev.* **2003**, *241*, 1−25. (d) *Aqueous-Phase Organometallic Catalysis*, 2nd ed.; Herrmann, W. A., Cornils, B., Eds.; Wiley-VCH: Weinheim, 2004. (e) Shaughnessy, K. H. *Chem. Rev.* **2009**, *109*, 643−710.

(2) (a) Duckmanton, P. A.; Blake, A. J.; Love, J. B. *Inorg. Chem.* **2005**, *44*, 7708−7710. (b) Knight, L. K.; Freixa, Z.; van Leeuwen, P. W. N. M.; Reek, J. N. H. *Organometallics* **2006**, *25*, 954−960. (c) Meeuwissen, J.; Detz, R. J.; Sandee, A. J.; de Bruin, B.; Reek, J. N. H. *Dalton Trans.* **2010**, *39*, 1929−1931. (d) Meeuwissen, J.; Detz, R.; Sandee, A. J.; de Bruin, B.; Siegler, M. A.; Spek, A. L.; Reek, J. N. H. *Eur. J. Inorg. Chem.* **2010**, 2992−2997.

(3) (a) *Ferrocenes: Ligands, Materials and Biomolecules*, Štěpnička, P., Ed.; Wiley & Sons: Chichester, 2008, Part I − Ligands, pp 1−277. (b) Štěpnička, P. In *The Chemistry of Organoiron Compounds*; Marek, I., Rappoport, Z., Eds.; Wiley & Sons: Chichester, 2013; Chapter 4, pp 103−154. (c) Atkinson, R. C. J.; Gibson, V. C.; Long, N. J. *Chem. Soc. Rev.* **2004**, *33*, 313−328. (d) Gómez Arrayás, R.; Adrio, J.; Carretero, J. C. *Angew. Chem., Int. Ed.* **2006**, *45*, 7674−7715.

(4) Representative examples: (a) Pugin, B.; Landert, H.; Spindler, F.; Blaser, H.-U. *Adv. Synth. Catal.* **2002**, *344*, 974−979. (b) Cvengroš, J.; Toma, Š.; Žemberyová, M.; Macquarrie, D. J. *Molecules* **2005**, *10*, 679−692. (c) Pugin, B.; Landert, H. (Novartis AG, Switzerland). Functionalized ferrocenyldiphosphines, a process for their preparation and their use. International Patent WO 9801457, 1998. (d) Pugin, B. (Solvias AG, Switzerland). Diphosphine ligands for metal complexes. International Patent WO 2001004131, 2001.

(5) Selected recent examples: (a) Simenel, A. A.; Morozova, E. A.; Snegur, L. V.; Zykova, S. I.; Kachala, V. V.; Ostrovskaya, L. A.; Bluchterova, N. V.; Fomina, M. M. *Appl. Organomet. Chem.* **2009**, *23*, 219−224. (b) Lapić, J.; Pavlović, G.; Siebler, D.; Heinze, K.; Rapić, V. *Organometallics* **2008**, *27*, 726−735. (c) Károlyi, B. I.; Bősze, S.; Orbán, E.; Sohár, P.; Drahos, L.; Gál, E.; Csámpai, A. *Molecules* **2012**, *17*, 2316−2329.

(6) Hayashi, T.; Mise, T.; Fukushima, M.; Kagotani, M.; Nagashima, N.; Hamada, Y.; Matsumoto, A.; Kawakami, S.; Konishi, M.; Yamamoto, K.; Kumada, M. *Bull. Chem. Soc. Jpn.* **1980**, *53*, 1138−1151.

(7) (a) Zhao, Q.; Li, S.; Huang, K.; Wang, R.; Zhang, X. *Org. Lett.* **2013**, *15*, 4014−4017. (b) Zhao, Q.; Wen, J.; Tan, R.; Huang, T.; Metola, P.; Wang, R.; Anslyn, E. V.; Zhang, X. *Angew. Chem., Int. Ed.* **2014**, *53*, 8467−8470.

(8) For structurally related, planar-chiral tertiary urea derivatives, see: Metallinos, C.; John, J.; Zaifman, J.; Emberson, K. *Adv. Synth. Catal.* **2012**, *354*, 602−606.

(9) Štěpnička, P. *Chem. Soc. Rev.* **2012**, *41*, 4273−4305.

(10) Solařová, H.; Císařová, I.; Štěpnička, P. *Organometallics* **2014**, *33*, 4131−4147.

(11) Selected reviews: (a) Beer, P. D.; Bayly, S. *Top. Curr. Chem.* **2005**, *255*, 125−162. (b) Bayly, S.; Beer, P. D.; Chen, G. Z. In *Ferrocenes: Ligands, Materials and Biomolecules*; Štěpnička, P., Ed.; Wiley & Sons: Chichester, 2008; Part II − Materials, Molecular Devices and Biomolecules, Chapter 8, pp 281−318. (c) Evans, N. H.; Beer, P. D. *Angew. Chem., Int. Ed.* **2014**, *53*, 11716−11754. Further recent examples: (d) Willener, Y.; Joly, K. M.; Moody, C. J.; Tucker, J. H. R. *J. Org. Chem.* **2008**, *73*, 1225−1233. (e) Cormode, D. P.; Evans, A. J.; Davis, J. J.; Beer, P. D. *Dalton Trans.* **2010**, 6532−6541. (f) Evans, N. H.; Serpell, C. J.; Christensen, K. E.; Beer, P. D. *Eur. J. Inorg. Chem.* **2012**, 939−944 and references therein. (g) Huang, X.; Wu, B.; Jia, C.; Hay, B. P.; Li, M.; Yang, X.-J. *Chem.—Eur. J.* **2013**, *19*, 9034−9041 and references therein.

(12) (a) Braunstein, P.; Naud, F. *Angew. Chem., Int. Ed.* **2001**, *40*, 680−399. (b) Slone, C. S.; Weinberger, D. A.; Mirkin, C. A. *Prog. Inorg. Chem.* **1999**, *48*, 233−350. (c) Bader, A.; Lindner, E. *Coord. Chem. Rev.* **1991**, *108*, 27−110.

(13) For examples of ferrocene phosphines bearing an additional $CH_2FG$ moiety (FG = donor functional group) in the position 1′, see: (a) Widhalm, M.; Nettekoven, U.; Mereiter, K. *Tetrahedron: Asymmetry* **1999**, *10*, 4369−4391. (b) Labande, A.; Daran, J.-C.; Manoury, E.; Poli, R. *Eur. J. Inorg. Chem.* **2007**, 1205−1209. (c) Gülcemal, S.; Labande, A.; Daran, J.-C.; Çetinkaya, B.; Poli, R. *Eur. J. Inorg. Chem.* **2009**, 1806−1815. (d) Štěpnička, P.; Schulz, J.; Klemann, T.; Siemeling, U.; Císařová, I. *Organometallics* **2010**, *29*, 3187. (e) Siemeling, U.; Klemann, T.; Bruhn, C.; Schulz, J.; Štěpnička, P. *Dalton Trans.* **2011**, *40*, 4722−4740. (f) Štěpnička, P.; Zábranský, M.; Císařová, I. *ChemistryOpen* **2012**, *1*, 71−79. (g) Štěpnička, P.; Císařová, I. *J. Organomet. Chem.* **2012**, *716*, 110−119. (h) Štěpnička, P.; Císařová, I. *Dalton Trans.* **2013**, *42*, 3373−3389. (i) Debono, N.; Daran, J.-C.; Poli, R.; Labande, A. *Polyhedron* **2015**, *86*, 57−63.

(14) Škoch, K.; Císařová, I.; Štěpnička, P. *Inorg. Chem.* **2014**, *53*, 568−577.

(15) Štěpnička, P.; Baše, T. *Inorg. Chem. Commun.* **2001**, *4*, 682−687.

(16) Transformation of primary amines to monosubstituted ureas are typically achieved through the action of alkali metal cyanate/acid mixtures.

(17) Xu, D.; Ciszewski, L.; Li, T.; Repič, O.; Blacklock, T. J. *Tetrahedron Lett.* **1998**, *39*, 1107−1110.

(18) (a) Henderson, W.; Oliver, A. G. *Polyhedron* **1996**, *15*, 1165−1173. (b) Nekrasov, Yu. S.; Skazov, R. S.; Simenel, A. A.; Snegur, L. V.; Kachala, I. V. *Russ. Chem. Bull.* **2006**, *55*, 1368−1371.

(19) See, for instance, the structure of (diphenylphosphino) ferrocene: Adeleke, J. B.; Liu, L.-K. *Acta Crystallogr., Sect. C: Cryst. Struct. Commun.* **1993**, *49*, 680−682.



DOI: 10.1021/acs.organomet.5b00197
*Organometallics* 2015, 34, 1942−1956

(20) Allen, F. H.; Kennard, O.; Watson, D. G.; Brammer, L.; Orpen, A. G.; Taylor, R. *J. Chem. Soc., Perkin Trans. 2* **1987**, S1−S19.
(21) Gan, K.-S.; Hor, T. S. A. In *Ferrocenes: Homogeneous Catalysis, Organic Synthesis, Materials Science*; Togni, A., Hayashi, T., Eds.; VCH: Weinheim, 1995; Chapter 1, Section 1.3, pp 18−35.
(22) The formed chains are built up from molecules related by the crystallographic *a* glide planes and, therefore, propagate in a direction parallel to the *a*-axis.
(23) (a) Etter, M. C. *Acc. Chem. Res.* **1990**, *23*, 120−126. (b) Custelcean, R. *Chem. Commun.* **2008**, 295−307.
(24) Štěpnička, P.; Císařová, I. *New J. Chem.* **2002**, *26*, 1389−1396.
(25) Evans, A. J.; Matthews, S. E.; Cowley, A. R.; Beer, P. D. *Dalton Trans.* **2003**, 4644−4650. Geometric parameters were calculated from the data deposited in the Cambridge Structural Database (refcode: EQOHIB).
(26) Etter, M. C.; MacDonald, J. C.; Bernstein, J. *Acta Crystallogr., Sect. B: Struct. Sci.* **1990**, *46*, 256−262.
(27) Štěpnička, P.; Císařová, I.; Gyepes, R. *Eur. J. Inorg. Chem.* **2006**, 926−938. See also ref 13h.
(28) (a) Teo, S.; Weng, Z.; Hor, T. S. A. *Organometallics* **2006**, *25*, 1199−1205. (b) Štěpnička, P.; Podlaha, J.; Gyepes, R.; Polášek, M. *J. Organomet. Chem.* **1998**, *552*, 293−301. See also ref 13h.
(29) For selected examples of complexes of the type $[PdCl(C_6H_4CH_2NMe_2\text{-}\kappa^2C^1,P)(Ph_2PfcX\text{-}\kappa P)]$ and related compounds, see: (a) Ma, J.-F.; Yamamoto, Y. *Inorg. Chim. Acta* **2000**, *299*, 164−171. (b) Štěpnička, P.; Císařová, I. *Organometallics* **2003**, *22*, 1728−1740. (c) Štěpnička, P.; Císařová, I. *Collect. Czech. Chem. Commun.* **2006**, *71*, 215−236. (d) Štěpnička, P.; Císařová, I. *Inorg. Chem.* **2006**, *45*, 8785−8789. (e) Tauchman, J.; Císařová, I.; Štepnička, P. *Organometallics* **2009**, *28*, 3288−3302. (f) Štěpnička, P.; Solařová, H.; Lamač, M.; Císařová, I. *J. Organomet. Chem.* **2010**, *695*, 2423−2431. (g) Štěpnička, P.; Solařová, H.; Císařová, I. *J. Organomet. Chem.* **2011**, *696*, 3727−3740. See also refs 10 and 13d.
(30) (a) Appleton, T. G.; Clark, H. C.; Manzer, L. E. *Coord. Chem. Rev.* **1973**, *10*, 335−422. (b) Hartley, F. R. *The Chemistry of Platinum and Palladium*; Applied Science: London, 1973; Chapter 11, p 299.
(31) (a) Štěpnička, P.; Císařová, I. *Collect. Czech. Chem. Commun.* **2006**, *71*, 279−293. (b) Tauchman, J.; Císařová, I.; Štěpnička, P. *Dalton Trans.* **2011**, *40*, 11748−11757.
(32) (a) Sundermeier, M.; Zapf, A.; Beller, M. *Eur. J. Inorg. Chem.* **2003**, 3513−3526. (b) Anbarasan, P.; Schareina, T.; Beller, M. *Chem. Soc. Rev.* **2011**, *40*, 5049−5067.
(33) (a) Schareina, T.; Zapf, A.; Beller, M. *Chem. Commun.* **2004**, 1388−1389. (b) Schareina, T.; Zapf, A.; Beller, M. *J. Organomet. Chem.* **2004**, *689*, 4576−4583.
(34) Butler, R. N.; Coyne, A. G. *Chem. Rev.* **2010**, *110*, 6302−6337.
(35) Schulz, J.; Císařová, I.; Štěpnička, P. *Organometallics* **2012**, *31*, 729−738.
(36) Electron-withdrawing substituents aid the base-induced hydrolysis of the nitriles via decreasing the electron density at the cyano group, thereby facilitating the attack of $OH^-$ on the cyanide carbon. In a model experiment, equimolar amounts of nitrile **9g** and $Na_2CO_3$ (1 mmol each) were allowed to react in dioxane−water (4 mL of 1:1 mixture) at 100 °C overnight, affording amide **10g** in virtually quantitative yield.
(37) Drew, D.; Doyle, J. R. *Inorg. Synth.* **1972**, *13*, 47−55.
(38) Cope, A. C.; Friedrich, E. C. *J. Am. Chem. Soc.* **1968**, *90*, 909−913.
(39) Sheldrick, G. M. *Acta Crystallogr., Sect. A: Found. Crystallogr.* **2008**, *64*, 112−122.
(40) van der Sluis, P.; Spek, A. L. *Acta Crystallogr., Sect. A: Found. Crystallogr.* **1990**, *46*, 194−201.
(41) Spek, A. L. *J. Appl. Crystallogr.* **2003**, *36*, 7−13.



DOI: 10.1021/acs.organomet.5b00197
*Organometallics* 2015, 34, 1942−1956

# Appendix 2

Karel Škoch, Ivana Císařová, Petr Štěpnička: "1′-(Diphenylphosphino)-1-cyanoferrocene: A Simple Ligand with Complicated Coordination Behavior toward Copper(I)". *Inorg. Chem.* **2014**, *53*, 568.

Inorganic Chemistry

Article

pubs.acs.org/IC

# 1′-(Diphenylphosphino)-1-cyanoferrocene: A Simple Ligand with Complicated Coordination Behavior toward Copper(I)

Karel Škoch, Ivana Císařová, and Petr Štěpnička*

Department of Inorganic Chemistry, Faculty of Science, Charles University in Prague, Hlavova 2030, 12840 Prague 2, Czech Republic

Supporting Information

**ABSTRACT:** 1′-(Diphenylphosphino)-1-cyanoferrocene (**3**), a new donor-asymmetric ferrocene ligand obtained in two steps from 1′-(diphenylphosphino)ferrocene-1-carboxaldehyde, reacts with CuCl at a Cu/**3** molar ratio of 1:1 to give the heterocubane complex $[Cu(\mu_3\text{-}Cl)(\mathbf{3}\text{-}\kappa P)]_4$ (**4**). When the Cu/**3** ratio is changed to 1:2 or 1:3, the reaction takes a different course, producing the P,N-bridged dimer $[CuCl(\mathbf{3}\text{-}\kappa P)(\mu(P,N)\text{-}\mathbf{3})]_2$ (**5**) after crystallization. Notably, CuBr and CuI behave differently, affording the corresponding 2D coordination polymers $[CuX(\mu(P,N)\text{-}\mathbf{3})]_n$ [X = I (**7**), and Br (**8**)], regardless of the Cu/**3** ratio. Reaction of **3** with sources of naked $Cu^+$, such as $[Cu(MeCN)_4]^+$ salts or their synthetic equivalents, provides the 1D coordination polymer $[Cu(MeCN\text{-}\kappa N)(\mu(P,N)\text{-}\mathbf{3})][BF_4]$ (**9**) or salts of a quadruply bridged dicopper(I) cation, $[Cu_2(\mu(P,N)\text{-}\mathbf{3})_4]X_2$ ($[\mathbf{10}]X_2$), depending on the Cu/**3** molar ratio (1:1 vs 1:2 and 1:3). Except for **4**, in which **3** binds as a simple P-monodentate ligand, the complexes reported here represent the first structurally characterized compounds in which a phosphinonitrile ligand coordinates through both of its soft donor moieties, thereby extending the coordination chemistry of these ligands.

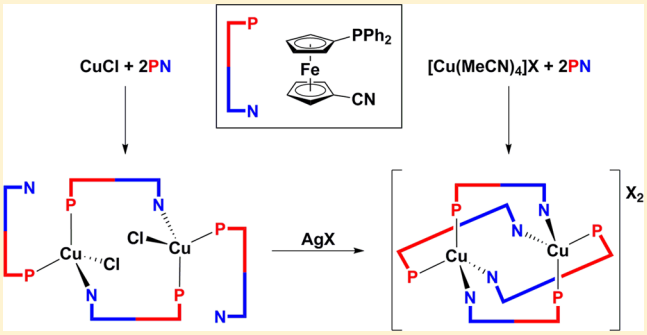


## INTRODUCTION

In the vast majority of coordination compounds containing simple (organic) phosphinonitrile donors, such as $Ph_2PCH_2CN$,[1] $(Ph_2P)_2CHCN$,[2] $Ph_2PCH(CN)_2$,[3] $Ph_{3-n}P(CH_2CH_2CN)_n$ ($n$ = 1−3),[4,5] 2- and 4-$Ph_2PC_6H_4CN$,[6−8] and similar compounds,[9] in their native (neutral) form,[10] these compounds coordinate as simple P-donors, with their cyano groups acting as auxiliary substituents. Compounds in which *both* functional groups are coordinated to a metal center remain extremely rare and have not been definitively confirmed using methods of direct structural analysis.[1b,11]

Given the numerous reports dealing with the multifaceted coordination chemistry of 1′-functionalized ferrocene phosphines,[12,13] we decided to prepare and study the new ferrocene-based mixed-donor ligand **3**, which combines the soft cyano and phosphine donor groups and formally represents a congener of the ubiquitous 1,1′-bis(diphenylphosphino)-ferrocene (dppf).[14] Compounds of this type are not entirely unprecedented, even among ferrocene derivatives, being represented by 1-(diphenylphosphino)-2-(cyanomethyl)-ferrocene[15] and its C$\alpha$-substituted derivatives,[16] 1-(diphenylphosphino)-2-cyano-3-ethylferrocene,[17] and 2-cyano-1-phosphaferrocene.[18] However, only the last of these compounds has been studied as a ligand in transition-metal complexes, coordinating as a P-monodentate donor.[18]

In this contribution, we report the synthesis and structural characterization of 1′-(diphenylphosphino)-1-cyanoferrocene (**3**) as a new ferrocene-based donor-asymmetric ligand and the copper(I) complexes resulting from its reactions with Cu(I) halides and $[Cu(MeCN)_4]^+$ salts or their synthetic equivalents. Because the stoichiometries of copper(I) complexes usually "give little clue to their structures, which can be very complicated",[19] we have focused mainly on the structural characterization of the prepared complexes and have thus identified both conventional and novel compound types.

## RESULTS AND DISCUSSION

**Synthesis of the Phosphinonitrile Ligand.** 1′-(Diphenylphosphino)-1-cyanoferrocene (**3**) was prepared in a standard manner starting from phosphinoaldehyde **1**[20] (Scheme 1). In the first step, the aldehyde was converted into the corresponding oxime **2** by reaction with hydroxylamine in methanol.[21] The oxime was subsequently dehydrated with

**Scheme 1. Preparation of Phosphinonitrile 3**[a]

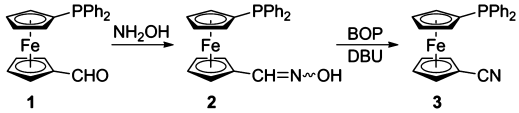


[a]BOP = (benzotriazol-1-yloxy)tris(dimethylamino)phosphonium hexafluorophosphate, DBU = 1,8-diazabicyclo[5.4.0]undec-7-ene.

**Received:** October 25, 2013
**Published:** December 17, 2013

   dx.doi.org/10.1021/ic4026848 | *Inorg. Chem.* 2014, 53, 568−577

BOP/DBU[22] to afford nitrile **3** as an orange, air-stable solid in a good overall yield (73% from **1**).[23]

The $^{1}H$ and $^{13}C$ NMR spectra of **2** and **3** show four signals typical for asymmetrically 1,1′-disubstituted ferrocene units and a characteristic multiplet of the $PPh_2$ substituents. The spectra of **2** also display additional signals of two nonequivalent CH═NOH moieties attributable to the (*E*) and (*Z*) double-bond isomers in a ca. 1:2 ratio. The $^{31}P$ NMR resonances of **2** and **3** are observed at approximately $\delta_P$ −17, close to that of the starting aldehyde.[20] In addition, compound **3** shows a characteristic C≡N stretching band at 2225 $cm^{-1}$ in its IR spectrum, well within the range typical for conjugated nitriles.[24] A cyclic voltammetry study (Figure 1) showed that nitrile **3** becomes oxidized in a single irreversible step at $E_{pa} \approx 0.48$ V[25] versus the ferrocene/ferrocenium reference. This primary, presumably iron-centered ($Fe^{II}/Fe^{III}$) oxidation shows signs of electrochemical reversibility at higher scan rates and is associated with another irreversible oxidation at more positive potentials, which was tentatively attributed to a redox response of a decomposition product (EC mechanism, Figure 1).[26]

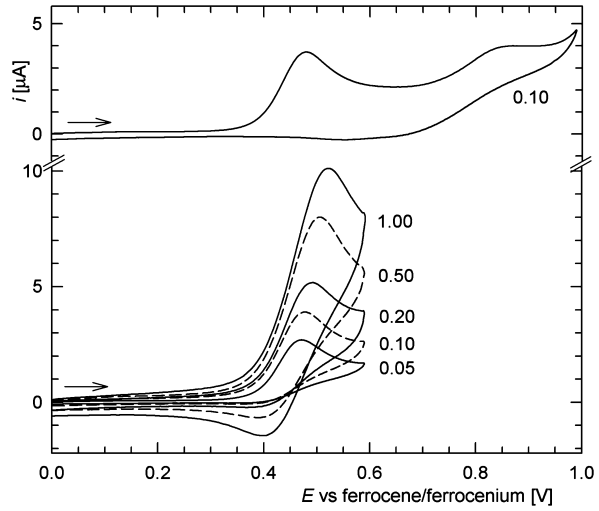


**Figure 1.** Cyclic voltammograms of **3**, as recorded on a Pt disk electrode in 1,2-dichloroethane ($c$ = 0.5 mM). The scan direction (arrow) and scan rates (in V $s^{-1}$) are indicated in the figure.

The solid-state structures of compounds **2** and **3** and the corresponding phosphine oxide **3O**[27] were determined by X-ray diffraction analysis (Figure 2). The CH═NOH moiety in the structure of **2** was found to be disordered over the two positions corresponding to the (*E*) and (*Z*) isomers [the refined (*E*)/(*Z*) ratio was ca. 34:66], which corresponds with the solution observations. The individual conformers assemble through O−H···N hydrogen bonds, forming dimers around the crystallographic inversion centers (see the Supporting Information, Figure S1). A similar mode of assembly was observed with FcCH═NOH[28] (Fc = ferrocenyl). Notably, compounds **3** and **3O** are practically isostructural. From a formal viewpoint, they differ only in the occupancy of one of the four compartments within the tetrahedron around the phosphorus atom (oxygen vs lone electron pair[29]), which has a rather minor impact on the overall molecular structure. Oxidation of the phosphorus atom results in shortening of the P−C bonds by ca. 0.03 Å, presumably due to an electron density transfer from the aromatic rings toward the electron-withdrawing phosphoryl moiety.[30] The C−P−C angles in **3O** are increased (by ca. 4°) by the higher steric demands of the fourth substituent (oxygen) at the phosphorus atom.

The molecular parameters of **2**, **3**, and **3O** presented in Table 1 are generally comparable with the corresponding data reported for simple ferrocene derivatives such as fc(CH═NOH)$_2$[31] (fc = ferrocene-1,1′-diyl; note that oxime FcCH═NOH is heavily disordered[28]), FcCN,[32] and $FcPPh_2$.[33] The ferrocene moieties exhibit balanced Fe−C distances and, consequently, practically negligible tilting. The cyclopentadienyl rings in **3** and **3O** are eclipsed, and their substituents assume a synclinal orientation (see $\tau$ angle in Table 1). In contrast, the substituents in **2** adopt an anti configuration, halfway between the eclipsed anticlinal ($\tau$ = 144°) and the staggered antiperiplanar ($\tau$ = 180°) conformations.

**Preparation of Complexes from Copper(I) Halides.** The copper(I) ion is a typical soft acid according to Pearson's hard and soft acids and bases concept.[34] Nevertheless, its character can be partly influenced by the attached donors (e.g., halides),[35] and a previous study on Cu(I)/dppf/$dppfO_2$ complexes ($dppfO_2$ = 1,1′-bis(diphenylphosphinoyl)ferrocene)

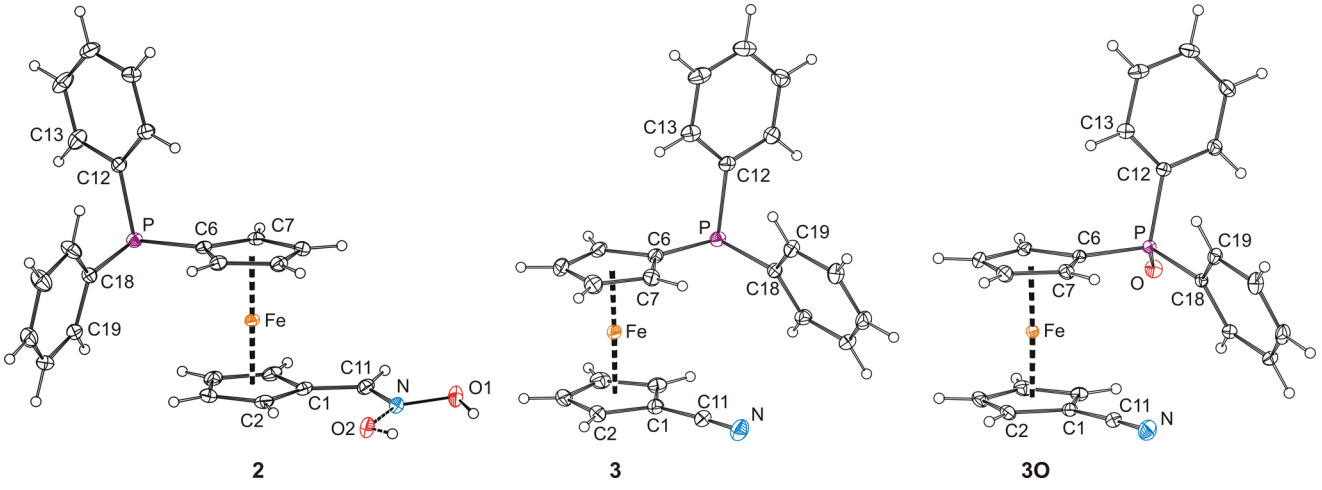


**Figure 2.** PLATON plots of the molecular structures of **2**, **3**, and **3O** showing the atom labeling scheme and the displacement ellipsoids at the 30% probability level. For oxime **2**, both orientations of the disordered OH group are shown.


dx.doi.org/10.1021/ic4026848 | Inorg. Chem. 2014, 53, 568−577

**Table 1. Selected Distances (Å) and Angles (deg) for Compounds 2, 3, and 3O**

| parameter[a] | 2[b] | 3 | 3O[c] |
|---|---|---|---|
| Fe−C (range) | 2.034(1)−2.057(1) | 2.024(2)−2.057(2) | 2.025(1)−2.062(1) |
| Fe−Cg1 | 1.6507(6) | 1.6456(8) | 1.6469(6) |
| Fe−Cg2 | 1.6531(6) | 1.6457(8) | 1.6422(6) |
| ∠Cp1, Cp2 | 1.08(8) | 0.9(1) | 0.38(8) |
| $\tau$ | 162.13(9) | 69.8(1) | 69.0(1) |
| C1−C11 | 1.452(2) | 1.430(2) | 1.430(2) |
| C11−N | 1.273(2) | 1.144(2) | 1.143(2) |
| C1−C11−N | 125.4(1) | 177.3(2) | 177.5(2) |
| P−C6 | 1.817(1) | 1.813(2) | 1.786(1) |
| P−C12 | 1.835(1) | 1.842(2) | 1.809(1) |
| P−C18 | 1.836(1) | 1.836(2) | 1.806(1) |

[a]Ring planes are defined as follows: Cp1 = C(1−5), C2 = C(6−10). Cg1 and Cg2 are the respective ring centroids. Parameter $\tau$ stands for the torsion angle C1−Cg1−Cg2−C6. [b]Further data: N−O1 = 1.424(2) Å, N−O2 = 1.436(3) Å. [c]Further data: P−O = 1.487(1) Å.

have suggested some borderline character for this metal ion.[36] Considering the nature of the donor groups available in **3** and the coordination variability of Cu(I)-complexes,[37] we decided to study the interactions of the newly prepared ligand **3** with Cu(I) by probing its reactivity toward copper(I) halides and precursors of the free $Cu^+$ ion.

Addition of ligand **3** (1, 2, or 3 molar equiv) to a suspension of CuCl in $CDCl_3$ led to complete dissolution of the solid copper(I) salt within hours. NMR analysis of the resulting solutions revealed that these reactions proceeded cleanly and afforded *three* different products at the three mentioned metal-to-ligand ratios (see the Supporting Information, Figure S2). An ESI mass spectrometric analysis performed in parallel was rather inconclusive. Regardless of the CuCl:**3** molar ratio, the mass spectra showed only fragments attributable to $[Cu_2Cl(\mathbf{3})_2]^+$ (*m*/*z* 951; the heaviest ionic species observed), $[Cu(\mathbf{3})_2]^+$ (*m*/*z* 853), $[Cu_2Cl(\mathbf{3})]^+$ (*m*/*z* 556), and $[Cu(\mathbf{3})]^+$ (*m*/*z* 458). However, the absence of higher molecular weight fragments is likely due to fragmentation during the ionization process and/or disintegration in the highly polar solvent used (methanol).

Subsequent evaporation and crystallization from an ethyl acetate/hexane mixture produced air-stable crystalline solids. The NMR spectra of the crystalline products isolated from the reactions performed at Cu/**3** ratios of 1:1 and 1:2 were identical with those recorded in situ. The compounds were characterized by X-ray diffraction analysis as a heterocubane comprising the ferrocene ligand as a P-monodentate donor, $[(\mu_3\text{-Cl})_4\{Cu(\mathbf{3}\text{-}\kappa P)\}_4]$ (**4**), and the ligand-bridged dimer $[(\mu(P,N)\text{-}\mathbf{3})\{CuCl(\mathbf{3}\text{-}\kappa P)\}]_2$ (**5**), respectively (Scheme 2). In contrast, the crystallization of the product obtained upon addition of 3 molar equiv of **3** to CuCl afforded exclusively the already mentioned dicopper(I) complex **5**. Because complexes of the type $[CuCl(PR_3)_3]$ are relatively common among Cu(I)-phosphine complexes,[38] we assume that the reaction of CuCl with 3 equiv of **3** indeed produced the tris-phosphine complex $[CuCl(\mathbf{3}\text{-}\kappa P)_3]$ (**6**) *in the solution* (perhaps in equilibrium with other species). However, upon crystallization, this species likely dissociated to give the less soluble dimer **5**, which then separated from the reaction mixture in pure crystalline form. The dissociative formation of **5** may be aided by steric destabilization of intermediate **6**, resulting from the presence of the bulky phosphinoferrocene ligand,[39] and the availability of another, much less sterically demanding soft donor group (nitrile).

**Scheme 2. Reactions of 3 with CuCl[a]**

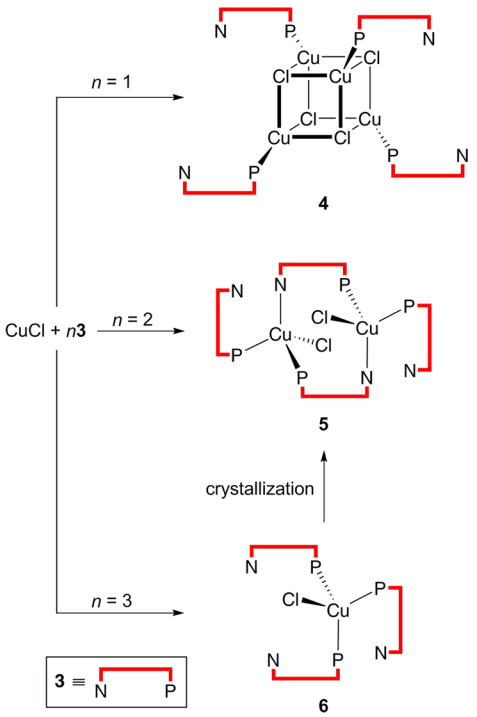


[a]As formulated, compound **6** represents a plausible intermediate that was characterized in solution but could not be isolated as a defined solid substance.

The $^{31}P$ NMR spectra of **4**-**6** showed broad singlets near $\delta_P$ = −13 ppm, suggesting coordination of the phosphine groups in all cases. The compounds were clearly distinguished by their $^1H$ NMR spectra, which showed the signals of the phosphinoferrocene ligand at different positions (Figure S2, Supporting Information). The observation of a single set of resonances in the $^1H$ NMR spectrum of **5** corroborates the fluxional nature of the Cu−**3** complexes. The IR spectra of crystalline complexes **4** and **5** differed mainly in the fingerprint region and provided limited diagnostic information. The spectrum of **5** showed a strong $\nu_{C\equiv N}$ band (2224 $cm^{-1}$) at a position identical to that observed for uncoordinated **3** (2225 $cm^{-1}$), whereas the $\nu_{C\equiv N}$ band in the spectrum of complex **4** (2241 $cm^{-1}$), which contains only uncoordinated C≡N moieties, was shifted to higher energies compared to free **3**.[40]


dx.doi.org/10.1021/ic4026848 | Inorg. Chem. 2014, 53, 568−577

The crystal structures of **4** and **5** are presented in Figures 3 and 4 (for complete views, see the Supporting Information,

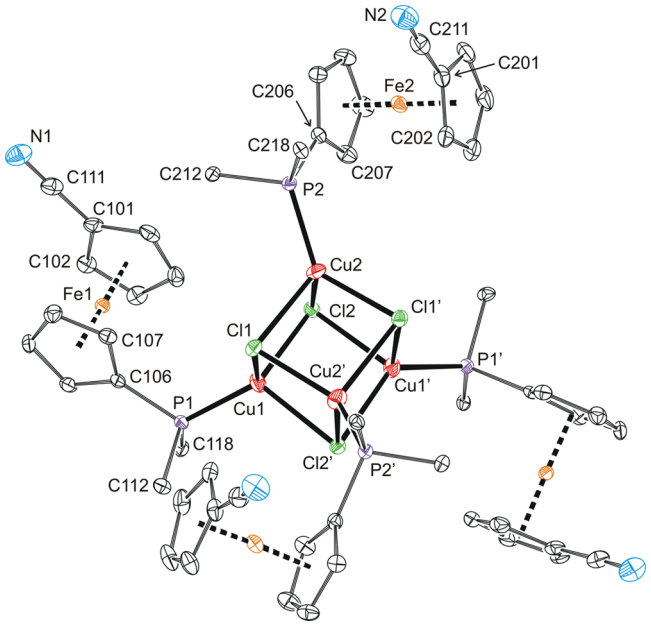


**Figure 3.** PLATON plot of the molecular structure of heterocubane **4** with 50% probability displacement ellipsoids. The phenyl ring carbons, except for those in ipso positions, and all hydrogens were omitted to simplify the figure. Atoms labeled with a prime are generated by the $(-x, y, {}^{3}/_{2} - z)$ symmetry operation. Selected distances (Å) and angles (deg): Cu1−P1 2.1760(8), Cu1−Cl1 2.4431(7), Cu1−Cl2 2.3595(5), Cu1−Cl2′ 2.4558(9), Cu2−P2 2.1856(8), Cu2−Cl1 2.5229(7), Cu2−Cl2 2.4820(7), Cu2−Cl1′ 2.3412(9), Cl1−Cu1−Cl2 99.41(2), Cl1−Cu1−Cl2′ 93.57(3), Cl2−Cu1−Cl2′ 96.36(2), Cl1−Cu2−Cl2 94.10(2), Cl1−Cu2−Cl1′ 93.31(3), Cl2−Cu2−Cl1′ 95.46(3), Cl−Cu−P 115.30(3)−132.26(3).

Figures S3 and S4). As indicated above, complex **4** adopts a typical[37,41] heterocubane structure in which each copper(I)

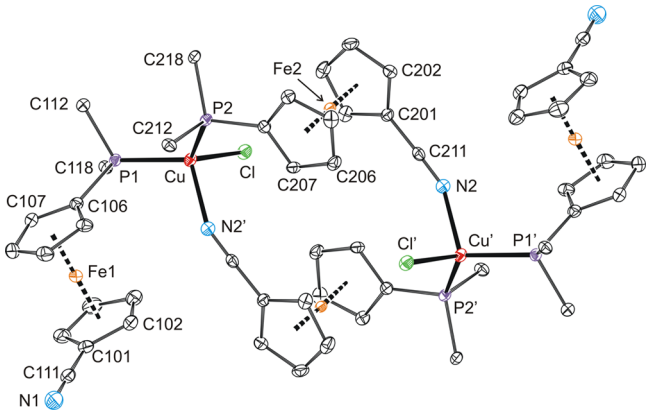


**Figure 4.** PLATON plot of the molecular structure of dimer **5** with 50% probability displacement ellipsoids. For clarity, the phenyl ring carbons, except for the ipso ones, and all hydrogens were omitted. The primed atoms are generated by crystallographic inversion. Selected distances (Å) and angles (deg): Cu−Cl 2.2877(4), Cu−P1 2.2558(5), Cu−P2 2.2673(4), Cu−N2′ 2.111(1), C111−N1 1.145(2), C211−N2 1.148(2), Cl−Cu−P1 113.38(1), Cl−Cu−P2 116.10(1), Cl−Cu−N2′ 98.16(4), P1−Cu−P2 117.62(2), P1−Cu−N2′ 108.16(4), P2−Cu−N2′ 99.97(4).

atom has a distorted $Cl_3P$ tetrahedral coordination environment. The heterocubane unit in **4** has an exact $C_2$ symmetry, residing on the crystallographic symmetry element. The interatomic distances within the $Cu_4Cl_4$ cube in **4** are within the range observed for other $[CuCl(PR_3)]_4$ complexes,[42] while the P−Cu bond lengths compare well with those reported for the $[CuI(L)]_4$ complexes obtained from phosphinoferrocene donors.[43] The faces of the heterocubane moiety (see the Supporting Information, Figure S5) are distorted from the ideal square shape. The intraface Cu···Cu contacts (3.1950(5)-3.3332(5) Å) are shorter than the Cl···Cl distances (3.540(1)-3.6634(8) Å), and the associated Cl−Cu−Cl angles (93.31(3)-99.41(2)°) are less acute that the Cu−Cl−Cu angles (81.89(2)-86.70(3)°). The ferrocene moieties that decorate the cubane unit at its exterior maintain their regular geometry [tilt angles ca. 2°; Fe−Cg 1.648(1)−1.653(2) Å] but assume different conformations ($\tau$ = −162.5(2)° (Fe1) and −66.4(2)° (Fe2)), which direct their arm-like cyano pendants into structural voids and away from the $Cu_4Cl_4$ core.

Complex **5**, obtained at CuCl:**3** ratios of 1:2 and 1:3 (after crystallization), is a dicopper(I) complex in which two phosphinoferrocene ligands coordinate as P-monodentate donors while the other two bridge the Cu(I) centers as P,N donors, thus resulting in identical $CuClP_2N$ centers (Figure 4). The symmetrical nature of the complex species is manifested in the crystal structure, in which the complex molecules reside on the crystallographic inversion centers.

The tetrahedral coordination environment of the Cu(I) ions in **5** is distorted, reflecting the dissimilar steric demands of the donor moieties attached to Cu(I) [cf. the interligand angles ranging from 98.16(4)° (Cl1−Cu−N2′) to 117.62(2)° (P1−Cu−P2)]. With respect to the Cu−donor distances, the coordination can be described as 3 + 1 because the rather similar Cu−Cl and Cu−P bonds are significantly longer that the remaining Cu−N bond (by ca. 0.15−0.18 Å). The ferrocene units are rotated into open intermediate conformations [$\tau$ = 159.0(1)° for Fe1, $\tau$ = −137.7(1)° for Fe2]. The bridging ligand shows a larger tilt and slightly shorter Fe−Cg distances [tilt 3.88(9)°, Fe−Cg 1.6475(7) and 1.6456(7) Å] than the P-coordinated one [tilt 1.8(1)°, Fe−Cg 1.6515(8) and 1.6559(8) Å].

As for the CuCl/**3** system, the NMR spectra of CuX−**3** (X = Br and I) mixtures obtained by mixing the appropriate copper(I) halide with **3** in $CDCl_3$ at metal-to-ligand ratios of 1:1, 1:2, or 1:3 suggested the formation of distinct species in each case. However, the subsequent crystallizations afforded only the insoluble polymeric complexes $[CuX(\mu(P,N)\text{-}\mathbf{3})]_n$ (**7** X = Br, **8** X = I) instead of the heterocubanes analogous to **4**. This confirms the dynamic nature of the $CuX(\mathbf{3})_n$ species in solution, which in turn enables the selective formation (upon crystallization) of the most stable and/or the least soluble product.

The crystal structures of **7** and **8** were determined by X-ray crystallography. In contrast to the other crystal structures reported in this paper, which were determined at 150 K, the diffraction data for **7** were recorded at 250 K because this compound undergoes a phase transition associated with a roughly 3-fold increase in the length of the monoclinic ($b$) axis. Differential scanning calorimetry (DSC) analysis demonstrated that the compound undergoes a reversible second-order phase transition at approximately −12 °C (see the Supporting Information). In addition, while compounds **7** and **8** have


dx.doi.org/10.1021/ic4026848 | Inorg. Chem. 2014, 53, 568−577

very similar structures, they are not isostructural (Figure S6, Supporting Information).[44]

The crystal structure of **8** is depicted in Figure 5, and the data for both polymeric complexes are given in the figure caption.

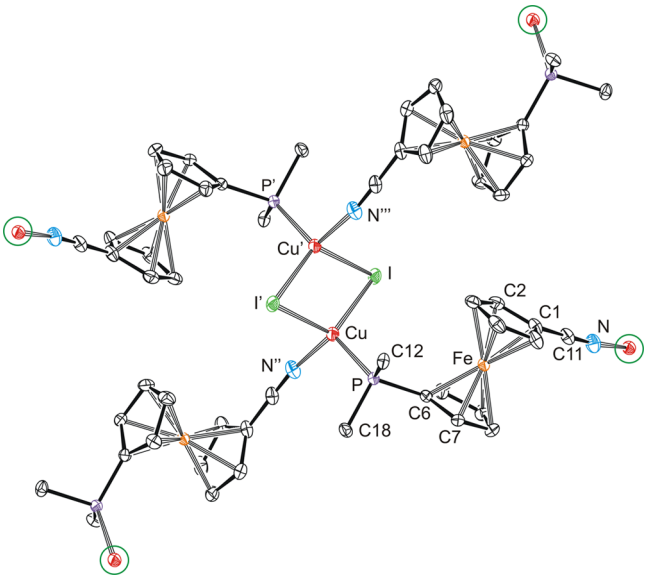


**Figure 5.** Section of the 2D polymeric structure of **8**, showing displacement ellipsoids at the 30% probability level. The circles indicate the atoms through which the propagation of the infinite assembly occurs. Selected distances (Å) and angles (deg) for **7** (X = Br) and [**8** (X = I)]: Cu−X 2.4494(5) [2.6027(3)], Cu−X′ 2.5224(5) [2.6857(3)], Cu−P 2.2169(9) [2.2394(6)], Cu−N″ 2.022(3) [2.016(2)], C11−N 1.137(4) [1.144(3)], X−Cu−X′ 109.96(2) [115.93(1)], X−Cu−P 118.25(2) [115.19(2)], X′−Cu−P 108.50(3) [105.21(2)], X−Cu−N″ 109.06(8) [112.34(6)], X′−Cu−N″ 99.96(8) [97.57(5)], Cu−X−Cu′ 70.04(1) [64.07(1)].

Each copper(I) ion in the structures of **7** and **8** is coordinated by two ligands (one through the phosphorus and one through its CN group), and the resulting $Cu(\mathbf{3})_2$ units are connected into a dimeric unit through asymmetric halide bridges[45] that complete the distorted tetrahedral coordination spheres around the Cu(I) ions. Because each ligand acts as a P,N bridge between two adjacent dicopper(I) units, the dimer units are interlinked into infinite corrugated layers (see the Supporting Information, Figure S7). The donor substituents in bridging **3** are rotated away from each other ($\tau$ = −158.9(2)° for **7** and −157.9(1)° for **8**). Otherwise, the ferrocene units remain regular [**7**: Fe−Cg 1.644(2)/1.647(1) Å; **8**: 1.647(1)/1.6480(9) Å] and display negligible tilting (below 1°).

**Reactions of 3 with Precursors of Bare $Cu^+$.** Similar to the above experiments, reactions were performed at metal-to-ligand ratios of 1:1, 1:2, and 1:3 using $[Cu(MeCN)_4]^+$ salts as the common precursors of Cu(I) ions devoid of any firmly bound supporting ligands. The reaction of $[Cu(MeCN)_4][BF_4]$ with 1 molar equiv of **3** in dichloromethane produced an orange precipitate, which redissolved upon addition of little acetonitrile. Layering with hexane and crystallization by liquid-phase diffusion afforded the *catena*-polymer $[Cu(\mu\text{-}\mathbf{3})(MeCN)]_n[BF_4]_n$ (**9**).

This compound was insoluble in common deuterated, nondonor solvents and could therefore not be analyzed by NMR spectroscopy. Its IR spectrum featured several $\nu_{C\equiv N}$ bands: a strong band at 2249 $cm^{-1}$ and two bands of medium intensity at 2314 and 2283 $cm^{-1}$. The crystal structure of **9** (Figure 6) confirmed the presence of different nitrile groups,

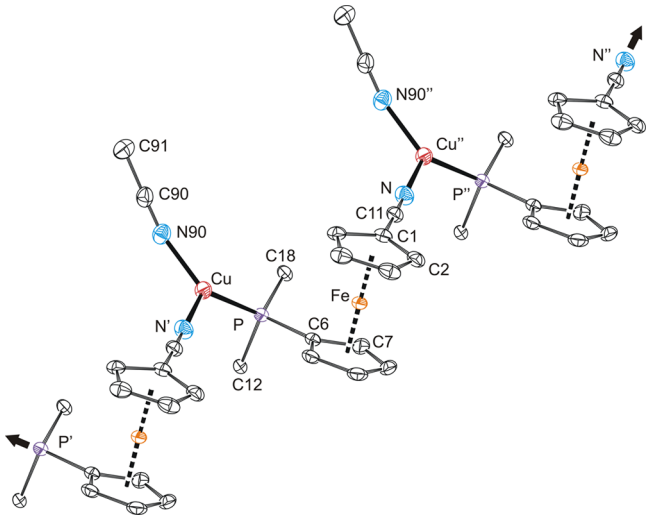


**Figure 6.** Section of the polymeric chain in the structure of **9**, in which the "monomer units" are related by elemental translation along the *a* axis. The counteranions ($BF_4^-$), phenyl ring carbons (except for those in ipso positions), and all hydrogens are omitted for clarity. Displacement ellipsoids are scaled to the 50% probability level. Selected distances (Å) and angles (deg): Cu−P 2.1985(5), Cu−N′ 1.954(2), Cu−N90 1.956(2), C11−N 1.141(3), C90−N90 1.136(3), P−Cu−N′ 120.19(5), P−Cu−N90 128.37(5), N′−Cu−N90 111.22(7).

indicating that **9** is a coordination polymer in which ligand **3** bridges the adjacent Cu(MeCN) units. The copper(I) centers are thus coordinated by two phosphinonitrile ligands and one acetonitrile, constituting an irregular trigonal $N_2P$ donor set. Because the disubstituted ferrocene unit [tilt 4.4(1)°, Fe−Cg 1.6474(9)/1.6398(9) Å] assumes a conformation similar to synclinal eclipsed [$\tau$ = −63.8(1)°, ideal value = 72°], the infinite chains are angular and, therefore, rather contracted (note that, owing to the overall symmetry, the Cu···Cu separation is exactly equal to the length of the crystallographic *a* axis). The $BF_4^-$ ions are located in between the chains and are fixed by the soft F···H−C interactions.[46]

Rather unexpectedly, increasing the Cu/**3** ratio to 1:2 and 1:3[47] in reactions of the phosphinonitrile with $[Cu(MeCN)_4]X$ [X = $BF_4$, $PF_6$, $CF_3SO_3$, or $B(C_6F_5)_4$[48]] resulted in the selective formation of the respective quadruply ligand-bridged dicopper(I) complex salts $\mathbf{10}X_2$ (Scheme 3, route *a*). These complexes, which were accessible equally well by the treatment of CuCl with 2 equiv of **3** and then by a silver(I) salt (i.e., from AgX and **5** formed in situ, Scheme 3, route *b*) or, similarly, by halogen removal from in situ generated **6** (Scheme 3, route *c*), represent an unprecedented structural type among Cu(I) complexes prepared from P,N donors. Previously structurally characterized compounds[49] in which a P,N donor bridges two discrete Cu(I) centers devoid of any supporting halide ligands include only asymmetric, triply bridged complexes of the type $[(MeCN)\text{-}Cu(\mu\text{-}P{-}N)_2(\mu\text{-}N{-}P)Cu]^{2+}$, where N−P is 2-(diphenylphosphino)pyridine[50] or 2-(diphenylphosphino)-1-methylimidazole.[51,52] The former ligand also forms a doubly bridged dicopper(I) cation having two or four additional acetonitrile ligands, viz. $[(MeCN)_nCu(\mu\text{-}P{-}N)(\mu\text{-}N{-}P)Cu\text{-}(MeCN)_n]^{2+}$ ($n$ = 1 or 2).[50,53] The different coordination


dx.doi.org/10.1021/ic4026848 | Inorg. Chem. 2014, 53, 568−577

**Scheme 3. Alternative Routes Leading to the Dicopper(I) Salts $10X_2$**[a]

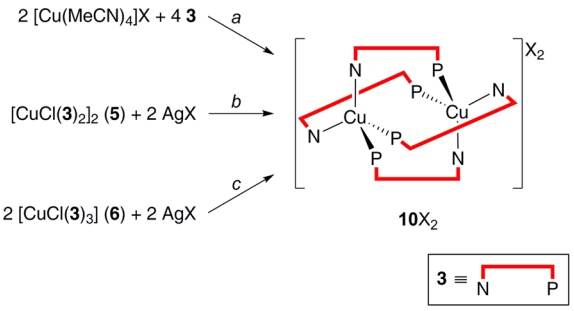


[a]Route a for X = $BF_4^-$, $PF_6^-$, $CF_3SO_3^-$, and $B(C_6F_5)_4^-$; route b for X = $SbF_6^-$ and $(CF_3SO_2)_2N^-$; and route c for X = $SbF_6^-$.

behavior of **3** is very likely due to the presence of the rather small, rod-like CN donor unit, which cannot easily participate in the chelation of the P-bonded metal ion but can be directed to another metal center (through practically unrestricted rotation of the ferrocene cyclopentadienyls) and thus supplement the preferred tetrahedral coordination environment around the "other" Cu(I) ion.

Although the salts of the cation $\mathbf{10}^{2+}$ crystallize readily, their structural characterization proved difficult owing to the presence of extensively disordered counteranions and/or solvent molecules. Good-quality, disorder-free crystals were ultimately obtained for $\mathbf{10}[SbF_6]_2$. The structure of the complex cation in this salt is presented in Figure 7. A complete view and a projection of the cation along the (Cu2, Cu1) vector are available in the Supporting Information (Figures S8 and S9), which also presents the structure of the less symmetric solvate $\mathbf{10}[SbF_6]_2{\cdot}2Me_2CO$ for comparison.

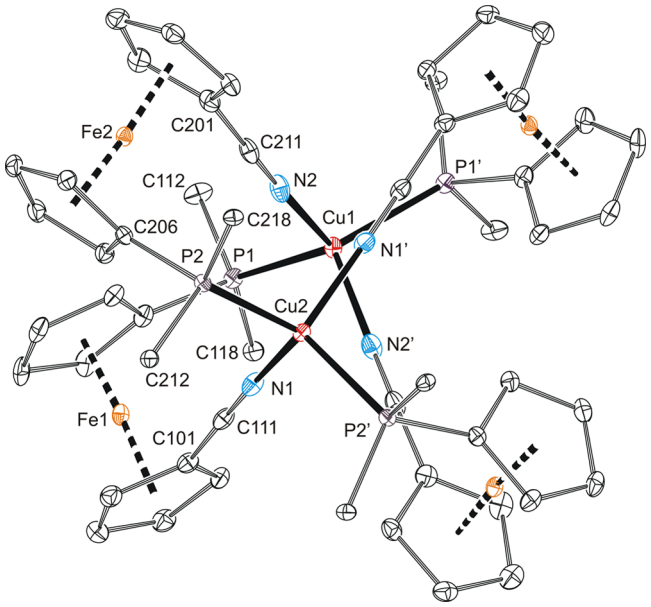


**Figure 7.** View of the complex cation in the structure of $\mathbf{10}[SbF_6]_2$, showing the displacement ellipsoids at the 30% probability level. The primed atoms are generated by the crystallographic 2-fold axis ($-x$, 2 $-$ $y$, $z$). Selected distances (Å) and angles (deg): Cu1–P1 2.3069(5), Cu1–N2 2.051(2), Cu2–P2 2.2807(5), Cu2–N1 2.016(2), C111–N1 1.143(3), C211–N2 1.144(3), P1–Cu1–P1′ 124.05(3), P1–Cu1–N2 104.52(5), P1–Cu1–N2′ 109.84(6), N2–Cu1–N2′ 102.05(8), P2–Cu2–P2′ 119.18(2), P2–Cu2–N1 107.10(5), P2–Cu2–N1′ 108.59(5), N1–Cu2–N1′ 105.49(7).

The structure of cation $\mathbf{10}^{2+}$ can be likened to a fragment of a quadruple helix consisting of pairs of chains with opposite polarity arranged around the central Cu1···Cu2 axis or, more figuratively, to a propeller with four blades (see Figure S9, Supporting Information). The compound crystallizes with the symmetry of the chiral orthorhombic space group *Aba*2 such that the copper atoms reside on the 2-fold axis. This "external" symmetry renders only one-half of the complex cation and one counterion ($SbF_6^-$) structurally independent.

The Cu1···Cu2 separation in $\mathbf{10}[SbF_6]_2$ is 5.4820(5) Å, which is considerably longer than the sum of covalent radii (2.64 Å[54]) or the Cu···Cu distances in heterocubane **4** [3.1950(5)–3.3332(4) Å] and much less than the Cu···Cu′ distances in **5** [8.2816(8) Å] and **9** [7.9595(5) Å]. Each copper(I) atom in $\mathbf{10}^{2+}$ forms two relatively shorter bonds to the nitrile groups and two longer bonds to the phosphine groups within a distorted tetrahedral coordination environment. The P–Cu–P angles are the largest, while the N–Cu–N angles are the most acute, reflecting the different steric properties of the donor moieties. The departure from the ideal tetrahedral angles is larger for Cu1 than for Cu2. The ferrocene units assume a synclinal eclipsed conformation [$\tau$ = 75.6(2)° for Fe1 and $\tau$ = 74.1(2)° for Fe2], which brings the donor moieties into positions suitable for bridging the two Cu(I) centers. However, this conformation of the donor units results in a mutual rotation of the $CuN_2P_2$ units (P1–Cu1···Cu2–N1 = 26.94(7)°, P2–Cu2···Cu1–N2 = 24.28(7)°) and, consequently, the helical character of the dicopper(I) cation.

The $\nu_{C\equiv N}$ bands in the IR spectrum of the $\mathbf{10}^{2+}$ salts appear shifted toward higher frequencies (2230 and 2237 $cm^{-1}$ for $\mathbf{10}[BF_4]_2$ and $\mathbf{10}[SbF_6]_2$, respectively) compared with the free ligand (2225 $cm^{-1}$). Together with a marginal variation of the lengths of the C≡N bonds,[55] this shift is in line with the usual trend, reflecting changes in the electronic structure of the nitrile moiety upon coordination.[40]

## CONCLUSIONS

The readily accessible phosphinonitrile **3** exhibits some unique properties, primarily due to the presence of the ferrocene moiety.[56] As a ligand, it can rotate along the axis of the ferrocene unit and thus undergo the rotational reorganization of the donor moieties, but it remains inflexible with respect to the tilting of the cyclopentadienyl rings. Furthermore, the entire molecule of **3** is conjugated and, because of strong electron-donating nature of the ferrocene unit, electron-rich. This results in unprecedented coordination behavior, which is exemplified herein for the soft Cu(I) ion.

In addition to conventional complexes in which the cyano groups remain uncoordinated and thus serve as spectators, albeit rather specific substituents, the structures determined for the Cu(I) complexes with ligand **3** reported in this Article demonstrate the ability of the phosphinonitrile donor to coordinate as a P,N bridge through both soft donor sites. The molecular structures of such complexes have been determined for the first time. Although limited to Cu(I) and a few coordination geometries (halide complexes $PX_3$ or $NPX_2$ tetrahedral donor sets, complexes without halide ligands $PN_2$ trigonal or $P_2N_2$ tetrahedral coordination environments), the results presented here demonstrate as yet undocumented coordination behavior of phosphinonitrile donors and stress the


dx.doi.org/10.1021/ic4026848 | *Inorg. Chem.* 2014, 53, 568–577

necessity of selecting the appropriate metal ions for evaluating the coordination potential of these donors.

## EXPERIMENTAL SECTION

**Materials and Methods.** The syntheses of **2** and **3** were performed in an argon atmosphere using standard Schlenk techniques.[57] Complexes with ligand **3** were prepared in argon-flushed vessels and in the dark. Aldehyde **1** was prepared according to the literature.[20] Dichloromethane and tetrahydrofuran (THF) were dried with a Pure Solv MD-5 Solvent Purification System (Innovative Technology, Amesbury, MA). Other chemicals and solvents utilized for crystallizations and chromatography were used as received (Sigma-Aldrich; solvents from Lachner, Brno, Czech Republic).

NMR spectra were measured with a Varian UNITY Inova 400 spectrometer ($^1$H 399.95, $^{13}$C 100.58, $^{31}$P 161.90 MHz) at 25 °C unless noted otherwise. Chemical shifts ($\delta$, ppm) are given relative to internal tetramethylsilane ($^1$H and $^{13}$C) or external 85% aqueous $H_3PO_4$ ($^{31}$P). In addition to the usual notation for signal multiplicity, vt and vq are used to denote virtual triplets and quartets arising from the AA′BB′ and AA′BB′X spin systems of the cyano- and $PPh_2$-substituted cyclopentadienyl rings, respectively (fc = ferrocene-1,1′-diyl). IR spectra were recorded with an FTIR Nicolet 760 instrument in the range 400−4000 cm$^{-1}$. Conventional (low-resolution) electrospray ionization mass spectra (ESI MS) were recorded on a Bruker Esquire 3000 spectrometer. The samples were dissolved in HPLC-grade methanol. High-resolution (HR) ESI MS measurements were obtained with an LTQ Orbitrap XL mass spectrometer. Elemental analyses were determined by a conventional combustion method with a PE 2400 Series II CHNS/O Elemental Analyzer (Perkin-Elmer). Melting points were determined with a melting point B-540 apparatus (Büchi, Flawil, Switzerland).

**1′-(Diphenylphosphino)ferrocene-1-carboxaldehyde Oxime (2).** A solution of sodium ethoxide prepared separately by dissolving sodium metal (0.063 g, 2.7 mmol) in anhydrous ethanol (5 mL) was added to a solution of hydroxylamine hydrochloride (0.190 g, 2.7 mmol) in absolute ethanol (15 mL), whereupon a fine white precipitate (NaCl) separated. The mixture was stirred for 10 min and then filtered through a polytetrafluoroethylene (PTFE) syringe filter into a suspension of 1′-(diphenylphosphino)ferrocene-1-carboxaldehyde (**1**; 0.360 g, 0.90 mmol) in anhydrous ethanol (20 mL). The resulting mixture was stirred at 60 °C for 3 h, cooled to room temperature, and diluted with brine (20 mL) and dichloromethane (20 mL). The organic layer was separated, washed with brine, dried over $MgSO_4$, and evaporated with chromatographic silica gel. The preadsorbed crude product was transferred onto a silica gel column packed in a hexane/diethyl ether (3:1) mixture. The same mobile phase was used to remove nonpolar impurities. The red band that eluted when the eluent was changed to hexane/diethyl ether (1:1) was collected and evaporated to afford aldoxime **2** as an orange solid (yield: 0.306 g, 82%). The compound was a mixture of (*E*) and (*Z*) isomers in ca. 2:1 ratio. Crystals suitable for X-ray diffraction analysis were grown by liquid-phase diffusion from an ethyl acetate/hexane mixture.

$^1$H NMR ($CDCl_3$): major isomer $\delta$ 4.13 (m, 2H, fc), 4.23 (vt, $J'$ = 1.9 Hz, 2H, fc), 4.43 (m, $J'$ = 1.8 Hz, 4H, fc), 7.30−7.39 (m, 10H, Ph), 7.71 (s, 1H, C*H*NOH), 7.96 (br s, 1H, CHNO*H*); minor isomer $\delta$ 4.11 (m, 2H, fc), 4.25 (vt, $J'$ = 1.9 Hz, 2H, fc), 4.41 (vt, $J'$ = 1.8 Hz, 2H, fc), 4.70 (vt, $J'$ = 1.9 Hz, 2H, fc), 6.96 (s, 1H, C*H*NOH), 7.30−7.39 (m, 10H, Ph), 7.96 (br s, 1H, CHNO*H*). $^{13}$C{$^1$H} NMR ($CDCl_3$): major isomer $\delta$ 68.44 (CH of fc), 71.28 (CH of fc), 72.16 (d, $J_{PC}$ = 4 Hz, CH of fc), 72.46 (d, $J_{PC}$ = 4 Hz, CH of fc), 73.88 (d, $^1J_{PC}$ = 14 Hz, C−P of fc), 76.86 (C−CHN of fc), 128.20 (d, $^2J_{PC}$ = 7 Hz, CH$^{ortho}$ of Ph), 128.62 (CH$^{para}$ of Ph), 133.47 (d, $^3J_{PC}$ = 20 Hz, CH$^{meta}$ of Ph), 138.71 (d, $^1J_{PC}$ = 9 Hz, C$^{ipso}$ of Ph). $^{31}$P{$^1$H} NMR ($CDCl_3$): −16.7 (major), −16.6 (minor). IR (Nujol): $\nu_{max}$ (cm$^{-1}$) 3280 br m, 3240 br m, 3160 br m, 3017 m, 1642 w, 1304 m, 1245 w, 1195 w, 1188 w, 1161 w, 1090 w, 1070 m, 1040 m, 997 w, 948 s, 897 m, 827 m, 783 m, 751 s, 703 m, 695 s, 636 w, 582 w, 569 w, 499 s, 453 w, 413 w. ESI+ MS: *m*/*z* 414 ([M + H]$^+$), 436 ([M + Na]$^+$). Anal. Calcd for $C_{23}H_{20}FeNOP{\cdot}0.2CH_3CO_2Et$ (430.8): C 66.34, H 5.05, N 3.25%. Found: C 66.24, H 4.73, N 3.28%. The amount of clathrated solvent was verified by NMR spectroscopy.

**1′-(Diphenylphosphino)-1-cyanoferrocene (3).** Oxime **2** (0.293 g, 0.71 mmol) and (benzotriazol-1-yloxy)tris(dimethylamino)-phosphonium hexafluorophosphate (BOP; 0.628 g, 1.42 mmol) were mixed in dry THF (15 mL). After the mixture had been stirred at room temperature for 5 min, 1,8-diazabicyclo[5.4.0]undec-7-ene (DBU; 0.25 mL, 1.7 mmol) dissolved in 5 mL of THF was added, and the stirring was continued for another 2 h. The mixture was washed with water (2× 5 mL) and brine (5 mL), and the organic phase was dried over $MgSO_4$ and evaporated with silica gel. The preadsorbed product was transferred to the top of a chromatographic column (silica gel; hexane/diethyl ether 1:1). Elution with the same solvent mixture afforded a single red band, which was collected and evaporated to give nitrile **3** as an orange microcrystalline solid (yield: 0.250 g, 89%). Crystals suitable for X-ray diffraction analysis were grown from ethyl acetate/hexane.

Mp 163−164 °C (ethyl acetate/hexane). $^1$H NMR ($CDCl_3$): $\delta$ 4.26 (vq, $J'$ = 1.9 Hz, 2H, fc), 4.28 (vt, $J'$ = 1.9 Hz, 2H, fc), 4.53 (vt, $J'$ = 1.9 Hz, 2H, fc), 4.56 (vt, $J'$ = 1.9 Hz, 2H, fc), 7.32−7.37 (m, 10H, Ph). $^{13}$C{$^1$H} NMR ($CDCl_3$): $\delta$ 52.62 (C−CN of fc), 72.17 (d, $J_{PC}$ = 1 Hz, CH of fc), 72.56 (CH of fc), 73.72 (d, $J_{PC}$ = 4 Hz, CH of fc), 74.87 (d, $J_{PC}$ = 14 Hz, CH of fc), 79.29 (d, $^1J_{PC}$ = 10 Hz, C−P of fc), 119.60 (C≡N), 128.35 (d, $^2J_{PC}$ = 7 Hz, CH$^{ortho}$ of Ph), 128.86 (CH$^{para}$ of Ph), 133.40 (d, $^3J$ = 20 Hz, CH$^{meta}$ of Ph), 138.03 (d, $^1J_{PC}$ = 10 Hz, C$^{ipso}$ of Ph). $^{31}$P{$^1$H} NMR ($CDCl_3$): $\delta$ −17.7. IR (Nujol): $\nu_{max}$ (cm$^{-1}$) 3114 w, 3100 w, 3082 w, 3055 w, 2225 m, 1232 w, 1194 w, 1160 m, 1090 w, 1232 w, 1032 m, 1027 m, 913 w, 848 w, 840 w, 823 m, 749 s, 699 s, 562 w, 555 w, 519 w, 510 m, 478 m, 495 m, 448 m, 450 m, 425 w. ESI+ MS: *m*/*z* 396 ([M + H]$^+$), 418 ([M + Na]$^+$), 434 ([M + K]$^+$). HR MS (ESI+): calcd for $C_{23}H_{19}FeNP$ ([M + H]$^+$) 396.0599, found 396.0599. Anal. Calcd for $C_{23}H_{18}FeNP$ (395.2): C 69.90, H 4.59, N 3.55%. Found: C 69.60, H 4.44, N 3.45%.

**Reactions of Ligand 3 with CuCl.** A solution of phosphine **3** in dichloromethane (1.5 mL) was added to a suspension of CuCl in the same solvent (0.5 mL). The resulting mixture was stirred at room temperature for 90 min, during which time all of the CuCl dissolved. Following evaporation under a vacuum, the solid products were analyzed by NMR spectroscopy and subsequently recrystallized by liquid-phase diffusion from ethyl acetate/hexane or chloroform/hexane.

*Complex* ***4***. Reaction between **3** (20 mg, 51 $\mu$mol) and CuCl (5.0 mg, 51 $\mu$mol) as described above gave **4** as a yellow microcrystalline solid (yield: 16 mg, 64%). $^1$H NMR ($CDCl_3$): $\delta$ 4.36 (br vt, $J'$ = 1.8 Hz, 2H, fc), 4.46 (vt, $J'$ =1.9 Hz, 2H, fc), 4.50−4.53 (br m, 4H, fc), 7.25−7.31 (m, 4H, Ph), 7.33−7.39 (m, 2H, Ph), 7.56−7.65 (m, 2H, Ph). $^{31}$P{$^1$H} NMR ($CDCl_3$): $\delta$ −13.3 (br s). IR (Nujol): $\nu_{max}$ (cm$^{-1}$) 3109 w, 3065 w, 3039 w, 2241 m, 1232 w, 1194 w, 1160 w, 1090 w, 1032 m, 1027 m, 913 w, 848w, 839 w, 823 m, 749 s, 699 s, 562 w, 558 w, 519 w, 511 m, 495 m, 478 m, 450 m, 425 w. ESI+ MS: *m*/*z* 458 ([Cu(**3**)]$^+$), 516 ([CuCl(**3**) + Na]$^+$), 558 ([$Cu_2Cl$(**3**)]$^+$), 853 ([Cu(**3**)$_2$]$^+$), 911 ([CuCl(**3**)$_2$ + Na]$^+$), 953 ([$Cu_2Cl$(**3**)$_2$]$^+$). Anal. Calcd for $(C_{23}H_{18}ClCuFeNP)_4$ (1976.8): C 55.89, H 3.67, N 2.83%. Found: C 55.91, H 3.60, N 2.59%.

*Complex* ***5***. Reaction of **3** (15 mg, 38 $\mu$mol) and CuCl (1.9 mg, 19 $\mu$mol) as described above produced **5** as a red crystalline solid (yield: 11 mg, 66%). $^1$H NMR ($CDCl_3$): $\delta$ 4.34 (br vt, 2H, fc), 4.46 (vt, $J'$ = 2.0 Hz, 2H, fc), 4.51 (vt, $J'$ = 2.0 Hz, 2H, fc), 4.54 (vt, $J'$ = 1.9 Hz, 2H, fc), 7.27−7.33 (m, 4H, Ph), 7.36−7.41 (m, 2H, Ph), 7.43−7.51 (br m, 4H, Ph). $^{31}$P{$^1$H} NMR ($CDCl_3$): $\delta$ −13.1 (br s). IR (Nujol): $\nu_{max}$ (cm$^{-1}$) 3101 w, 3047 m, 2224 s, 1586 w, 1236 w, 1192 w, 1167 w, 1035 w, 1026 w, 846 w, 833 w, 755 m, 740 m, 696 s, 630 w, 595 w, 553 w, 530 m, 510 m, 476 m, 458 m, 425 w. ESI+ MS: *m*/*z* 458 ([Cu(**3**)]$^+$), 516 ([CuCl(**3**) + Na]$^+$), 558 ([$Cu_2Cl$(**3**)]$^+$), 853 ([Cu(**3**)$_2$]$^+$), 911 ([CuCl(**3**)$_2$ + Na]$^+$), 953 ([$Cu_2Cl$(**3**)$_2$]$^+$). Anal. Calcd for $C_{46}H_{36}ClCuFe_2N_2P_2$ (889.4): C 62.12, H 4.08, N 3.15%. Found: C 61.87, H 3.94, N 3.10%.

According to monitoring by NMR spectroscopy, when the reaction was performed similarly with 3 equiv of **3** (**3**: 15 mg, 38 $\mu$mol; CuCl


dx.doi.org/10.1021/ic4026848 | *Inorg. Chem.* 2014, 53, 568−577

1.3 mg, 13 μmol), it produced a different product (formulated as [CuCl(**3**)$_3$] (**6**)), which was converted completely to complex **5** during the subsequent crystallization from ethyl acetate/hexane (yield of **5**: 11 mg, 95%). Data recorded for **6** in situ. $^1$H NMR ($CDCl_3$): δ 4.31 (br vt, $J'$ = 1.8 Hz, 2H, fc), 4.42 (br vt, $J'$ = 1.8 Hz, 2H, fc), 4.50 (vt, $J'$ = 1.9 Hz, 2H, fc), 4.56 (vt, $J'$ = 1.9 Hz, 2H, fc), 7.28−7.43 (m, 10H, Ph). $^{31}$P{$^1$H} NMR ($CDCl_3$): δ −15.0 (br s). ESI+ MS: *m*/*z* 458 ([Cu(**3**)]$^+$), 516 ([CuCl(**3**) + Na]$^+$), 558 ([Cu$_2$Cl(**3**)]$^+$), 853 ([Cu(**3**)$_2$]$^+$), 911 ([CuCl(**3**)$_2$ + Na]$^+$), 953 ([Cu$_2$Cl(**3**)$_2$]$^+$). The NMR and IR spectra of the crystallized samples were identical to those of **5**.

*[CuBr(3)]$_n$ (**7**).* CuBr (7.3 mg, 51 μmol) and **3** (20 mg, 51 μmol) were reacted in dry chloroform (2 mL) for 1 h to afford a clear solution, which was partly evaporated under a vacuum (to ca. 1 mL) and filtered through a PTFE syringe filter. The filtrate was layered with chloroform (1 mL) and hexane (10 mL), and the mixture was allowed to crystallize by diffusion to produce **8** as an orange-red crystalline solid (yield: 19 mg, 70%). Note: Complete solvent removal produces a glassy solid, which can be dissolved in ethyl acetate. The solution, however, rapidly deposits **8** as an orange precipitate.

$^1$H NMR (in situ, $CDCl_3$): δ 4.38 (vt, $J'$ = 1.9 Hz, 2H, fc), 4.40 (vt, $J'$ =1.9 Hz, 2H, fc), 4.57 (vt, $J'$ = 1.7 Hz, 2H, fc), 4.59 (br s, 2H, fc), 7.28−7.34 (m, 4H, Ph), 7.36−7.42 (m, 2H, Ph), 7.56−7.63 (m, 4H, Ph). $^{31}$P{$^1$H} NMR (in situ, $CDCl_3$): δ −16.1 (br s). IR (Nujol): $\nu_{max}$ ($cm^{-1}$) 3112 w, 3103 w, 3061 w, 3040w, 2243 s, 1238 m, 1193 w, 1167 s, 1033 s, 914 s, 890 w, 753 s, 745 s, 697 s, 636 w, 535 s, 517 s, 509 m, 481 s, 457 m, 432 m. Anal. Calcd for $C_{23}H_{18}BrCuFeNP$ (538.7): C 51.28, H 3.37, N 2.60%. Found: C 50.90, H 3.29, N 2.34%.

The NMR spectra recorded for the reaction mixtures obtained similarly at Cu/**3** molar ratios of 1:2 and 1:3 were different, but the subsequent crystallization always produced only complex **8**. **Cu/3 = 1:2.** $^1$H NMR (in situ, $CDCl_3$): δ 4.39 (br vt, $J'$ = 1.7 Hz, 2H, fc), 4.45 (vt, $J'$ = 1.9 Hz, 2H, fc), 4.48 (vt, $J'$ = 1.9 Hz, 2H, fc), 4.54 (vt, $J'$ = 1.9 Hz, 2H, fc), 7.27−7.32 (m, 4H, Ph), 7.36−7.41 (m, 2H, Ph), 7.43−7.48 (m, 4H, Ph). $^{31}$P{$^1$H} NMR (in situ, $CDCl_3$): δ −13.6 (br s). **Cu/3 = 1:3.** $^1$H NMR (in situ, $CDCl_3$): δ 4.35 (br vt, $J'$ = 1.8 Hz, 2H, fc), 4.42 (br vt, $J'$ = 1.9 Hz, 2H, fc), 4.49 (vt, $J'$ = 1.9 Hz, 2H, fc), 4.56 (vt, $J'$ = 1.9 Hz, 2H, fc), 7.28−7.33 (m, 4H, Ph), 7.35−7.41 (m, 6H, Ph). $^{31}$P{$^1$H} NMR (in situ, $CDCl_3$): δ −14.7 (br s).

*[CuI(3)]$_n$ (**8**).* Ligand **3** (50 mg, 0.13 mmol) and CuI (24 mg, 0.13 mmol) were reacted in dry $CHCl_3$ as described above. After filtration, the clear, orange solution was layered with chloroform (2 mL) and hexane (20 mL) and set aside for crystallization to produce **8** in the form of orange-red crystals (yield: 65 mg, 87%).

$^1$H NMR (in situ, $CDCl_3$): δ 4.07 (br s, 2H, fc), 4.26 (br s, 2H, fc), 4.52−4.56 (m, 4H, fc), 7.39−7.45 (m, 4H, Ph), 7.47−7.60 (m, 6H, Ph). $^{31}$P{$^1$H} NMR (in situ, $CDCl_3$): δ −27.9 (br s). IR (Nujol): $\nu_{max}$ ($cm^{-1}$) 3112 w, 3103 m, 3089 w, 3065 m, 3041 m, 2242 s, 1586 w, 1237 m, 1193 m, 1165 s, 1098 m, 1070 w, 1050 w, 1033 s, 999 w, 987 w, 914 m, 889 w, 865 w, 839 s, 832 s, 809 m, 952 s, 744 s, 697 s, 635 w, 577 w, 534 s, 516 s, 509 m, 478 s, 459 s, 432 m. Anal. Calcd for $C_{23}H_{18}CuFeINP$ (585.7): C 47.17, H 3.10, N 2.39%. Found: C 46.90, H 3.03, N 2.20%.

Similar to the CuBr/**3** system, the reaction mixtures obtained at CuI/**3** ratios of 1:2 and 1:3 gave different NMR spectra but provided only complex **9** upon crystallization. **CuI/3 = 1:2.** $^1$H NMR (in situ, $CDCl_3$): δ 4.41−4.46 (m, 6H, fc), 4.54 (vt, $J'$ =1.9 Hz, 2H, fc), 7.26−7.31 (m, 4H, Ph), 7.35−7.43 (m, 6H, Ph). $^{31}$P{$^1$H} NMR (in situ, $CDCl_3$): δ −14.8 (br s). **CuI/3 = 1:3.** $^1$H NMR (in situ, $CDCl_3$): δ 4.39−4.42 (m, 4H, fc), 4.48 (vt, $J'$ =1.9 Hz, 2H, fc), 4.48 (vt, $J'$ =1.9 Hz, 2H, fc), 4.55 (vt, $J'$ =1.9 Hz, 2H, fc), 7.27−7.32 (m, 4H, Ph), 7.34−7.40 (m, 6H, Ph). $^{31}$P{$^1$H} NMR (in situ, $CDCl_3$): δ −14.9 (br s).

**Preparation of [Cu(3)(MeCN)]$_x$[BF$_4$]$_x$ (9).** A solution of **3** (20 mg, 51 μmol) in dichloromethane (2 mL) was added to a suspension of solid [Cu(MeCN)$_4$][BF$_4$] (16 mg, 51 μmol) in the same solvent (1 mL), and the resulting mixture was stirred for 1 h. The separated solid was dissolved by addition of acetonitrile (2 drops), and the solution was filtered through a syringe filter. The filtrate was layered with hexane (ca. 6 mL) and set aside for crystallization. The dark orange-red crystals, which separated over several days, were filtered off, washed with pentane, and dried under a vacuum to afford analytically pure **9** (yield: 25 mg, 84%).

IR (Nujol): $\nu_{max}$ ($cm^{-1}$) 3099 w, 3071 w, 3048 w, 2314 w, 2283 m, 2249 s, 1306 w, 1285 w, 1242 m, 1195 w, 1169 m, 1102 s, 1075 s, 1052 s, 1027 s, 997 m, 916 m, 845 m, 831 w, 749 s, 699 s, 538 s, 519 s, 488 s, 481 s, 464 m, 429 w. Anal. Calcd for $C_{25}H_{21}N_2BF_4PFeCu$ (586.6) C 51.18, H 3.61, N 4.78%. Found: C 51.48, H 3.59, N 4.59%.

*Complex **10**[BF$_4$]$_2$ (Route a in Scheme 3).* A solution of **3** (15 mg, 38 μmol) in dry dichloromethane was added to a suspension of [Cu(MeCN)$_4$][BF$_4$] in the same solvent (6.0 mg, 19 μmol in 0.5 mL). The resulting mixture was stirred for 1 h and evaporated under a vacuum. The residue was taken up with acetone (5 mL) and filtered through a syringe filter. Evaporation of the filtrate under vacuum gave **10**[BF$_4$]$_2$ as a yellow solid (yield: 14 mg, 78%). IR (Nujol): $\nu_{max}$ ($cm^{-1}$) 2230 s, 1712 w, 1618 w, 1237 m, 1166 m, 1071 s, 1044 s, 999 m, 913 w, 741 m, 722 m, 696 w, 635 w, 532 w, 511 s, 490 s, 476 s, 463 s, 433 m. ESI+ MS: *m*/*z* 458 [Cu(**3**)$^+$]. Anal. Calcd for $C_{92}H_{72}B_2Cu_2F_8Fe_4N_4P_4{\cdot}H_2O$ (1899.6): C 58.17, H 3.93, N 2.95%. Found: C 57.85, H 4.00, N 2.95%. (Note: Salts with other anions were obtained similarly.)

*Complex **10**[SbF$_6$]$_2$ (Route c in Scheme 3).* A solution of ligand **3** (30 mg, 76 μmol) in dichloromethane (3 mL) was added to a suspension of CuCl (3.8 mg, 38 μmol) in the same solvent (1 mL). After being stirred for 60 min, the resulting solution was treated with a suspension of Ag[SbF$_6$] (13 mg, 38 μmmol) in dichloromethane (3 mL), and the reaction mixture was stirred for another 30 min and filtered through a PTFE syringe filter. The filtrate was evaporated under a vacuum, and the residue was taken up with acetone (1.5 mL) and filtered into a 5 mm NMR tube. The solution was carefully layered with acetone (0.5 mL) and hexane (ca. 2 mL), and the mixture was allowed to crystallize at room temperature. The separated crystalline solid was filtered off, washed with pentane, and dried under a vacuum. Yield of **10**[SbF$_6$]$_2$: 34 mg (82%), red crystalline solid. IR (Nujol): $\nu_{max}$ ($cm^{-1}$) 3122 w, 3055 w, 2237 s, 1587 w, 1481 m, 1435 s, 1238 m, 1196 w, 1099 m, 1041 m, 999 w, 912 w, 830 m, 741 m, 695 s, 659 s, 577 w, 531 w, 511 s, 487 s, 478 s, 466 m, 433 w. ESI+ MS: *m*/*z* 458 [Cu(**3**)$^+$]. Anal. Calcd for $C_{92}H_{72}Cu_2F_{12}Fe_4P_4N_4Sb_2$ (2179.4) C 50.70, H 3.33, N 2.57%. Found: C 50.43, H 3.33, N 2.36%.

## ■ ASSOCIATED CONTENT

### Ⓢ Supporting Information

Additional structural diagrams, NMR spectra of CuCl/**3** mixtures, results of DSC measurements for **7**, description of single-crystal X-ray diffraction analyses, and copies of NMR and IR spectra. Complete crystallographic data in standard CIF format (CCDC deposition numbers 966377−966386). This material is available free of charge via the Internet at http://pubs.acs.org.

## ■ AUTHOR INFORMATION

### Corresponding Author

*E-mail: stepnic@natur.cuni.cz.

### Notes

The authors declare no competing financial interest.

## ■ ACKNOWLEDGMENTS

This contribution is based on work supported by the Czech Science Foundation (Project 13-08890S) and the Grant Agency of Charles University in Prague (Project 108213).

## ■ REFERENCES

(1) (a) Braunstein, P.; Matt, D.; Mathey, F.; Thavard, D. *J. Chem. Res. Synop.* **1978**, 232−233. (b) Braunstein, P.; Matt, D.; Dusausoy, Y.; Fischer, J.; Mitschler, A.; Ricard, L. *J. Am. Chem. Soc.* **1981**, *103*, 5115−5125. (c) Klasen, C.; Lorenz, I. P.; Schmid, S.; Beuter, G. *J. Organomet. Chem.* **1992**, *428*, 363−378.

(2) (a) Braun, L.; Liptau, P.; Kehr, G.; Ugolotti, J.; Fröhlich, R.; Erker, G. *Dalton Trans.* **2007**, 1409−1415. (b) Sithole, S. V.; Staples, R. J.; van Zyl, W. E. *Acta Crystallogr. E: Struct. Rep. Online* **2011**, *67*, m64. (c) Sithole, S. V.; Staples, R. J.; van Zyl, W. E. *Inorg. Chem. Commun.* **2012**, *15*, 216−220.

(3) (a) Maraval, A.; Owsianik, K.; Arquier, D.; Igau, A.; Coppel, Y.; Donnadieu, B.; Zablocka, M.; Majoral, J.-P. *Eur. J. Inorg. Chem.* **2003**, 960−968. (b) Minko, Y. A.; Belina, N. V.; Sushev, V. V.; Fukin, G. K.; Bubnov, M. P.; Kornev, A. N. *J. Organomet. Chem.* **2007**, *692*, 4157−4160.

(4) Selected examples: (a) Meriwether, L. S.; Fiene, M. L. *J. Am. Chem. Soc.* **1959**, *81*, 4200−4208. (b) Meriwether, L. S.; Colthup, E. C.; Fiene, M. L.; Cotton, F. A. *J. Inorg. Nucl. Chem.* **1959**, *11*, 181−183. (c) Magee, T. A.; Matthews, C. N.; Wang, T. S.; Wotiz, J. H. *J. Am. Chem. Soc.* **1961**, *83*, 3200−3203. (d) Cotton, F. A.; Oldham, C.; Walton, R. A. *Inorg. Chem.* **1967**, *6*, 214−223. (e) Ross, E. P.; Dobson, G. R. *Inorg. Chem.* **1967**, *6*, 1256−1257. (f) Houk, L. W.; Dobson, G. R. *J. Chem. Soc. A* **1968**, 1846−1849. (g) Forbus, N. P.; Brown, T. L. *Inorg. Chem.* **1981**, *20*, 4343−4347. (h) Habib, M.; Trujillo, H.; Alexander, C. A.; Storhoff, B. N. *Inorg. Chem.* **1985**, *24*, 2344−2349. (i) Gutiérrez Alonso, A.; Ballester Reventós, L. *J. Organomet. Chem.* **1988**, *338*, 249−259. (j) Pringle, P. G.; Smith, M. B. *J. Chem. Soc., Chem. Commun.* **1990**, 1701−1702. (k) Khan, M. N. I.; King, C.; Fackler, J. P., Jr.; Winpenny, R. E. P. *Inorg. Chem.* **1993**, *32*, 2502−2505. (l) Liu, C. W.; Pan, H.; Fackler, J. P., Jr.; Wu, G.; Wasylishen, R. E.; Shang, M. *J. Chem. Soc., Dalton Trans.* **1995**, 3691−3697. (m) Rosi, L.; Bini, A.; Frediani, P.; Bianchi, M.; Salvini, A. *J. Mol. Catal. A: Chem.* **1996**, *112*, 367−383. (n) Hussain, M. S.; Al-Arfaj, A. R.; Akhtar, M. N.; Isab, A. A. *Polyhedron* **1996**, *15*, 2781−2785. (o) Orpen, A. G.; Pringle, P. G.; Smith, M. B.; Worboys, K. *J. Organomet. Chem.* **1998**, *550*, 255−266. (p) Pruchnik, F. P.; Smolenski, P.; Wajda-Hermanowicz, K. *J. Organomet. Chem.* **1998**, *570*, 63−69. (q) Blin, J.; Braunstein, P.; Fischer, J.; Kickelbick, G.; Knorr, M.; Morise, X.; Wirth, T. *J. Chem. Soc., Dalton Trans.* **1999**, 2159−2170. (r) Chantler, J.; Fanwick, P. E.; Walton, R. A. *Inorg. Chim. Acta* **2000**, *305*, 215−220. (s) Smolenski, P. *J. Organomet. Chem.* **2011**, *696*, 3867−3872. (t) Boschi, A.; Cazzola, E.; Uccelli, L.; Pasquali, M.; Ferretti, V.; Bertolasi, V.; Duatti, A. *Inorg. Chem.* **2012**, *51*, 3130−3137. (u) Kihara, K.; Suzuki, T.; Kita, M.; Sunatsuki, Y.; Kojima, M.; Takagi, H. D. *Bull. Chem. Soc. Jpn.* **2012**, *85*, 1160−1166.

(5) For examples of donors containing longer aliphatic spacers, $Ph_2P(CH_2)_nCN$ ($n \geq 3$), see: (a) Storhoff, B. N.; Harper, D. P.; Saval, I. H.; Worstell, J. H. *J. Organomet. Chem.* **1981**, *205*, 161−166. (b) Pitter, S.; Dinjus, E.; Jung, B.; Görls, H. *Z. Naturforsch. B, Chem. Sci.* **1996**, *51*, 934−946.

(6) (a) Payne, D. H.; Frye, H. *Inorg. Nucl. Chem. Lett.* **1972**, *8*, 73−77. (b) Hatano, M.; Asai, T.; Ishihara, K. *Chem. Lett.* **2006**, *35*, 172−173. (c) Kawatsura, M.; Yamamoto, M.; Namioka, J.; Kajita, K.; Hirakawa, T.; Itoh, T. *Org. Lett.* **2011**, *13*, 1001−1003 and refs 4h and 5a.

(7) For complexes featuring the analogous di- and trinitriles, $PhP(C_6H_4CN\text{-}2)_2$ and $P(C_6H_4CN\text{-}2)_3$, see: (a) Chapman, S.; Kane-Maguire, L. A. P. *J. Chem. Soc., Dalton Trans.* **1995**, 2021−2026. (b) Elliott, M. E.; Kimmerling, T. S.; Zhu, L.; Storhoff, B. N.; Huffman, J. C. *Polyhedron* **1999**, *18*, 1603−1608. (c) Klein, H.-F.; Beck, R.; Florke, U.; Haupt, H.-J. *Eur. J. Inorg. Chem.* **2003**, 853−862. (d) Szesni, N.; Weibert, B.; Fischer, H. *Inorg. Chim. Acta* **2004**, *357*, 1789−1798.

(8) 2-(Diphenylphosphino)benzonitrile has been used as a synthetic precursor in the preparation of various phosphinoheterocyclic donors: (a) Koch, G.; Lloyd-Jones, G. C.; Loiseleur, O.; Pfaltz, A.; Pretot, R.; Schaffner, S.; Schnider, P.; von Matt, P. *Recl. Trav. Chim. Pays-Bas* **1995**, *114*, 206−210; *Chem. Abstr.* **1995**, *123*, 198930. (b) Baltzer, N.; Macko, L.; Schaffner, S.; Zehnder, M. *Helv. Chim. Acta* **1996**, *79*, 803−812. (c) Cahill, J. P.; Bohnen, F. M.; Goddard, R.; Kruger, C.; Guiry, P. J. *Tetrahedron: Asymmetry* **1998**, *9*, 3831−3839. (d) Kündig, E. P.; Meier, P. *Helv. Chim. Acta* **1999**, *82*, 1360. (e) Lait, S. M.; Parvez, M.; Keay, B. A. *Tetrahedron: Asymmetry* **2004**, *15*, 155−158.

(9) 1-(Diphenylphosphino)cyclopropanecarbonitrile: (a) Vinogradova, N. M.; Odinets, I. L.; Lyssenko, K. A.; Pasechnik, M. P.; Petrovskii, P. V.; Mastryukova, T. A. *Mendeleev Commun.* **2001**, 219−221. (b) Odinets, I. L.; Vinogradova, N. M.; Matveeva, E. V.; Golovanov, D. D.; Lyssenko, K. A.; Keglevich, G.; Kollár, L.; Roëschenthaler, G.-V.; Mastryukova, T. A. *J. Organomet. Chem.* **2005**, *690*, 2559−2570. 1-Cyano-2-(diphenylphosphino)cyclopentane and -cyclohexane: (c) Blinn, D. A.; Button, R. S.; Farazi, V.; Neeb, M. K.; Tapley, C. L.; Trehearne, T. E.; West, S. D.; Kruger, T. L.; Storhoff, B. N. *J. Organomet. Chem.* **1990**, *393*, 143−152. (d) Fredericks, E. J.; Gindling, M. J.; Kroll, L. C.; Storhoff, B. N. *J. Organomet. Chem.* **1994**, *465*, 289−296. 1,3,5-Tricyano-1,3,5-tris(diphenylphosphino)cyclohexane: (e) Mayer, H. A.; Stössel, P.; Fawzi, R.; Steimann, M. *Chem. Ber.* **1995**, *128*, 719−723. (f) Stössel, P.; Heins, W.; Mayer, H. A.; Fawzi, R.; Steinman, M. *Organometallics* **1996**, *15*, 3393−3403. (g) Heins, W.; Stössel, P.; Mayer, H. A.; Steinmann. *J. Organomet. Chem.* **1999**, *587*, 258−266.

(10) Phosphinonitrile $Ph_2PCH_2CN$ easily undergoes deprotonation at the methylene group. The resulting C anion can be used as a ligand in transition-metal complexes. For a review, see: Braunstein, P. *Chem. Rev.* **2006**, *106*, 134−159.

(11) Barratt, D. S.; Hosseiny, A.; McAuliffe, C. A.; Stacey, C. *J. Chem. Soc., Dalton Trans.* **1985**, 135−139.

(12) Štěpnička, P. In *Ferrocenes: Ligands, Materials and Biomolecules*; Štěpnička, P., Ed.; Wiley: Chichester, U.K., 2008; Chapter 5, pp 177−204.

(13) Selected recent examples of $Ph_2PfcY$-type donors: (a) Y = OH: Atkinson, R. C. J.; Gibson, V. C.; Long, N. J.; White, A. J. P. *Dalton Trans.* **2010**, *39*, 7540−7546. (b) Y = $B(2,4,6\text{-}Me_3C_6H_2)_2$: Bebbington, M. W. P.; Bontemps, S.; Bouhadir, G.; Hanton, M. J.; Tooze, R. P.; van Rensburg, H.; Bourissou, D. *New J. Chem.* **2010**, *34*, 1556−1559. (c) Y = $CH_2$(benzimidazolium): Gülcemal, S.; Labande, A.; Daran, J.-C.; Çetinkaya, B.; Poli, R. *Eur. J. Inorg. Chem.* **2009**, 1806−1815. (d) Y = 2-Py, 3-Py, and $CH_2$(2-Py) (Py = pyridyl): Štěpnička, P.; Schulz, J.; Klemann, T.; Siemeling, U.; Císařová, I. *Organometallics* **2010**, *29*, 3187−3200. (e) Siemeling, U.; Klemann, T.; Bruhn, C.; Schulz, J.; Štěpnička, P. *Dalton Trans.* **2011**, *40*, 4722−4740. (f) Y = $CH_2NMe_2$: Štěpnička, P.; Zábranský, M.; Císařová, I. *ChemistryOpen* **2012**, *1*, 71−79. (g) Y = CH═NR′: Teo, S.; Weng, Z.; Hor, T. S. A. *J. Organomet. Chem.* **2011**, *696*, 2928−2934. (h) Y = $CH_2PPh_2$: Štěpnička, P.; Císařová, I.; Schulz, J. *Organometallics* **2011**, *30*, 4393−4403. (i) Štěpnička, P.; Císařová, I. *J. Organomet. Chem.* **2012**, *716*, 110−119. (j) Y = $CH_2OMe$: Štěpnička, P.; Císařová, I. *Dalton Trans.* **2013**, *42*, 3373−3389. (k) Y = CONHR (R = H, Cy, Ph, $NH_2$): Štěpnička, P.; Solařová, H.; Lamač, M.; Císařová, I. *J. Organomet. Chem.* **2010**, *695*, 2423−2431. (l) Štěpnička, P.; Solařová, H.; Císařová, I. *J. Organomet. Chem.* **2011**, *696*, 3727−3740. (m) Y = $CONHCH(R)CO_2Me$ and related compounds: Tauchman, J.; Císařová, I.; Štepnička, P. *Organometallics* **2009**, *28*, 3288−3302. (n) Tauchman, J.; Císařová, I.; Štěpnička, P. *Eur. J. Org. Chem.* **2010**, 4276−4287. (o) Tauchman, J.; Císařová, I.; Štěpnička, P. *Dalton Trans.* **2011**, *40*, 11748−11757. (p) Tauchman, J.; Therrien, B.; Süss-Fink, G.; Štěpnička, P. *Organometallics* **2012**, *31*, 3985−3994. (q) Y = $CONHCH_{(3-n)}(CH_2OH)_n$ ($n$ = 1−3) and analogues: Schulz, J.; Císařová, I.; Štěpnička, P. *J. Organomet. Chem.* **2009**, *694*, 2519. (r) Schulz, J.; Císařová, I.; Štěpnička, P. *Eur. J. Inorg. Chem.* **2012**, 5000−5010. (s) Y = $CONH(CH_2)_nSO_3[HNEt_3]$ ($n$ = 1−3): Schulz, J.; Císařová, I.; Štěpnička, P. *Organometallics* **2012**, *31*, 729−738.

(14) (a) Chien, S. W.; Hor, T. S. A. In *Ferrocenes: Ligands, Materials and Biomolecules*; Štěpnička, P., Ed.; Wiley: Chichester, U.K., 2008; Chapter 2, pp 33−116. (b) Gan, K.-S.; Hor, T. S. A. In *Ferrocenes: Homogeneous Catalysis, Organic Synthesis, Materials Science*; Togni, A., Hayashi, T., Eds.; Wiley-VCH: Weinheim, Germany, 1995; Chapter 1, pp 3−104; (c) Young, D. J.; Chien, S. W.; Hor, T. S. A. *Dalton Trans.* **2012**, *41*, 12655. (d) Bandoli, G.; Dolmella, A. *Coord. Chem. Rev.* **2000**, *209*, 161.

(15) Štěpnička, P.; Císařová, I. *Organometallics* **2003**, *22*, 1728−1740.

(16) Lamač, M.; Štěpnička, P. *Inorg. Chem. Commun.* **2006**, *9*, 319−321.

(17) Zirakzadeh, A.; Schuecker, R.; Weissensteiner, W. *Tetrahedron: Asymmetry* **2010**, *21*, 1494−1502.
(18) Fassbender, J.; Frank, W.; Ganter, C. *Eur. J. Inorg. Chem.* **2012**, 4356−4364.
(19) Cotton, F. A.; Wilkinson, G.; Murillo, C. A.; Bochmann, M. *Advanced Inorganic Chemistry*, 6th ed.; Wiley: New York, 1999; Chapter 17-H, p 858.
(20) Štěpnička, P.; Baše, T. *Inorg. Chem. Commun.* **2001**, *4*, 682−687.
(21) This standard approach was also employed in the original preparations of FcCH═NOH: (a) Lindsay, J. K.; Hauser, C. R. *J. Org. Chem.* **1957**, *22*, 355−358. (b) Graham, P. J.; Lindsey, R. V.; Parshall, G. W.; Peterson, M. L.; Whitman, G. M. *J. Am. Chem. Soc.* **1957**, *79*, 3416−3420.
(22) Singh, M. K.; Lakshman, M. L. *J. Org. Chem.* **2009**, *74*, 3079−3084.
(23) A one-pot procedure based on the reaction of aldehydes with $NH_2OH{\cdot}HCl/KI/ZnO$ in hot acetonitrile, which was shown to work well with (unsubstituted) ferrocenecarboxaldehyde, gave disappointing results in the case of **1**. Using this procedure, nitrile **3** was not only isolated in a low yield but was also contaminated with the difficult-to-separate starting aldehyde. See: Kivrak, A.; Zora, M. *J. Organomet. Chem.* **2007**, *692*, 2346−2349.
(24) Kitson, R. E.; Griffith, N. E. *Anal. Chem.* **1952**, *24*, 334−337.
(25) $E_{pa}$ is the anodic peak potential in cyclic voltammetry. The value was recorded at a scan rate of 0.1 V $s^{-1}$ in 1,2-dichloromethane solution ($c$ = 0.5 mM) containing 0.1 M $Bu_4N[PF_6]$ as the supporting electrolyte using a $\mu$Autolab III instrument (Eco Chemie, Utrecht, The Netherlands), a Pt disk working electrode, a Pt sheet auxiliary electrode, and a Ag/AgCl (3 M KCl) reference electrode.
(26) Electrochemical oxidations of phosphinoferrocenes to the respective ferrocenia are often associated with followup chemical reactions that render the redox response irreversible. For selected examples, see: (a) Ong, J. H. L.; Nataro, C.; Golen, J. A.; Rheingold, A. L. *Organometallics* **2003**, *22*, 5027−5032. (b) Zanello, P.; Opromolla, G.; Giorgi, G.; Sasso, G.; Togni, A. *J. Organomet. Chem.* **1996**, *506*, 61−65. (c) Pilloni, G.; Longato, B.; Corain, B. *J. Organomet. Chem.* **1991**, *420*, 57−65. (d) Podlaha, J.; Štěpnička, P.; Ludvík, J.; Císařová, I. *Organometallics* **1996**, *15*, 543−550.
(27) Crystals of **3O** were isolated accidentally from an attempted preparation of $[Cu_2(\mathbf{3})_4][BPh_4]_2$ by the metathesis of in situ formed $[Cu_2(\mathbf{3})_4][PF_6]_2$ with solid $Na[BPh_4]$ in dichloromethane during crystallization of the crude reaction mixture from ethyl acetate/hexane.
(28) Ferguson, G.; Bell, W.; Glidewell, C. *J. Organomet. Chem.* **1991**, *405*, 229−236.
(29) The electron density corresponding to the lone electron pair can be refined as a He atom (two electrons), although with a large displacement factor [$U_{iso}$(He)/$U_{eq}$(P) ≈ 10]. The refinement leads to a reasonable geometry [P···He 1.25(2) Å, C—P···He angles ca. 115−118°) and markedly decreases the residual electron density (0.96 → 0.33 e $Å^{-3}$). However, the reliability factor ($R$) for the observed diffractions changes only marginally (from 2.72% to 2.63%).
(30) Compare the Hammett $\sigma_p$ constants for $PPh_2$ and $P(O)Ph_2$, at 0.19 and 0.53, respectively. Data from: Hansch, C.; Leo, A.; Taft, R. W. *Chem. Rev.* **1991**, *91*, 165−195.
(31) Ossola, F.; Tomasin, P.; Benetollo, F.; Foresti, E.; Vigato, P. A. *Inorg. Chim. Acta* **2003**, *353*, 292−300.
(32) Bell, W.; Ferguson, G.; Glidewell, C. *Acta Crystallogr. C: Cryst. Struct. Commun.* **1996**, *52*, 1928−1930.
(33) Adeleke, J. A.; Liu, L.-K. *Acta Crystallogr. C: Cryst. Struct. Commun.* **1993**, *49*, 680−682.
(34) Pearson, R. G. *J. Am. Chem. Soc.* **1963**, *85*, 3533−3539.
(35) Pearson, R. G. *Inorg. Chem.* **1988**, *27*, 734−740.
(36) Pilloni, G.; Corain, B.; Degano, M.; Longato, B.; Zanotti, G. *J. Chem. Soc., Dalton Trans.* **1993**, 1777−1778.
(37) Hathaway, B. J. In *Comprehensive Coordination Chemistry*; Wilkinson, G., Gillard, R. D., McCleverty, J. A., Eds.; Pergamon Press: New York, 1987; Vol. 5, Chapter 53, p 533−774.
(38) Representative early examples: (a) L = $PPh_3$: Lippard, S. J.; Ucko, D. A. *Inorg. Chem.* **1968**, *7*, 1051−1056 and references therein. (b) Gill, J. T.; Mayerle, J. J.; Welcker, P. S.; Lewis, D. F.; Ucko, D. A.; Barton, D. J.; Stowens, D.; Lippard, S. J. *Inorg. Chem.* **1976**, *15*, 1155−1168 (crystal structure determination). (c) L = $PMe_3$: Schmidbaur, H.; Adlkofer, J.; Schwirten, K. *Chem. Ber.* **1972**, *105*, 3382−3388.
(39) (a) Lippard, S. J.; Mayerle, J. J. *Inorg. Chem.* **1972**, *11*, 753−759. (b) Fife, D. J.; Moore, W. M.; Morse, K. W. *Inorg. Chem.* **1984**, *23*, 1684−1691.
(40) Coordination of a nitrile usually results in a shift of the C≡N stretching band toward higher energies because of the removal of electron density from a weakly antibonding molecular orbital ($\sigma$-donation of the lone pair at N). The associated $\pi$-back-donation, which has the opposite effect of increasing the population of antibonding $\pi$-orbitals, is relatively weak. See: (a) Nakamoto, K. *Infrared and Raman Spectra of Inorganic and Coordination Compounds. Part B: Applications in Coordination, Organometallic, and Bioinorganic Chemistry*, 5th ed.; Wiley: New York, 1997; Section III-15, p 105−115. (b) Kuznetsov, M. L. *Russ. Chem. Rev.* **2002**, *71*, 265−282.
(41) According to DFT calculations, the closed heterocubane structures represent global energy minima for the $[CuX(PH_3)]_4$ tetramers: Schwerdtfeger, P.; Krawczyk, R. P.; Hammerl, A.; Brown, R. *Inorg. Chem.* **2004**, *43*, 6707−6716.
(42) Vega, A.; Saillard, J.-Y. *Inorg. Chem.* **2004**, *43*, 4012−4018.
(43) (a) Štěpnička, P.; Gyepes, R.; Podlaha, J. *Collect. Czech. Chem. Commun.* **1998**, *63*, 64−74. (b) Štěpnička, P.; Císařová, I. *Collect. Czech. Chem. Commun.* **2006**, *71*, 215−236.
(44) The same set of symmetry elements is distributed differently in the crystal lattices of **7** and **8** (see Supporting Information, Figure S6).
(45) The halide bridges are asymmetrical, with slightly different distances to the two bridged Cu atoms [Δ(Cu−X) ≈ 0.08 Å].
(46) Mainly C15—H15···F3&($x$ − 1, $y$, $z$) with C15···F3 = 3.399(3) Å and C22—H22···F4&(1 − $x$, 2 − $y$, 1 − $z$) with C22···F4 = 3.333(3) Å.
(47) The reaction of $[Cu(MeCN)_4][BF_4]$ with 3 equiv of **3** in $CH_2Cl_2$ afforded a mixture of unreacted **3** and $[\mathbf{10}][BF_4]_2$, from which the latter compound separated upon crystallization.
(48) $[Cu(MeCN)_4][B(C_6F_5)_4]$ was prepared according to the literature: Liang, H.-C.; Kim, En.; Incarvito, C. D.; Rheingold, A. L.; Karlin, K. D. *Inorg. Chem.* **2002**, *41*, 2209−2212. Other $[Cu(MeCN)_4]^+$ salts were commercially available.
(49) According to a search in the Cambridge Structural Database, version 5.33, in Nov 2011 with updates from Nov 2011 and from Feb, May, and Aug 2012.
(50) Lastra, E.; Gamasa, M. P.; Gimeno, J.; Lanfranchi, M.; Tiripicchio, A. *J. Chem. Soc., Dalton Trans.* **1989**, 1499−1506.
(51) Abdul Jalil, M.; Yamada, T.; Fujinami, S.; Honjo, T.; Nishikawa, H. *Polyhedron* **2001**, *20*, 627−633.
(52) The reaction of $Cu[BF_4]_2$ with an excess of 2-(diphenylphoshino)-1-benzylimidazole yielded a similar complex containing one $\eta^1$-coordinated $BF_4$ anion per the metal center (Cu−F ≈ 2.7−2.8 Å): Bachechi, F.; Burini, A.; Fontani, M.; Galassi, R.; Machioni, A.; Pietroni, B. R.; Zanello, P.; Zuccaccia, C. *Inorg. Chim. Acta* **2001**, *323*, 45−54.
(53) Maekawa, M.; Munakata, M.; Kitagawa, S.; Yonezawa, T. *Bull. Chem. Soc. Jpn.* **1991**, *64*, 2286−2288.
(54) Cordero, B.; Gómez, V.; Platero-Prats, A. E.; Revés, M.; Echeverría, J.; Cremades, E.; Barragán, F.; Alvarez, S. *Dalton Trans.* **2008**, 2832.
(55) With the exception of the value determined for **7** [C≡N = 1.137(4) Å at 250 K], the length of the C≡N bond remained statistically constant in the *entire* series of structurally characterized compounds (ca. 1.144 Å at 150 K). The C—C≡N angle spanned the range from 176.6(2)° to 179.1(2)°.
(56) For an overview of the chemistry of ferrocene ligands, see: *Ferrocenes: Ligands, Materials and Biomolecules*; Štěpnička, P., Ed.; Wiley: Chichester, U.K., 2008.
(57) Shriver, D. F. *The Manipulation of Air-Sensitive Compounds*; McGraw-Hill: New York, 1969.

# Appendix 3

Karel Škoch, Ivana Císařová, Petr Štěpnička: "Phosphinoferrocene Ureas: Synthesis, Structural Characterization, and Catalytic Use in Palladium-Catalyzed Cyanation of Aryl Bromides". *Organometallics*, **2015**, *34*, 1942.

Dalton Transactions

PAPER

Cite this: *Dalton Trans.*, 2016, **45**, 10655

# Silver(I) complexes with 1′-(diphenylphosphino)-1-cyanoferrocene: the art of improvisation in coordination†

Karel Škoch,[a] Filip Uhlík,[b] Ivana Císařová[a] and Petr Štěpnička*[a]

1′-(Diphenylphosphino)-1-cyanoferrocene (**1**) reacts with silver(I) halides at a 1 : 1 metal-to-ligand ratio to afford the heterocubane complexes $[Ag(\mu_3\text{-}X)(\mathbf{1}\text{-}\kappa P)]_4$, where X = Cl (**2**), Br (**4**), and I (**5**). In addition, the reaction with AgCl with 2 equiv. of **1** leads to chloride-bridged dimer $[(\mu\text{-}Cl)_2\{Ag(\mathbf{1}\text{-}\kappa P)_2\}_2]$ (**3**) and, presumably, also to $[(\mu(P,N)\text{-}\mathbf{1})\{AgCl(\mathbf{1}\text{-}\kappa P)\}]_2$ (**3′**). While similar reactions with AgCN furnished only the insoluble coordination polymer $[(\mathbf{1}\text{-}\kappa P)_2Ag(NC)Ag(CN)]_n$ (**6**), those with AgSCN afforded the heterocubane $[Ag(\mathbf{1}\text{-}\kappa P)(\mu\text{-}SCN\text{-}S,S,N)]_4$ (**7**) and the thiocyanato-bridged disilver(I) complex $[Ag(\mathbf{1}\text{-}\kappa P)_2(\mu\text{-}SCN\text{-}S,N)]_2$ (**8**), thereby resembling reactions in the AgCl–**1** system. Attempted reactions with AgF led to ill-defined products, among which $[Ag(\mathbf{1}\text{-}\kappa P)_2(\mu\text{-}HF_2)]_2$ (**9**) and $[(\mu\text{-}SiF_6)\{Ag(\mathbf{1}\text{-}\kappa P)_2\}_2]$ (**10**) could be identified. The latter compound was prepared also from $Ag_2[SiF_6]$ and **1**. Reactions between **1** and $AgClO_4$ or $Ag[BF_4]$ afforded disilver complexes $[(\mu(P,N)\text{-}\mathbf{1})Ag(ClO_4\text{-}\kappa O)]_2$ (**11**) and $[(\mu(P,N)\text{-}\mathbf{1})Ag(BF_4\text{-}\kappa F)]_2$ (**12**) featuring pseudolinear Ag(I) centers that are weakly coordinated by the counter anions. A similar reaction with $Ag[SbF_6]$ followed by crystallization from ethyl acetate produced an analogous complex, albeit with coordinated solvent, $[(\mu(P,N)\text{-}\mathbf{1})Ag(AcOEt\text{-}\kappa O)]_2[SbF_6]_2$ (**13**). Ultimately, a compound devoid of any additional ligands at the Ag(I) centers, $[(\mu(P,N)\text{-}\mathbf{1})Ag]_2[B(C_6H_3(CF_3)_2\text{-}3,5)_4]_2$ (**14**), was obtained from the reaction of **1** with silver(I) tetrakis-[3,5-bis(trifluoromethyl)phenyl]borate. The reaction of $Ag[BF_4]$ with two equivalents of **1** produced unique coordination polymer $[Ag(\mathbf{1}\text{-}\kappa P)(\mu(P,N)\text{-}\mathbf{1})]_n[BF_4]_n$ (**15**), the structure of which contained one of the phosphinoferrocene ligands coordinated as a P,N-chelate and the other forming a bridge to an adjacent Ag(I) center. All of these compounds were structurally characterized by single-crystal X-ray crystallography, revealing that the lengths of the bonds between silver and its anionic ligand(s) typically exceed the sum of the respective covalent radii, which is in line with the results of theoretical calculations at the density-functional theory (DFT) level, suggesting that standard covalent dative bonds are formed between silver and phosphorus (soft acid/soft base interactions) while the interactions between silver and the ligand's nitrile group (if coordinated) or the supporting anion are of predominantly electrostatic nature.

Received 10th May 2016,
Accepted 1st June 2016

DOI: 10.1039/c6dt01843b

www.rsc.org/dalton

## Introduction

Because of a $d^{10}$ valence shell configuration, soft[1] silver(I) ions have no stereochemical preference due to the lack of ligand field stabilization. As a result, the coordination geometry of Ag(I) complexes is determined by an interplay of electrostatic and steric factors and is, therefore, difficult to predict.[2] Thus, although the Ag(I)–phosphine complexes are accessible through simple reactions of silver(I) salts with phosphines, they form a wide variety of structures ranging from mononuclear species to complicated multinuclear, often polymeric, assemblies and clusters.[3] This also holds true for silver(I) complexes with 1,1′-bis(diphenylphosphino)ferrocene (dppf), an archetypal and widely studied bidentate metalloligand,[4] which has been demonstrated in numerous systematic and focused studies devoted to Ag(I)–dppf complexes with various supporting (mostly simple anionic) ligands[5,6] as well as on multimetallic complexes and transition metal clusters featuring Ag(I)(dppf) fragments.[7] In contrast, the structural chemistry of Ag(I)

[a]*Department of Inorganic Chemistry, Faculty of Science, Charles University in Prague, Hlavova 2030, 128 40 Prague, Czech Republic.*
*E-mail: petr.stepnicka@natur.cuni.cz*
[b]*Department of Physical and Macromolecular Chemistry, Faculty of Science, Charles University in Prague, Hlavova 2030, 128 40 Prague, Czech Republic*

†Electronic supplementary information (ESI) available: Full experimental and characterization data for all newly prepared compounds, IR spectra of **3′** and $[(\mu(P,N)\text{-}\mathbf{1})\{CuCl(\mathbf{1}\text{-}\kappa P)\}]_2$, complete structural drawings, a summary of relevant crystallographic data, additional plots of the calculated electron density and its Laplacian. CCDC 1470453–1470466. For ESI and crystallographic data in CIF or other electronic format see DOI: 10.1039/c6dt01843b

complexes with other phosphinoferrocene donors remains largely unexplored, being limited to compounds prepared from (ferrocenylmethyl)diphenylphosphine,[8] diferrocenyl(phenyl)phosphine,[9] a cyclic ferrocene triphosphine[10] or (2-ferrocenylethyl)phosphines $(FcCH_2CH_2)_nPH_{3-n}$ (Fc = ferrocenyl, $n$ = 1–3)[11] for the non-functional ferrocene phosphines, and a handful of dppf congeners with one of their phosphine groups replaced by another functional moiety.[12] To date, the latter compounds include only Ag(I) complexes with phosphino-chalcogen donors (**A** and **B** in Scheme 1)[13] or phosphinoferrocene pyridines (**C**–**E** in Scheme 1)[14] and Ag(I) carboxylates prepared from 1′-(diphenylphosphino)-1-ferrocenecarboxylic acid (Hdpf).[15]

In view of our recent investigations into the coordination chemistry of 1′-(diphenylphosphino)-1-cyanoferrocene (**1** in Scheme 1) that led to structurally unique Cu(I) complexes[16] and hemilabile Au(I) complexes with favorable catalytic properties,[17] we aimed to complete our study with this new, donor-unsymmetric dppf analogue by focusing on complexes with Ag(I). Attention was directed mainly to the structural chemistry of the **1**–Ag(I) complexes because a search in the Cambridge Structural Database[18] revealed that silver(I) complexes with phosphinonitrile donors whose crystal structure has been determined are very rare, consisting of $[Ag\{P(CH_2CH_2CN)_3\text{-}\kappa P\}_2]NO_3$ featuring linearly coordinated Ag(I) centers[19] and complex $[Ag_2(\mu\text{-}L)_2(MeCN)_2][SbF_6]_2$, where L is 2,6-bis(diphenylphosphino)benzonitrile coordinated as a P,P′-bridge between the trigonal and tetrahedral Ag(I) centers.[20]

This contribution describes the structural characterization of products arising from the interactions of various AgX salts with phosphinonitrile **1** at varying metal-to-ligand ratios. Because of the specific features detected in the structures of some of these complexes, attention is also paid to the bonding situation in the representative complexes, which is discussed in view of the results of density-functional theory (DFT) computations.

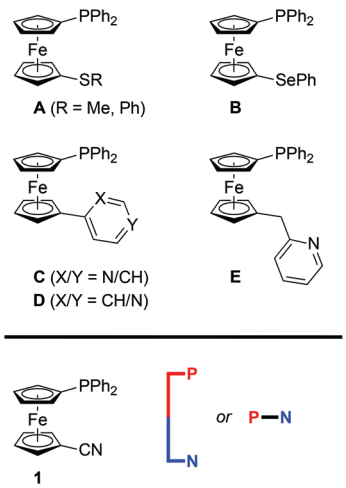


Scheme 1

## Results and discussion

### General comments

Considering the structural complexity of Ag(I)–phosphine complexes, the reaction studies were performed using silver(I) salts with a wide selection of counter anions and at varying metal-to-ligand ratios. The screening experiments were performed in deuterated solvents to allow for *in situ* NMR monitoring. Typically, ligand **1** was added to a suspension of the respective AgX salt (mostly at Ag : **1** ratios of 1 : 1 and 1 : 2) in $CDCl_3$, and the resulting mixture was stirred for 90 min, during which time the silver salt dissolved. After filtration, the reaction mixture was monitored by $^1H$ and $^{31}P\{^1H\}$ NMR spectroscopy and, finally, crystallized by the addition of a poor solvent (sometimes after evaporation and re-dissolution). The conditions were kept as similar as possible to minimize possible influence of complexation and solvolytic equilibria[21] on the reaction outcome.

Notably, the NMR spectra of the reaction mixtures provided little diagnostic information because the dynamic nature of the Ag–**1** complexes resulted in a broadening and averaging of the NMR resonances.[22] Little structural information was inferred also from the IR spectra of solid samples except for the characteristic bands due to C≡N stretching vibrations that are observed in the narrow range of 2223–2228 $cm^{-1}$ for compounds featuring uncoordinated nitrile groups (*cf.* 2225 $cm^{-1}$ for ligand **1**)[16] and that shifted upon coordination of the nitrile group.

### Complexes with halide-supporting ligands

Aiming at a systematic survey of the coordination properties of **1** toward silver(I), attention was first paid to compounds resulting from the action of the phosphinonitrile on Ag(I) halides (Scheme 2).

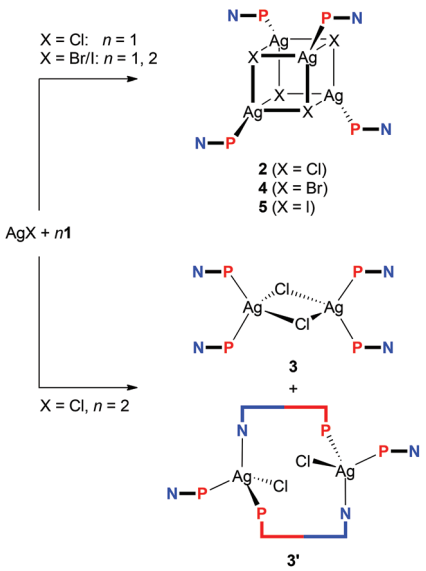


Scheme 2 Synthesis of Ag(I)–**1** complexes from silver(I) halides.

The $^{31}P\{^1H\}$ NMR spectrum of the solution obtained after addition of one molar equivalent of **1** into a suspension AgCl in $CDCl_3$ showed a broad doublet at $\delta_P$ −1.4, confirming that the phosphinonitrile was indeed coordinated (*cf.* $\delta_P$ −17.7 for **1** in $CDCl_3$).[16] Moreover, the relatively large $^1J_{AgP}$ coupling constant of 604 Hz suggested that the reaction stoichiometry was very likely maintained in the reaction product (*i.e.*, that "AgCl·**1**" was formed *in situ*).[21,23] A subsequent crystallization from wet acetone–hexane afforded orange crystals of hydrated heterocubane **2**·$H_2O$, which was structurally characterized (see below). Unsolvated **2** could be similarly isolated from acetone–hexane (*i.e.*, in the absence of added water). However, the crystals suffered from extensive disorder.

Upon increasing the amount of the ligand to two equivalents, the reaction in $CDCl_3$ and crystallization by the addition of methyl *tert*-butyl ether and hexane furnished a mixture of two products. The dominating, larger orange prismatic crystals were identified by X-ray crystallography as dinuclear complex **3**, in which two chloride ligands bridge two Ag(**1**-κ*P*)$_2$ units (Scheme 2). The minor product separated in the form of fine yellow needles was tentatively formulated as [(μ(P,N)-**1**){AgCl(**1**-κ*P*)}]$_2$ (**3′**) based on the similarity of its IR spectrum with the spectrum obtained for an analogous Cu(I) complex studied previously (see the ESI, Fig. S1†).[16] Upon increasing the amount of **1** to 3 equiv., however, dimer **3** became the only crystalline product isolated from the reaction mixture under otherwise identical conditions, although $^{31}P\{^1H\}$ NMR indicates that some other species (or perhaps equilibria) might be involved (*cf.* $\delta_P$ of −5.0 and −6.9 for the AgCl : **1** mixtures with Ag : **1** = 1 : 2 and 1 : 3, respectively).

In contrast, the similar reactions of **1** with the heavier silver(I) halides gave rise to heterocubanes [Ag(μ$_3$-X)(**1**-κ*P*)]$_4$ (**4**: X = Br, **5**: X = I) irrespective of the Ag : **1** molar ratio (Ag : **1** = 1 : 1 and 1 : 2). The bromide-bridged heterocubane was isolated in the form of a solvate **4**·0.25$H_2O$ after crystallization from ethyl acetate–hexane. Under similar conditions, the iodide analogue was separated as **5**·3AcOEt, while crystallization from chloroform–hexane provided **5**·4$CHCl_3$.

A representative crystal structure of **2**·$H_2O$ is shown in Fig. 1, and all heterocubane cores are depicted in Fig. 2 (*N.B.* complete structural drawings for all compounds are presented in the ESI†). Selected geometric parameters for the heterocubanes are presented in Table 1 and 2, and in the ESI.†

The pairs of compounds **2**·$H_2O$/**4**·0.25$H_2O$ and **5**·3AcOEt/**5**·4$CHCl_3$ are essentially isostructural. The former structures actually differ only in the abundance of the water molecules in the crystal lattice. Apparently, the water molecules can penetrate into the structures built up from these bulky complexes without changing the overall crystal assembly. In fact, they fill the structural voids left between the complex molecules and form hydrogen bridges toward the in-cage halide ions and uncoordinated cyano groups (for a structural diagram, see the ESI, Fig. S3†). The latter interactions appear to be essential for the construction of a regular structural assembly because the structure determined for crystals of unsolvated **2** was disordered at the exterior of the heterocubane molecule mainly at

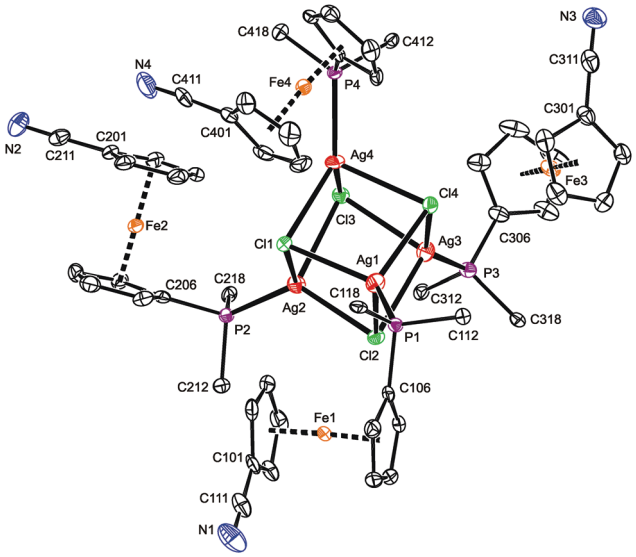


**Fig. 1** PLATON plot of the cubane complex in the structure of **2**·$H_2O$ showing 50% probability ellipsoids. For clarity, only the pivotal atoms from the phenyl rings are shown, and the hydrogens are omitted.

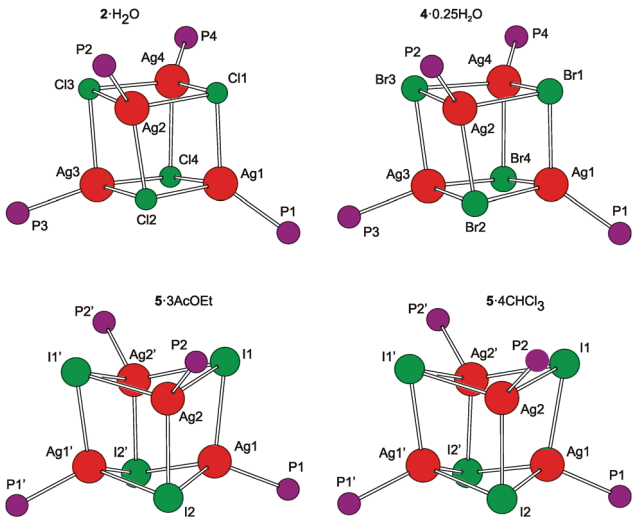


**Fig. 2** View of the $Ag_4X_4P_4$ cores in the four structurally characterized heterocubanes. The prime-labeled atoms in the structures of the iodide-bridged compounds are generated by the crystallographic two-fold axes.

the terminal $C_5H_4CN$ moieties.[24] The isostructural relationship between **5**·3AcOEt and **5**·4$CHCl_3$ also indicates that the crystal structures of these compounds are determined mainly by the packing of the bulky building blocks, leaving vacancies that can be filled by solvent molecules whose size and shape determine the stoichiometry (*i.e.*, relative amount) without affecting the crystal structure.

According to recent DFT calculations,[25] closed heterocubanes are energetically favored over opened, chair-like assemblies for {MX(PH$_3$)}$_4$ tetramers with M = Cu and Ag. These cubanes can be described as distorted tetrahedral arrays of

Table 1 The ranges of selected interatomic distances and angles for the heterocubane cores in **2**·$H_2O$, **4**·0.25$H_2O$, **5**·3AcOEt, and **5**·4$CHCl_3$ (in Å and °)

| Parameter [$n$][a] | **2**·$H_2O$ | **4**·0.25$H_2O$ | **5**·3AcOEt | **5**·4$CHCl_3$ |
|---|---|---|---|---|
| Ag–X [12/6] | 2.5550(7)–2.7481(7) | 2.6801(3)–2.8375(3) | 2.8215(3)–3.0094(3) | 2.8141(4)–3.0185(4) |
| Ag–P [4/2] | 2.3709(7)–2.3841(8) | 2.3947(5)–2.4083(5) | 2.4508(8) and 2.458(1) | 2.4535(8) and 2.4592(8) |
| Ag–X–Ag [12/6] | 78.98(2)–89.85(2) | 76.34(1)–86.72(1) | 65.99(1)–77.86(1) | 65.23(1)–75.57(1) |
| X–Ag–X [12/6] | 89.24(2)–102.02(2) | 91.11(1)–104.42(1) | 96.65(1)–113.77(1) | 99.35(1)–114.07(1) |
| P–Ag–X [12/6] | 104.62(3)–146.73(3) | 103.15(2)–143.41(2) | 104.26(2)–125.87(2) | 100.62(2)–125.02(2) |

[a] $n$ gives the number of observed independent values for **2**·$H_2O$, **4**·0.25$H_2O$/**5**·3AcOEt and **5**·4$CHCl_3$.

metal ions embedded within an $X_4$ tetrahedron of the face-capping halide ions. However, their geometry can change rather broadly depending on the relative sizes of the M/X ions and the steric properties of the metal-bound ligands (possible crowding around the compact $M_4X_4$ unit), as well as on the symmetry of the crystal assembly.[26] In the present case, the heterocubane units in the structures of **2**·$H_2O$ and **4**·0.25$H_2O$ lack any imposed symmetry, while those in **5**·3AcOEt and **5**·4$CHCl_3$ reside on the crystallographic two-fold axes, which makes only their halves structurally independent.

The geometric data reported in Tables 1 and 2 indicate that the intra-cluster parameters vary considerably across the series of structurally characterized compounds as well as for the individual representatives. Both the particular data and asymmetry parameters $Q$, defined as a ratio of the Ag···Ag and X···X separations (diagonals) for the six faces of the cube-like $Ag_4X_4$ array given in Table S2,† suggest an increasing distortion of the heterocubane cores with an increasing size of the halide anion. The Ag–X bond distances are similar or longer than the sum of the respective covalent radii ($\sum r_{cov}$; Ag–Cl 2.47, Ag–Br 2.65, and Ag–I 2.84 Å)[27] and expectedly lengthen upon replacing Cl with Br and then I, which is associated with a less pronounced elongation of the Ag–P bonds and, mainly, with a closing of the Ag–X–Ag angles and an opening of the X–Ag–X angles. Changes in the angles at the vertices of the heterocubane moiety manifest an increasing departure from a nearly planar rhomboidal shape of the $Ag_2X_2$ faces toward a butterfly-like arrangement resulting from a disparity between the sizes of atoms forming the cage. Typically, a short in-face Ag···Ag distance is associated with a long X···X contact and *vice versa*. All observed intermolecular Ag···Ag contacts were longer than double the covalent radius for silver ($2r_{cov} \approx 2.90$ Å).[27] Moreover, because the large iodine anions are displaced from the heterocubane core, the Ag···Ag distances within the faces of the $Ag_4I_4$ core are slightly shorter than those observed for **2**·$H_2O$ and **4**·0.25$H_2O$ that are in turn quite similar. These trends are generally consistent with those observed for $[AgX(PR_3)]_4$ complexes resulting from simple phosphines (see ref. 26).

The ferrocene moieties in the structure of the heterocubanes adopt their regular geometry. Their cyclopentadienyl rings are tilted by less than *ca.* 6° and assume conformations[4a] that direct the cyanide groups away from the central $Ag_4X_4$ moiety (see Fig. 1). This can be demonstrated by the dihedral angles $\tau_n$ = C$n$01–Cg$n$1–Cg$n$2–C$n$06, where Cg$n$1 and Cg$n$2 denote the centroids of the cyclopentadienyl rings C($n$01–$n$05) and C($n$06–$n$10), respectively. In the case of **2**·$H_2O$/**4**·0.25$H_2O$, these angles are $\tau_1$ = −134.0(2)/−136.3(2)°, $\tau_2$ = 144.0(2)/143.1(2)°, $\tau_3$ = −155.8(2)/−153.6(2)°, and $\tau_4$ = −63.6(2)/−67.6(2)°, while for **5**·3AcOEt/**5**·4$CHCl_3$: $\tau_1$ = 135.1(3)/131.6(3)°, and $\tau_2$ = 75.4(3)/77.3(2)°.

The crystal structure of **3**·$CH_2Cl_2$ (Fig. 3) reveals a symmetric dimeric structure in which two chloride anions bridge two equivalent Ag(**1**-κ$P$)$_2$ units, thereby completing the tetrahedral donor array around the Ag(I) ions. The atoms constituting the central $Ag_2Cl_2$ ring in the molecule of **3** are coplanar within 0.008(1) Å. The variation of the Ag–Cl bond lengths within this ring is marginal (*ca.* 0.02 Å), but the $Ag_2Cl_2$ core is rhomboidal in shape (Cl–Ag–Cl ≫ Ag–Cl–Ag). In addition, the adjacent $P_2Ag$ planes are not perpendicular to the $Ag_2Cl_2$ ring as expected for two regular, edge-sharing tetrahedra but

Table 2 The Ag···Ag and X···X in-face diagonal distances for the heterocubane units in the structure of **2**·$H_2O$, **4**·0.25$H_2O$, **5**·3AcOEt and **5**·4$CHCl_3$ (in Å)

| Compound | Parameter | $i/j$ = 1/2 | 1/3 | 1/4 | 2/3 | 2/4 | 3/4 |
|---|---|---|---|---|---|---|---|
| **2**·$H_2O$ | Ag$i$···Ag$j$ | 3.7212(3) | 3.5511(4) | 3.6119(3) | 3.4364(3) | 3.7043(3) | 3.7262(3) |
| | Cl$i$···Cl$j$ | 3.739(1) | 3.780(1) | 3.904(1) | 4.113(1) | 3.912(1) | 3.7503(9) |
| **4**·0.25$H_2O$ | Ag$i$···Ag$j$ | 3.7784(2) | 3.5604(2) | 3.6163(2) | 3.4494(2) | 3.7107(2) | 3.7544(2) |
| | Br$i$···Br$j$ | 3.9458(3) | 4.0575(3) | 4.1661(3) | 4.3624(3) | 4.1831(3) | 3.9836(3) |
| Compound | Parameter | $i/j$ = 1/2 | 1/1′ | 1/2′ | 2/2′ | 2/1′ | 1′/2′ |
| **5**·3AcOEt | Ag$i$···Ag$j$ | 3.1841(4) | 3.6670(3) | 3.4557(4) | 3.3812(4) | ≡1/2′ | ≡1/2 |
| | I$i$···I$j$ | 4.8029(3) | 4.5341(3) | 4.5938(3) | 4.3570(3) | ≡1/2′ | ≡1/2 |
| **5**·4$CHCl_3$ | Ag$i$···Ag$j$ | 3.1576(4) | 3.5773(4) | 3.3775(4) | 3.2264(4) | ≡1/2′ | ≡1/2 |
| | I$i$···I$j$ | 4.8117(3) | 4.6302(3) | 4.6286(3) | 4.4485(3) | ≡1/2′ | ≡1/2 |

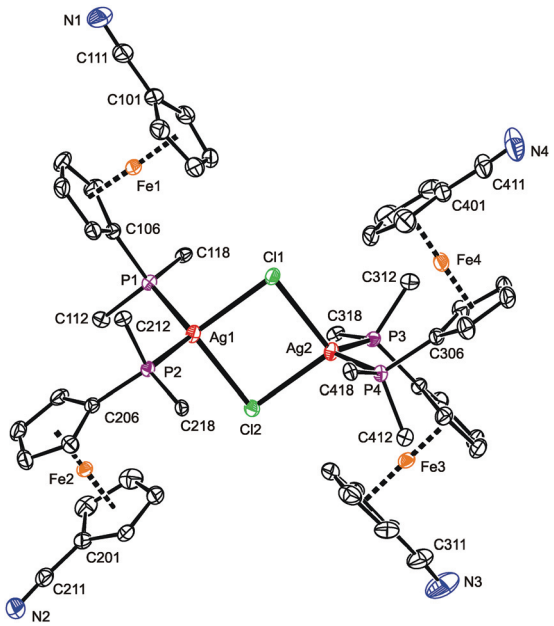


**Fig. 3** PLATON plot of the complex molecule in the structure of **3**·$CH_2Cl_2$. Displacement ellipsoids are scaled to the 50% probability level. The hydrogen atoms and phenyl ring carbons (except for pivotal ones) are omitted for clarity. Selected distances and angles (in Å and °): Ag1–Cl1 2.6671(7), Ag1–Cl2 2.6499(7), Ag2–Cl1 2.6675(7), Ag2–Cl2 2.6563(7), Ag1–P1 2.4791(7), Ag1–P2 2.4800(7), Ag2–P3 2.4817(7), Ag4–P3 2.4804(7), Cl1–Ag1–Cl2 91.24(2), Cl1–Ag1–P1 100.58(2), Cl1–Ag1–P2 117.11(2), Cl2–Ag1–P1 119.34(2), Cl2–Ag1–P2 103.91(2), P1–Ag1–P2 121.24(2), Cl1–Ag2–Cl2 91.09(2), Cl1–Ag2–P3 114.64(2), Cl1–Ag2–P4 104.73(2), Cl2–Ag2–P3 104.81(2), Cl2–Ag2–P4 116.68(2), P3–Ag2–P4 121.14(2), Ag1–Cl1–Ag2 88.53(2), Ag1–Cl2–Ag2 89.13(2).

appear tilted by 77.93(3)° (Ag1) and 81.78(3)° (Ag2) in mutually opposite directions. These distortions can be attributed to the steric strain imparted by the bulky, Ag-bound phosphine ligands (correspondingly, the P–Ag–P angles are the most opened among the interligand angles). Similar features and Ag-donor distances were described for an analogous triphenylphosphine complex, $[Ag(\mu\text{-}Cl)(PPh_3)_2]_2{\cdot}2CHCl_3$.[28] As in **3**·$CH_2Cl_2$, the $Ag–Cl^{bridge}$ in the mentioned $PPh_3$ complex (2.625(3) and 2.630(3) Å) is longer than the sum of the respective covalent radii ($\sum r_{cov}$ = 2.47 Å).

The four structurally independent ferrocene units in the structure of **3**·$CH_2Cl_2$ have similar opened conformations ($\tau$ = 154.9(2)° (Fe1), 156.5(2)° (Fe2), 153.7(2)° (Fe3), and 155.3(2)° (Fe4)) that divert their nitrile substituents from the sterically congested Ag(I) centers. These units also exert similar Fe–C distances and, consequently, the observed tilt angles do no exceed *ca.* 3°. The conformation of the substituents on the phosphorus atoms seems to be controlled through their spatial contacts and further stabilized *via* intramolecular, π···π stacking interactions of phenyl rings above and below the $Ag_2Cl_2$ ring.[29]

The experiments with simple Ag(I) halides were further extended to reactions of silver(I) pseudohalides, whose anions are potentially polydentate. The reactions of silver(I) cyanide with **1** at metal-to-ligand ratios of 1 : 1 and 1 : 2 produced identical, insoluble orange crystalline products, which were found to be coordination polymer **6** (Scheme 3), wherein the linear $Ag(C{\equiv}N\text{-}\kappa C)_2^-$ moieties interconnect the $Ag(\mathbf{1}\text{-}\kappa P)_2^+$ fragments into an infinite zig-zag chain.[30] Although formal, this description is supported by the structural parameters determined for solvated **6** (Fig. 4), showing that the Ag2–C bonds (Ag2–C50 = 2.055(2) Å; Ag2–C60 = 2.053(2) Å) are significantly shorter than the Ag1–N bonds (Ag1–N50 = 2.341(2) Å, Ag1–$N60^i$ = 2.344(2) Å; i = 1/2 + *x*, 1/2 − *y*, 1/2 + *z*). Such a formulation further corresponds to the high stability of the $[Ag(CN)_2]^-$ ions[31] that may be, together with solubility issues, responsible for the preferential formation of polymeric **6**. Analogous complexes have been isolated from reactions of AgCN with triphenyl- and tricyclohexylphosphine.[32,33]

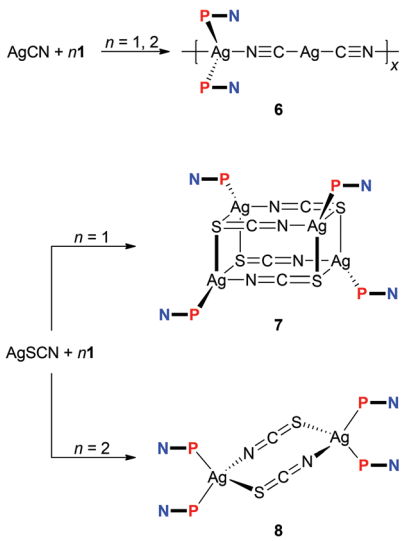


**Scheme 3** Reactions of **1** with AgCN and AgSCN.

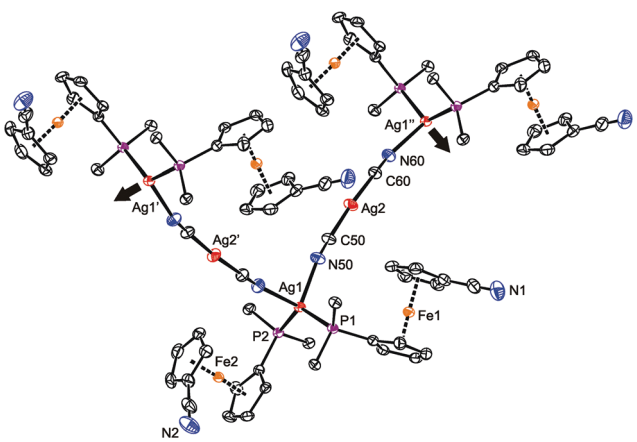


**Fig. 4** Section of the infinite chain in the structure of **6**. The displacement ellipsoids are scaled to the 50% probability level. For clarity, only the pivotal atoms from the phenyl rings are shown, and the hydrogen atoms are omitted (for a complete drawing, see the ESI†).

The $Ag(CN)_2^-$ connecting moiety in the structure of **6** is essentially linear with a C50–Ag2–C60 angle of 175.86(9)° and possesses Ag–C distances similar to those determined for isolated dicyanoargentate(1−) anions.[34] In contrast, the tetrahedral coordination environment of the second Ag(I) ion in the structure of **6** is severely distorted, apparently due to the steric demands of the phosphine ligands. This distortion can be demonstrated by the interligand angles at Ag1 ranging from 96.27(6)–130.30(2)°, with the limits set by the N50–Ag1–N60 (most acute) and P1–Ag1–P2 (most opened) angles. The Ag1–P distances are 2.4489(5) and 2.4527(5) Å for P1 and P2, respectively. Finally, the ferrocene units in the two structurally independent phosphinonitrile donors exert negligible tilting (1.7(1)° for Fe1, 2.7(1)° for Fe2), and their cyanide pendants are rotated away from the ligated Ag(I) ion so that the ferrocene units adopt conformations around anticlinal eclipsed ($\tau$ = 137.8(2)/−145.6(1)° for Fe1/Fe2; *cf.* ideal value: $\tau$ = 144°).

Unlike the previous case, the reactions of silver(I) thiocyanate with **1** (Scheme 3) led to different products when the amount of **1** was varied, virtually paralleling the reactivity patterns observed in the AgCl–**1** system. Thus, the reaction of AgSCN with one molar equivalent of **1** led to a cuboidal tetrameric complex **7**, whereas the reaction at a Ag : P ratio of 1 : 2 produced a symmetrical, thiocyanato-bridged dimer $[Ag(\mathbf{1}\text{-}\kappa P)_2(\mu\text{-SCN-}S,N)]_2$ (**8**). Complexes **7** and **8** have different $^1$H NMR signatures (in solution), and their $^{31}$P NMR resonances were observed at $\delta_P$ *ca.* −1.0 and −2.6 ppm, respectively. The bands of the uncoordinated nitrile groups ($\nu_{C\equiv N}$) in their IR spectra were observed at positions similar to **1–5**. On the other hand, the absorptions attributable to stretching vibrations of the thiocyanate groups differ ($\nu_{max}$/cm$^{-1}$; **7**: 2122 m + 2094 vs **8**: 2098 vs), reflecting different roles of these anionic ligands.

Repeated crystallization experiments with **7** only yielded poor-quality crystals. For instance, those utilized for X-ray diffraction analysis contained heavily disordered chloroform (the pendant $C_5H_4CN$ moieties were also partly disordered) and suffered from twinning. Although these complications lowered the overall precision, the structural determination is unambiguous.

Compound **7** (Fig. 5) crystallized with four complete tetramers per monoclinic unit cell (space group *P*2/*n*) and with two halves of the $[Ag(\mathbf{1}\text{-}\kappa P)(\mu\text{-SCN})]_4$ array in the asymmetric unit, each located around the crystallographic two-fold axis. The thiocyanate groups act as S,N-bridges between two silver atoms at the elongated $Ag_2(SCN)_2$ faces. Their sulfur atoms further coordinate silver atoms in adjacent $Ag_2(SCN)_2$ moieties and thus interlink the final cuboidal assembly. Such an arrangement formally corresponds with the bonding ability of the SC≡N moiety, namely with the number of lone electron pairs available at the N and S atoms, and can be alternatively described as a dimer of dimers (*i.e.*, as $[\{(\mathbf{1}\text{-}\kappa P)Ag(SCN)\}_2]_2$), as was suggested for the only analogous compound whose crystal structure was determined: $[(Ph_2PPy\text{-}\kappa P)Ag(\mu\text{-SCN-}S,S,N)]_4$ (Py = 2-pyridyl).[35]

The two independent heterocubanes found in the structure of **7** differ only marginally, and their geometry is generally similar to that of the mentioned $Ph_2PPy$ analogue. Each silver atom in **7** is surrounded by two sulfur atoms, a thiocyanate nitrogen and a phosphine phosphorus, forming a distorted tetrahedral donor set (see parameters in Table 3). The distances between Ag1 and the two bonded sulfur atoms (S20 and S10′) differ by *ca.* 0.13 Å. A similar feature is also observed for Ag4, while the Ag2 and Ag3 atoms bind to their two *S*-thiocyanate ligands more symmetrically. The SCN-bridged edges of the cuboidal assembly are bent at the nitrogen atoms

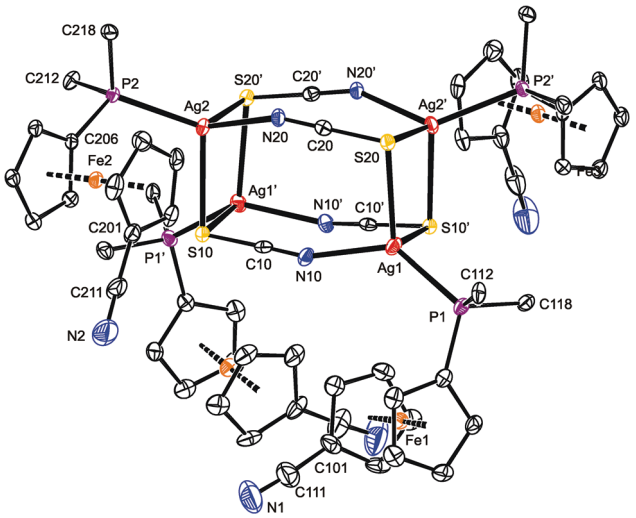


Fig. 5 PLATON plot of one of the structurally independent heterocubane molecules in the structure of solvated **7** at the 30% probability level. The prime-labeled atoms are generated by the crystallographic two-fold axis. For clarity, hydrogen atoms and phenyl ring carbons (except for pivotal ones) are omitted.

Table 3 Selected geometric parameters for the two independent tetrameric cages in the structure of solvated complex **7** (in Å and °)[a]

| Molecule 1 | | Molecule 2 | |
|---|---|---|---|
| Ag1–S20 | 2.652(1) | Ag3–S40 | 2.660(1) |
| Ag1–N10 | 2.214(5) | Ag3–N30 | 2.227(5) |
| Ag1–S10′ | 2.782(1) | Ag3–S30′ | 2.770(2) |
| Ag1–P1 | 2.389(1) | Ag3–P3 | 2.391(1) |
| S20–Ag1–N10 | 96.7(1) | S40–Ag3–N30 | 97.0(1) |
| S20–Ag1–S10′ | 95.80(4) | S40–Ag3–S30′ | 96.62(4) |
| N10–Ag1–S10′ | 97.3(1) | N30–Ag3–S30′ | 96.3(1) |
| P1–Ag1–S20 | 122.19(5) | P3–Ag3–S40 | 121.23(5) |
| P1–Ag1–N10 | 132.8(1) | P3–Ag3–N30 | 131.8(1) |
| P1–Ag1–S10′ | 103.55(4) | P3–Ag3–S30′ | 106.18(5) |
| Ag2–S10 | 2.648(1) | Ag4–S30 | 2.638(1) |
| Ag2–N20 | 2.262(4) | Ag4–N40 | 2.241(5) |
| Ag2–S20′ | 2.660(1) | Ag4–S40′ | 2.672(2) |
| Ag2–P2 | 2.397(1) | Ag4–P4 | 2.387(1) |
| S10–Ag2–N20 | 100.2(1) | S30–Ag4–N40 | 100.5(1) |
| S10–Ag2–S20′ | 98.90(4) | S30–Ag4–S40′ | 99.56(4) |
| N20–Ag2–S20′ | 98.3(1) | N40–Ag4–S40′ | 100.8(1) |
| P2–Ag2–S10 | 110.44(4) | P4–Ag4–S30 | 110.88(5) |
| P2–Ag2–N20 | 126.3(1) | P4–Ag4–N40 | 127.5(1) |
| P2–Ag2–S20′ | 118.16(4) | P4–Ag4–S40′ | 113.69(5) |

[a] The prime-labeled atoms are generated by crystallographic two-fold axes (*N.B.* the symmetry operations are different for molecules 1 and 2).

(Ag–N–C angles: 151.2(4)–157.8(4)°), which in turn results in an expansion of the central part of the heterocubane core, albeit without any notable twisting at the $Ag_2(SCN)_2$ faces.[36]

As indicated above, compound **8** is a dimer in which the thiocyanate anions interconnect two Ag(1-κ*P*)$_2$ units (Fig. 6). In the crystal, its molecules are arranged around the inversion centers and, hence, only their half is structurally independent. Analogous structures have been reported for $[L_2Ag(\mu\text{-SCN-}S,N)]_2$ with various monophosphine (L = $PPh_3$,[37] $P(C_6H_4Me\text{-}4)_3$,[38] $P(C_6H_4F\text{-}4)_3$ [39] and $Ph_2PPy$)[35] and chelating diphosphine donors.[40] Similar to these compounds, the Ag–S3 and Ag–N3 distances in **8** are longer than the sum of the respective covalent radii ($\sum r_{cov}$ = 2.50 (Ag/S) and 2.16 (Ag/N) Å).

The eight-membered ring in the structure of **8** is rectangular in shape due to the presence of the rigid, rod-like SCN bridges and the fact that the S–Ag–N angle of 93.79(4)° departs considerably from the tetrahedral value, being diminished due to the steric demands of the Ag-bound phosphines. The central $(AgSCN)_2$ ring has a chair-like conformation (Fig. S11†) with the silver atoms displaced by 0.541(1) Å above and below the "central" $(SCN)_2$ plane.[41] The latter plane thus appears tilted by 14.2(7)° with respect to the {Ag, S3, N3′} plane but is perpendicular to the plane defined by atoms Ag, P1, and P2. Even in this case, the nitrile substituents at the ferrocene units remain uncoordinated and are directed away from the phosphine groups ($\tau$ = 152.0(1)° (Fe1) and 141.0(1)° (Fe2)).

To complete our investigation of the reactions of **1** with silver(I) halides and pseudohalides, reaction tests were also performed with silver(I) fluoride. Unfortunately, experiments with AgF were complicated by the highly hygroscopic nature of this salt and typically led to non-crystallizing, extensively decomposed reaction mixtures. Nonetheless, several of the repeated experiments performed with AgF and **1** at Ag : **1** ratios of both 1 : 1 and 1 : 2 provided few crystals (always along with a black tarry material) that were structurally characterized as a dimer similar to **3** but with linear $HF_2^-$ bridges between the Ag(I) centers, $[Ag(\mathbf{1}\text{-}\kappa P)_2(\mu\text{-}HF_2)]_2$ (**9**). Unfortunately, all crystals obtained were affected by a substitutional disorder, resulting from the alternation of $HF_2^-$ and chloride anions as the bridges in between the sterically encumbered Ag(**1**-κ*P*)$_2$ units.[42] The chloride ions necessary for the formation of **3** most likely came from the starting silver(I) salt[43] or arose *via* decomposition of the halogenated solvent. Yet another experiment at a Ag : **1** molar ratio of 1 : 2 resulted in few crystals that —despite their low quality and extensive disorders—allowed the product to be unequivocally formulated as a hexafluorosilicate-bridged disilver(I) complex, $[(\mu\text{-}SiF_6)\{Ag(\mathbf{1}\text{-}\kappa P)_2\}_2]$ (**10**). Obviously, some hydrogen fluoride was formed by decomposition of the hygroscopic AgF during the crystallization, which in turn reacted with the starting AgF and **1** (or any **1**–AgF intermediate) to afford compound **9** or attacked the glass tube used for crystallization, producing some $H_2[SiF_6]$ (or any hexafluorosilicate salt) and then complex **10**. These rather unexpected results prompted us to attempt at a reproducible synthesis of **10** and, mainly, to study the Ag(I)–**1** complexes with "non-coordinating" supporting anions in more detail.

To prepare **10** in a rational manner, defined $Ag_2[SiF_6]$ was synthesized from $Ag_2O$ and $H_2[SiF_6]$ and reacted with four equivalents of the phosphinonitrile ligand in chloroform. The resulting mixture displayed a very broad $^{31}P$ NMR resonance at around $\delta_P$ −2. The $^{19}F$ NMR spectrum revealed one singlet at $\delta_F$ −131 with $^{29}Si$ satellites ($^1J_{SiF}$ = 115 Hz),[44] suggesting a rapid interchange or no interaction between Ag(I) and the anion in solution. The IR spectrum of crystalline **10** contained band attributable to the ligand's C≡N group and solvating acetone at 2223 $cm^{-1}$ and 1705 $cm^{-1}$, respectively, and a strong band due to the hexafluorosilicate anion ($\nu_3$ vibration at 749 $cm^{-1}$).

Crystallization from chloroform–acetone/hexane afforded orange crystals of **10**·½$CHCl_3$·½$Me_2CO$, which were structurally characterized. The compound crystallizes with the symmetry of the monoclinic space group *C*2/*c*, with both the solvent molecules and the nitrile groups disordered (Fig. 7 and Table 4). Otherwise, however, the molecular symmetry is rather high because the silicon atom resides on the inversion center, which in turn renders only the half of the complex molecule structurally independent. The hexafluorosilicate anion, symmetrically placed between two Ag(**1**-κ*P*)$_2$, forms two Si–F→Ag bridges toward each silver(I) ion. Coordination of the $[SiF_6]^{2-}$ anion results in a slight yet statistically significant elongation of the bridging Si–F bonds (*cf.* Si–F1/2 = 1.691(2)/1.704(2) Å *vs.* Si–F3 = 1.669(2) Å (ref. 45)), though without angular distortion of the octahedral anion (see the *cis*-F–Si–F angles in Table 4). Because the bridging fluorine atoms are a part of the $[SiF_6]^{2-}$ anion and thus occur in constrained proximal positions, the donor array around Ag(I) departs from a regular tetrahedron even more than in the other structurally characterized compounds that comprise two Ag(I)(**1**-κ*P*)$_2$

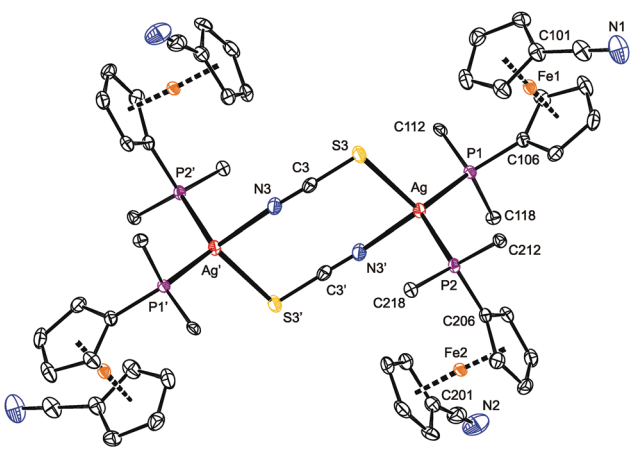


**Fig. 6** PLATON plot of **8** showing the 30% probability displacement ellipsoids. The prime-labeled atoms were generated by crystallographic inversion. Hydrogen atoms and phenyl carbons (except for pivotal ones) are omitted for clarity. Selected distances and angles (in Å and °): Ag–P1 2.4589(5), Ag–P2 2.4763(5), Ag–S3 2.6365(5), Ag–N3′ 2.338(2), S3–C3 1.658(2), C3–N3 1.157(3), N1–C111 1.140(3), N2–C211 1.145(3), P1–Ag–P2 120.27(2), P1–Ag–S3 116.06(2), P2–Ag–S3 107.71(2), P1–Ag–N3′ 108.15(4), P2–Ag–N3′ 107.28(4), S3–Ag–N3′ 93.79(4), Ag–S3–C3 99.29(7), S3–C3–N3 178.7(2), C3–N3–Ag′ 158.0(2).

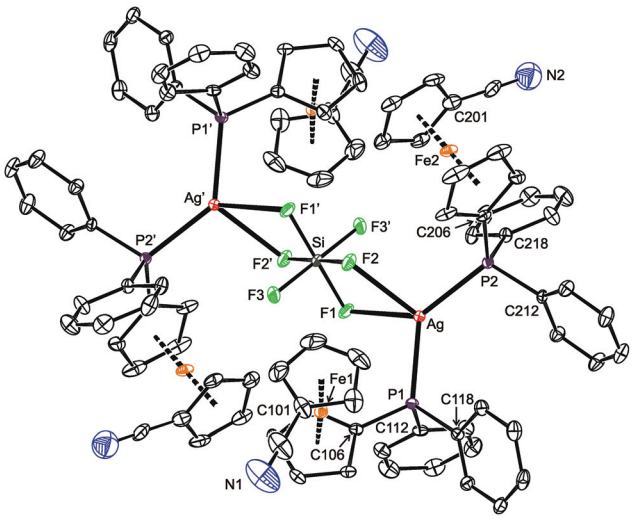


Fig. 7 PLATON plot of the complex molecules in the structure of solvated **10**, showing displacement ellipsoids at the 30% probability level. For clarity, the hydrogen atoms and the less populated orientation of the disordered C≡N group at ligand 2 (Fe2) are omitted. Note: the prime-labeled atoms are generated by crystallographic inversion.

Table 4 Selected interatomic distances and angles for solvated **10** (in Å and °)

| | | | |
|---|---|---|---|
| Ag–P1 | 2.421(1) | P1–Ag–P2 | 132.44(3) |
| Ag–P2 | 2.4160(9) | P1–Ag–F1 | 89.93(6) |
| Ag–F1 | 2.542(2) | P1–Ag–F2 | 122.30(6) |
| Ag–F2 | 2.482(2) | P2–Ag–F1 | 130.00(6) |
| Si–F1 | 1.691(2) | P2–Ag–F2 | 103.08(6) |
| Si–F2 | 1.704(2) | F1–Ag–F2 | 56.68(7) |
| Si–F3 | 1.669(2) | *cis*-F–Si–F | 89.3(1)–90.7(1) |

moieties connected by anionic bridging ligands. This distortion is clearly manifested in the interligand angles ranging from 56.68(7)° for F1–Ag–F2 to 132.44(3)° for P1–Ag–P2. Because of the twisting, the {Ag, F1, F2} and {Ag, P1, P2} planes are rotated by 56.1(1)°, and the central $Ag(\mu\text{-}F)_2Si(\mu\text{-}F)_2Ag$ moiety is undulated (the dihedral angle of the {Ag, F1, F2} and {Si, F1, F2} planes is 18.77(9)°; see Fig. S13†).

While the Ag–P bond lengths in **10** fall within the common ranges and below the sum of the covalent radii (2.421(1) and 2.4160(9) for P1 and P2, respectively; $\sum r_{cov}$ = 2.52 Å), the Ag–F distances of 2.542(2) and 2.482(2) Å for F1 and F2, respectively, are considerably longer than the sum of the covalent radii ($\sum r_{cov}$ = 2.02 Å) as well as the Ag–F separations in the "true" fluoride-bridged complex $[(\mu\text{-}F)\{AgL\}_2][BF_4]$ (L = 1,3-bis(2,6-diisopropylphenyl)imidazol-2-ylidene; 2.0671(7) and 2.0672(7) Å).[46] This suggests a predominantly electrostatic nature of the interaction between the Ag(I)(**1**-κ*P*)$_2$ units and the hexafluorosilicate anion whose closer contact is sterically hindered (*N.B.* the anion is surrounded by four sterically demanding phosphinoferrocene moieties). In fact, the structure of **10** can be adequately compared with only $[Ag(MeCN)_2]_2[SiF_6]$ in which the hexafluorosilicate anion interacts with four adjacent Ag(I) ions (twice *via* two and twice through one fluorine atom).[47]

## DFT study of the bridged disilver(I) complexes

Peculiar structural features detected in the solid-state structures of **3**·$CH_2Cl_2$, **8** and **10** led us to investigate the bonding situation in these compounds theoretically using DFT calculations (details are given in the ESI†). As mentioned earlier, in many cases, the observed bonding distances, particularly the Ag–X (X = S, N, Cl and F) "dative bonds" in these compounds, were found to be significantly longer than sum of the corresponding covalent radii, raising the question of whether the bonding has more ionic than covalent character. A useful clue about ionicity can be derived from the partial charges assigned by a population analysis. Although this assignment is somewhat arbitrary, as can be demonstrated by the sole existence of several dozens of such partitioning schemes, the concept of partial charges proved to be quite useful. We used a natural population analysis (NPA)[48] that has a rather small basis-set dependence, but even the results of the basic Mulliken population analysis were similar. In general, there is no correlation between the charge transfer and strength of a donor–acceptor bond.[49] For this reason, we also followed an unambiguous description of bonding using the properties of the experimentally observable electron density, applying the concepts from the Atoms in Molecules (AIM) theory.[50] Herein, we give contour plots of the electron density in planes defined by the Ag center and two coordinated atoms as well as their Laplacian, the sum of the second partial derivatives with respect to coordinates. The latter quantity indicates the local concentration of electrons if negative and depletion if positive. Negative values of the density Laplacian around a critical bond point (the saddle point of the electron density) indicate the formation of a covalent bond with electrons concentrated in this region.[49] For ionic bonds, no such negative region exists, and the density Laplacian remains positive. This property allows for distinguishing between different types of bonding.

The bonding situation for compound **3** is depicted in Fig. 8 (for additional plots, see the ESI†). Already on the electron density map, one can see an increased bonding density between the Ag and P centers, but no such charge concentration between Ag and Cl. The same projection mapping the Laplacian of the electron density reveals a negative basin between Ag and P and a positive region between Ag and Cl. The NPA charges (in units of the elementary charge) for Ag, P and Cl in **3** are 0.52, 0.88 and −0.74, respectively, corroborating an ionic nature of the Ag–Cl bonding interaction.

In complex **8**, the other coordination partners of Ag(I) (besides the phosphine) are the N and S atoms of the thiocyanate ligand. The NPA charges for Ag, P, N and S are 0.48, 0.90, −0.59 and −0.30, respectively (the nitrogen in the SCN ligand is significantly more negative than sulfur, which corresponds to its higher electronegativity). The character of the nitrogen coordination can be thus described as more ionic, whereas that of sulfur is more covalent, as further indicated by a basin in the negative Laplacian of the electron density shown in Fig. 9. The situation observed for complex **10** (Fig. 9) is quite similar to **3**. The sum of the covalent radii for Ag and F

 

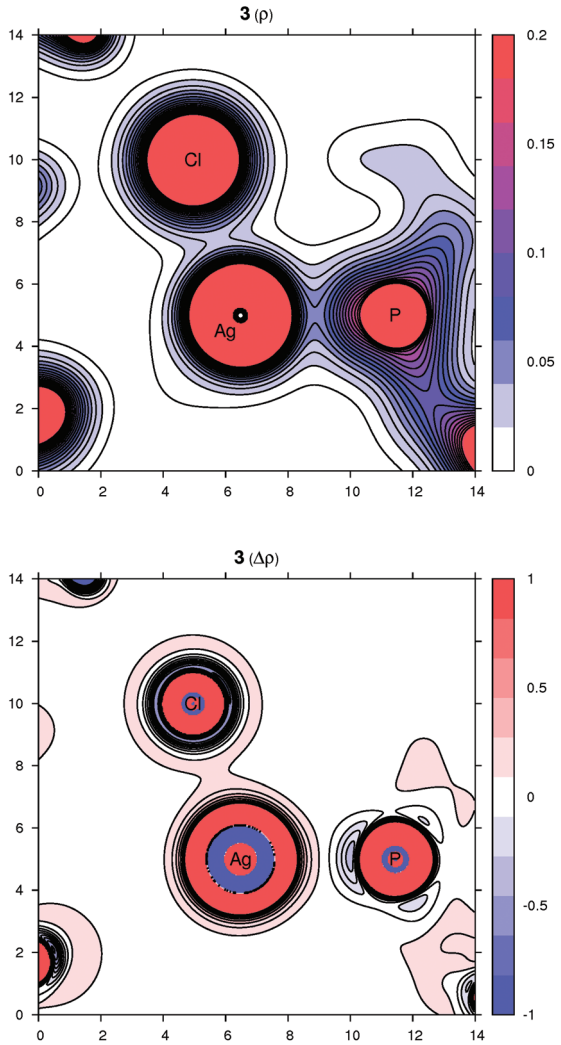


Fig. 8 Contour plots of the electron density $\rho(r)$ (top) and its Laplacian $\Delta\rho(r)$ (bottom) in the plane defined by Ag, P and Cl atoms for compound **3**. All values are in atomic units.

is again significantly shorter than the observed Ag–F separation, suggesting a prevalently electrostatic interaction between the Ag(I) center and bridging anion. This observation is in agreement with the calculated NPA partial charges for Ag, P, F and Si of 0.56, 0.88, −0.67 and 2.46, respectively, and also with the area of negative density Laplacian found between Ag and F (Fig. 9). In contrast, the P→Ag dative bonds retained their covalent nature in all studied cases (see additional plots in the ESI†).

### Complexes resulting from Ag(I) salts with weakly coordinating anions

The phosphinonitrile ligand **1** in all its Ag(I) complexes with anionic supporting ligands mentioned above behaves as a simple phosphine. In order to enforce the coordination of the nitrile moiety, we next investigated reactions between **1** and silver(I) salts with common "non-coordinating" anions,[51] *viz.* $AgClO_4$, $Ag[BF_4]$ and $Ag[SbF_6]$. Indeed, the reactions performed with these salts at a 1 : 1 Ag : **1** molar ratio afforded symmetric, dimer-like disilver(I) complexes **11–13** in which the two equivalent Ag(I) centers are connected by two P,N-bridging phosphinonitrile ligands (Scheme 4). However, the coordination environments of the Ag(I) ions (in the solid state) are completed by compensating anions ($ClO_4^-$ and $[BF_4]^-$) or the solvent used during crystallization (ethyl acetate in the case of the $[SbF_6]^-$ salt).

The IR spectra of solid perchlorate **11** and tetrafluoroborate **12** contain bands related to $\nu_{C\equiv N}$ at 2272/2283 $cm^{-1}$ and at 2275/2285 $cm^{-1}$. The shift of these bands to higher energies relative to free **1** suggests a low contribution of π-back bonding to the C≡N→Ag interaction.[52] Also observed are strong bands characteristic of the anions, namely composite $\nu_3$ bands of $ClO_4^-$ and $BF_4^-$ at 1025–1125 and 995–1100 $cm^{-1}$, respectively.

Because the product isolated from the reaction of **1** with $Ag[SbF_6]$ proved to be poorly soluble, it was recrystallized from ethyl acetate/hexane.[53] Under such conditions, however, the plausible "primary" product was converted to $[Ag\{\mu(P,N)\text{-}\mathbf{1}\}(AcOEt\text{-}\kappa O)]_2[SbF_6]_2$ (**13**). The coordination of the solvent is indicated by a strong $\nu_{C=O}$ band in the IR spectrum of the crystallized sample at 1703 $cm^{-1}$, shifted toward lower energies with respect to ethyl acetate itself (1742 $cm^{-1}$ in a $CCl_4$ solution).[54] The $\nu_{C\equiv N}$ bands are observed at 2255 (m), 2267 (s) and 2280 (m) $cm^{-1}$, while the $[SbF_6]^-$ anion gives rise to a strong band at 661 $cm^{-1}$.

Compounds **11** and **12** are isostructural and crystallize as compact dimers around the crystallographic inversions centers (Fig. 10, parameters in Table 5). The O- and F-monodentate anions are located within the pocket defined by the bulky phosphinoferrocene moieties. While the Ag–P and Ag–N bond lengths are less than the sum of the covalent radii, suggesting a real bonding interaction, the distances between the silver(I) centers and O or F donor atoms from the anions markedly exceed the respective "threshold" values ($\sum r_{cov}$ = 2.11 (Ag/O) and 2.02 (Ag/F) Å). The P–Ag–N angles in **11** and **12** are *ca.* 156° and 162°, respectively, with the more acute angle for **11** reflecting a closer approach of the "additional" donor to silver. Otherwise, however, these angles suggest the cationic Ag(I) centers to be essentially linearly dicoordinate, weakly interacting with the counter anions. Such a description is in line with the results of the DFT computations (*vide infra*).

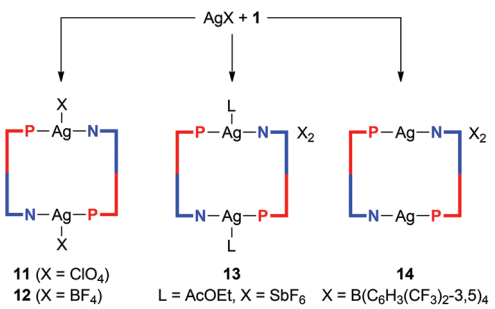


Scheme 4 Synthesis of disilver(I) complexes **11–14**.

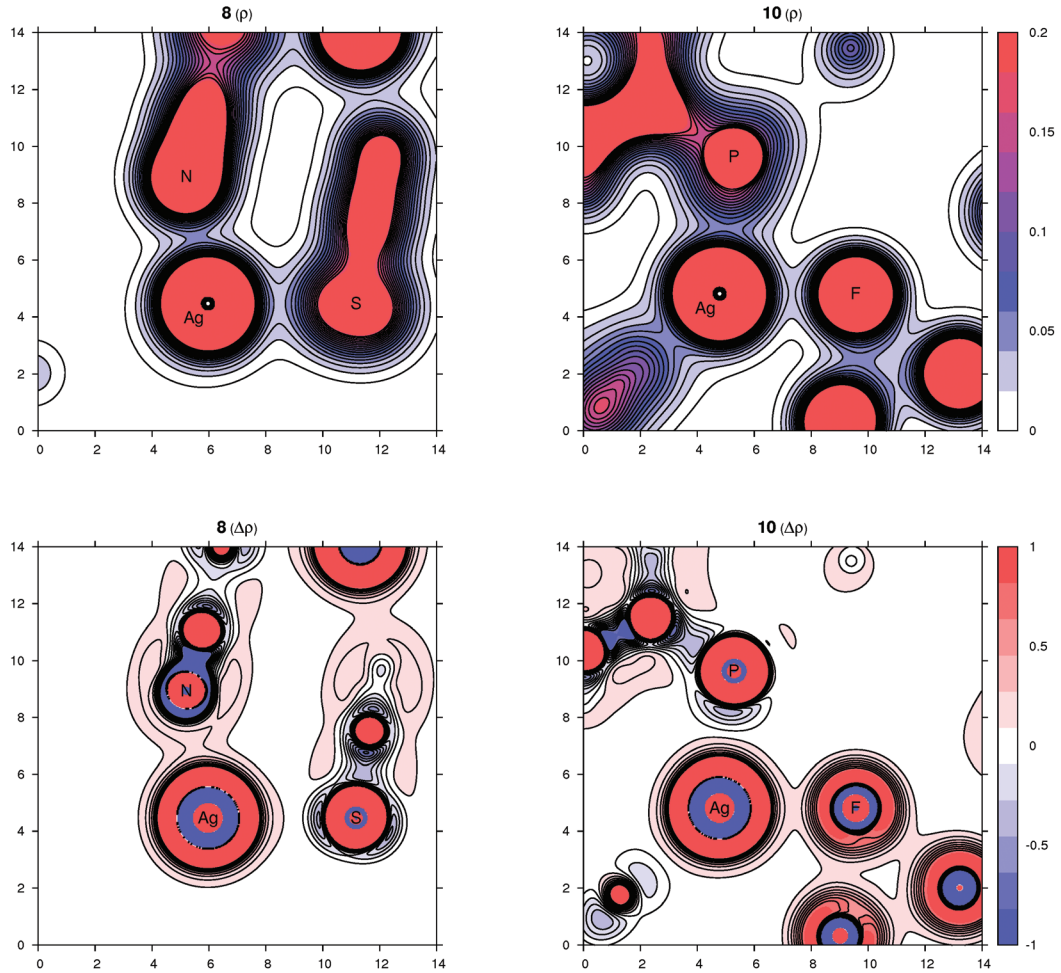


Fig. 9 Contour plots of the electron density $\rho(r)$ (top panel) and its Laplacian $\Delta\rho(r)$ (bottom panel) for compounds **8** (left part) and **10** (right part) in planes defined by three atoms whose symbols are shown. All values are in atomic units.

The ferrocene units in **11** and **12** exert negligible tilting (1.2(2)° and 1.6(1)°) and their substituents, now both involved in coordination, adopt positions approximately halfway between synclinal eclipsed ($\tau$ = 72°) and anticlinal staggered ($\tau$ = 108°). In such a conformation, the C6–P and C1–CN bonds are nearly perpendicular,[55] giving rise to a side-by-side arrangement of the two Ag(**1**) subunits. The $PPh_2$ moiety is oriented such that the Ag–P bond is directed inward the $Ag_2(\mathbf{1})_2$ core.[56] The CN bond lengths in **11** and **12** are the same (within the 3σ-level) as in uncoordinated **1** (1.144(2) Å).[16]

As opposed to the structures of **11** and **12**, the ethyl acetate in **13** is directed to the sides of the $Ag_2(\mathbf{1})_2$ core and displaced away from its center (Fig. 11). The coordinated oxygen atom is closer to the Ag-bound phosphorus, diminishing the P–Ag–O1S and opening the N–Ag–O1S angle. As judged from the displacement of the Ag atom from the plane of the directly bonded atoms, P, N′ and X [0.076(1) Å for **11** (X = O1), 0.116(1) Å for **12** (X = F1), and 0.227(1) Å for **13** (X = O1S)], twisting of the coordination environment of the Ag(I) ion increases from **11** through **12** to **13**. On the other hand, the conformation of the ferrocene ligand in **13** is nearly the same as in **11** and **12**.

Eventually, the elusive $[Ag_2(\mathbf{1})_2]^{2+}$ complex devoid of any additional ligands at the Ag(I) ions was obtained from the reaction between **1** and the silver(I) salt with tetrakis[3,5-bis(trifluoromethyl)phenyl]borate (BARF) anion (Scheme 4). The $^{31}$P NMR spectrum of **14** displays a doublet at $\delta_P$ 5.5 ppm with $^1J_{AgP}$ = 765 Hz, the relatively large $^1J_{AgP}$ coupling constant being in accordance with the presence of linear, sp-hybridized silver.[23,57] The $\nu_{C\equiv N}$ bands in the IR spectrum of a crystalline sample are observed at 2282 (w) and 2258 (s) $cm^{-1}$.

The structure of $[Ag_2\{\mu(P,N)\text{-}\mathbf{1}\}_2][BARF]_2$ (**14**; see Fig. 11) resembles that of the analogous Au(I) complexes $[Au_2\{\mu(P,N)\text{-}\mathbf{1}\}_2]X_2$, where X = $N(SO_2CF_3)_2$ and $[SbF_6]$,[17] consisting of discrete dimeric units $[Au_2(\mathbf{1})_2]^{2+}$ and isolated anions. Because of the absence of an additional donor protruding into the coordination sphere of Ag(I), the Ag–P/N distances in **14** are slightly shorter, the P–Ag–N angle is less acute,[58] and the ferrocene substituents are rotated closer to each other ($\tau$ = 80.1(2)°, tilt angle: 2.7(2)°) than in the structures of **11–13**. Additionally, the Ag···Ag distances in **14** are the shortest among complexes **11–14**, with the observed trend (**14** < **12** < **11** < **13**) reflecting

 

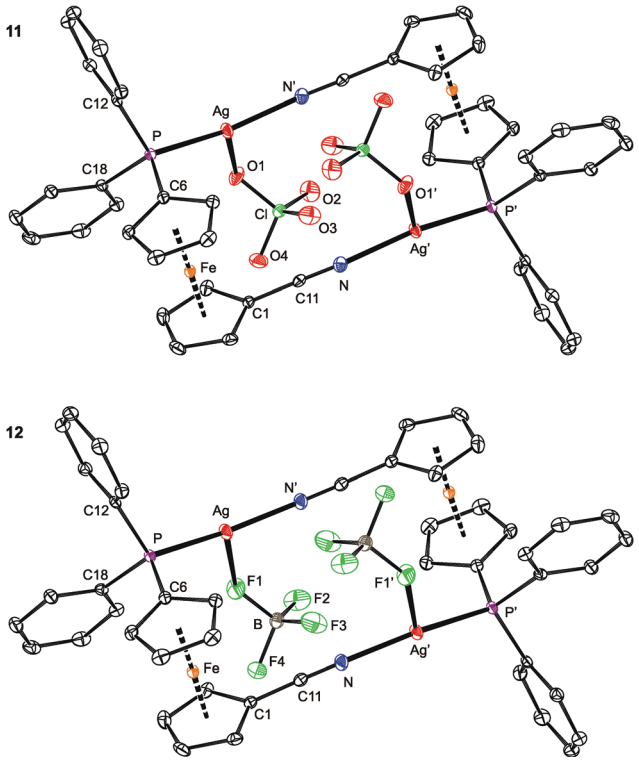


Fig. 10 PLATON plots of the molecular structures of **11** (top) and **12** (bottom) showing displacement ellipsoids at the 30% probability level. The hydrogen atoms are omitted for clarity. Note: the prime-labeled atoms are generated by crystallographic inversion.

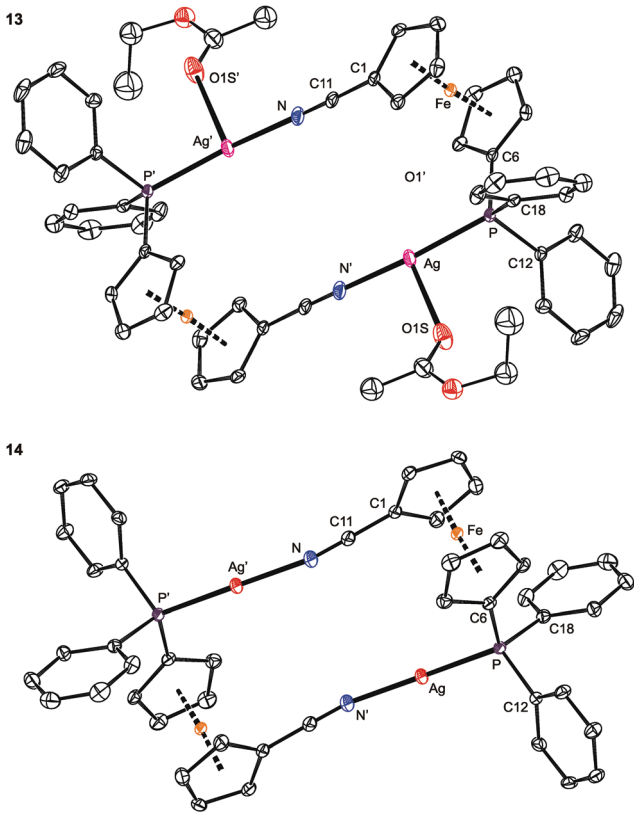


Fig. 11 PLATON plots of the complex cations in the structures of **13** (top) and **14** (bottom). Displacement ellipsoids enclose the 30% probability level. All hydrogen atoms are omitted, and only one position of the disordered ethyl acetate is shown (for **13**) for clarity. Complete structural diagrams are available in the ESI.†

**Table 5** Selected geometric parameters for disilver(I) complexes **11–14** (in Å and °)[a]

| Parameter | **11**[b] | **12**[c] | **13**[d] | **14** |
|---|---|---|---|---|
| X | O1 | F1 | O1S | None |
| Ag–P | 2.3564(7) | 2.3513(5) | 2.3583(9) | 2.3508(6) |
| Ag–N | 2.141(2) | 2.124(2) | 2.133(3) | 2.120(2) |
| Ag–X | 2.550(2) | 2.624(2) | 2.648(3) | n.a. |
| P–Ag–N | 156.50(6) | 161.87(5) | 161.67(8) | 169.36(7) |
| P–Ag–X | 112.59(4) | 109.79(4) | 92.90(7) | n.a. |
| N–Ag–X | 90.45(7) | 87.03(6) | 100.2(1) | n.a. |
| Ag···Ag | 5.6145(3) | 5.5859(3) | 5.9009(5) | 5.4674(3) |
| C≡N | 1.140(3) | 1.139(3) | 1.135(5) | 1.135(3) |
| C≡N–Ag | 171.7(2) | 171.2(2) | 170.8(3) | 168.8(2) |
| $\tau$ | 87.2(2) | 85.9(1) | −87.1(3) | 80.1(2) |

[a] n.a. = not applicable. [b] Further data: Cl–O1 1.447(2), Cl–O2 1.419(2), Cl–O3 1.431(2), Cl–O4 1.440(2). [c] Further data: B–F1 1.398(3), B–F2 1.364(3), B–F3 1.365(3), B–F4 1.397(3). [d] Further data: C1S–O1S 1.211(5).

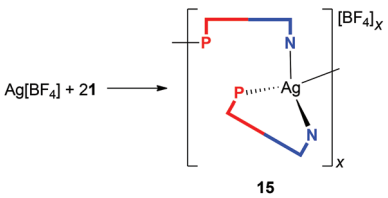


Scheme 5 Reaction of $Ag[BF_4]$ with **1** at a 1 : 2 metal-to-ligand ratio, leading to **15**.

the presence and size of the additional ligands coordinated to the $[Ag_2(\mathbf{1})_2]^{2+}$ moiety.

Upon increasing the amount of ligand **1** to 2 or even 3 equiv., the reaction with $Ag[BF_4]$ proceeded differently, leading to an unusual coordination polymer $[Ag\{\mu(P,N)\text{-}\mathbf{1}\}(\mathbf{1}\text{-}\kappa^2P,N)]_n[BF_4]_n$ (**15** in Scheme 5).[59] The IR spectrum of crystalline **15** contains three bands attributable to C≡N stretching vibrations at 2242, 2228 and 2214 $cm^{-1}$, all shifted to lower wavenumbers compared to those of the dimeric complex **12**. The anion gives rise to a strong composite band between *ca.* 1085–1025 $cm^{-1}$.

Presumably because of its polymeric nature, compound **15** proved to be very difficult to crystallize. Eventually, one of the numerous repeated experiments, during which the solvents, sample concentration, temperature and mode of crystallization were varied, produced crystals of solvate **15**·AcOEt that were suitable for X-ray diffraction analysis. The crystal structure of **15**·AcOEt (Fig. 12 and Table 6) revealed tetracoordinate Ag(I) centers, ligated from two bridging phosphinonitrile ligands responsible for linear propagation of the polymeric chain and further by another molecule of **1** bonded in a P,N-chelating manner. Such a particular combination of P,N-bridging[60] and

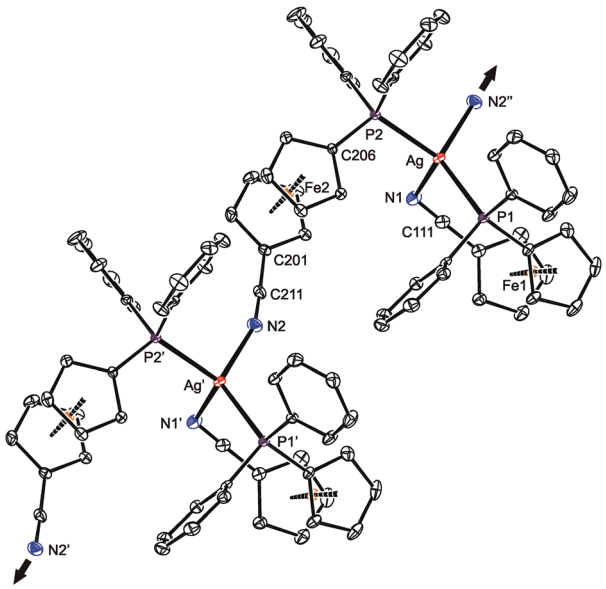


Fig. 12 Section of the infinite polymeric chain in the structure of **15**·AcOEt (30% probability ellipsoids). Hydrogen atoms are omitted for clarity. The arrows indicate the propagation of the linear assembly.

Table 6 Selected distances and angles for **15**·AcOEt (in Å and °)[a]

| | | | |
|---|---|---|---|
| Ag–P1 | 2.4345(7) | Ag–P2 | 2.4402(7) |
| Ag–N1 | 2.485(2) | Ag–N2$^{i}$ | 2.330(2) |
| P1–Ag–N1 | 100.35(5) | P2–Ag–N2$^{i}$ | 99.65(6) |
| P1–Ag–N2$^{i}$ | 120.83(6) | P2–Ag–N1 | 108.90(6) |
| P1–Ag–P2 | 129.20(2) | N1–Ag–N2$^{i}$ | 90.94(8) |
| C111–N1 | 1.150(3) | C211–N2 | 1.136(3) |
| C101–C111–N1 | 178.7(3) | C201–C211–N2 | 177.9(3) |
| C111–N1–Ag | 109.4(2) | C211–N2–Ag$^{ii}$ | 159.9(2) |
| $\tau_1$ | 5.6(2) | $\tau_2$ | 144.6(2) |
| $\varphi_1$ | 5.3(2) | $\varphi_2$ | 2.1(1) |

[a] Symmetry operations: i = $x + 1, y, z$; ii = $x - 1, y, z$. $\tau_n$ is the torsion angle Cn1–C*gn*1–C*gn*2–C*n*6, $\varphi_n$ is the dihedral angle of the cyclopentadienyl planes.

chelating coordination of a phosphinonitrile donor is unprecedented and leads to an abnormal geometry at the C≡N–Ag fragment.

As stated above, compound **15** is a coordination polymer in which one of the phosphinonitrile donors bridges two adjacent Ag(I) centers related by elemental translation along the crystallographic axis *a* in the space group $P2_12_12_1$. The silver(I) ion in **15** possesses a distorted tetrahedral $P_2N_2$ donor set. While the Ag–P distances to the two phosphine groups are similar in length, the Ag–N1 separation pertaining to the chelating ligand is significantly longer (by *ca.* 0.16 Å) than the Ag–N2 bond involving the bridging phosphinonitrile, but both Ag–N distances are well below the sum of the covalent radii ($\sum r_{cov}$ = 2.16 Å). The CN group of the bridging ligand is coordinated with a departure from linearity (Ag–N≡C ≈ 160°) but is still within the ranges common for Ag(I) complexes with nitrile donors (see the distribution in Fig. 13).[18] In contrast, the Ag–N≡C angle of *ca.* 109° found for the chelating ligand is

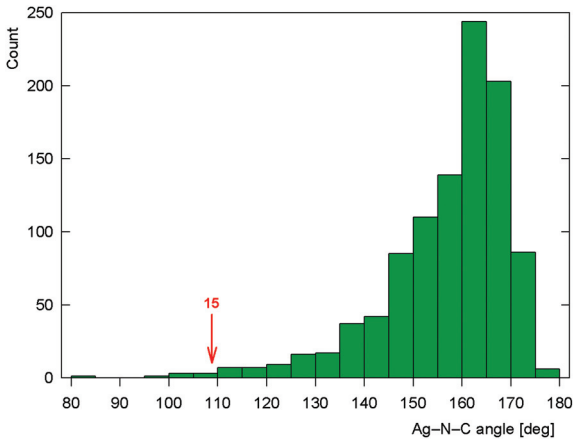


Fig. 13 Histogram showing the distribution of the C≡N–Ag angles in the structurally characterized Ag–nitrile complexes (the angle encountered for chelating **1** in complex **15** is indicated).

unusually acute. Indeed, compounds with C≡N–Ag angles below 110° are not entirely unprecedented but remain quite scarce, being found in only 5 out of 1016 C≡N–Ag fragments (<0.5%)[61] encountered in 853 structurally characterized Ag(I)–nitrile complexes featuring the C–C≡N–Ag moieties (repeated structure determinations are not excluded). In neither case, however, the coordinated bent nitrile group is a part of a simple chelating ligand. Furthermore, the geometry encountered in the crystal structure of **15** also differentiates this compound from transition metal complexes with $\eta^2$-coordinated nitriles, in which the C≡N bonds are oriented laterally with respect to the metal center and bonded in an approximately symmetrical fashion (*i.e.*, with *d*(M–CN) ≈ *d*(M–NC); *cf.* Ag–N1/C111 of 2.485(2)/3.065(3) Å in **15**·AcOEt).[62]

Notably, the conformation of the flexible phosphinoferrocene ligands in **15** changes with their coordination mode. The ferrocene substituents in chelating **1** (Fe1) are nearly synclinal eclipsed, and the cyclopentadienyl rings are slightly tilted (by *ca.* 5°). In contrast, the ferrocene moiety in the bridging ligand has an opened conformation near ideal anticlinal eclipsed that allows for efficient bridging while maintaining a relatively compact arrangement without much steric crowding.

### DFT study of the bonding situation in 11, 12 and 15

DFT calculations suggest that the bonding situation in dimeric complexes **11** and **12** is similar to that in compounds **3** and **10**. The calculated NPA atomic charges on Ag, P and N are, in both cases, approximately 0.61, 0.88 and −0.42, respectively. The charges on the O atoms in the perchlorate anion in **11** range from −0.80 to −0.90 (the most negative being the O atom coordinated to silver), while those on the F atoms in the $BF_4^-$ anion of **12** are all *ca.* −0.56. The ionic character of the coordination of $ClO_4^-$ and $BF_4^-$ was confirmed by the positive electron density Laplacians (see the ESI†).

The coordination of the nitrile groups deserves more comments. In general, nitrile ligands are weak π-acceptors

 

with usually insignificant π-back donation,[52,63] which can be deduced from the negligible contribution of nitrile antibonding π* molecular orbitals (MOs) to the occupied MOs of the complex. The main components of the Ag–N coordination bond are thus the σ-donation of the nitrile lone pair to the silver(I) ion and the electrostatic interaction.[52] These general conclusions from MO theory are supported by AIM concept. The relevant cross-sections containing the Ag and N atoms of the electron density map and its Laplacian are shown in Fig. 14 (see also the ESI†). The region of the N atom is essentially unperturbed upon coordination and shows a charge concentration corresponding to a slight distortion of the lone electron pair on N toward the Ag(I) center. The nitrile group becomes more polarized upon coordination, with partial charges changing from −0.32 (N) and 0.30 (C) for the free ligand to −0.44 (N) and 0.42 (C) for the coordinated one in both **11** and **12**. Otherwise, the bonding region resembles the situation for the closed-shell interaction and corresponds to the Coulomb interaction between Ag and the nitrile group due to a significant partial charge on N.[49,52]

Neither σ-donation nor Coulomb interaction is sensitive to the Ag–N–C coordination angle, which explains the unusually small value of this angle observed for **15** and also applies to model compounds **F** and **G** (Scheme 6) that were studied instead of polymeric **15**. The dependence of the (relative) energy on the coordination angle is shown in Fig. 15, where the all other coordinates were relaxed and the energy was minimized with respect to them. The minima are quite shallow corresponding to approximately $1–2k_BT$ at room temperature, thus allowing for adjustment of the coordination angle due to other interactions without significant penalty.

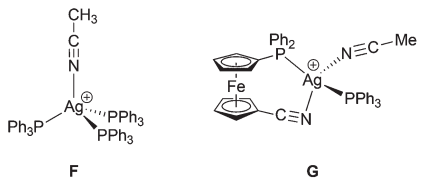


**Scheme 6** Model species for the DFT study.

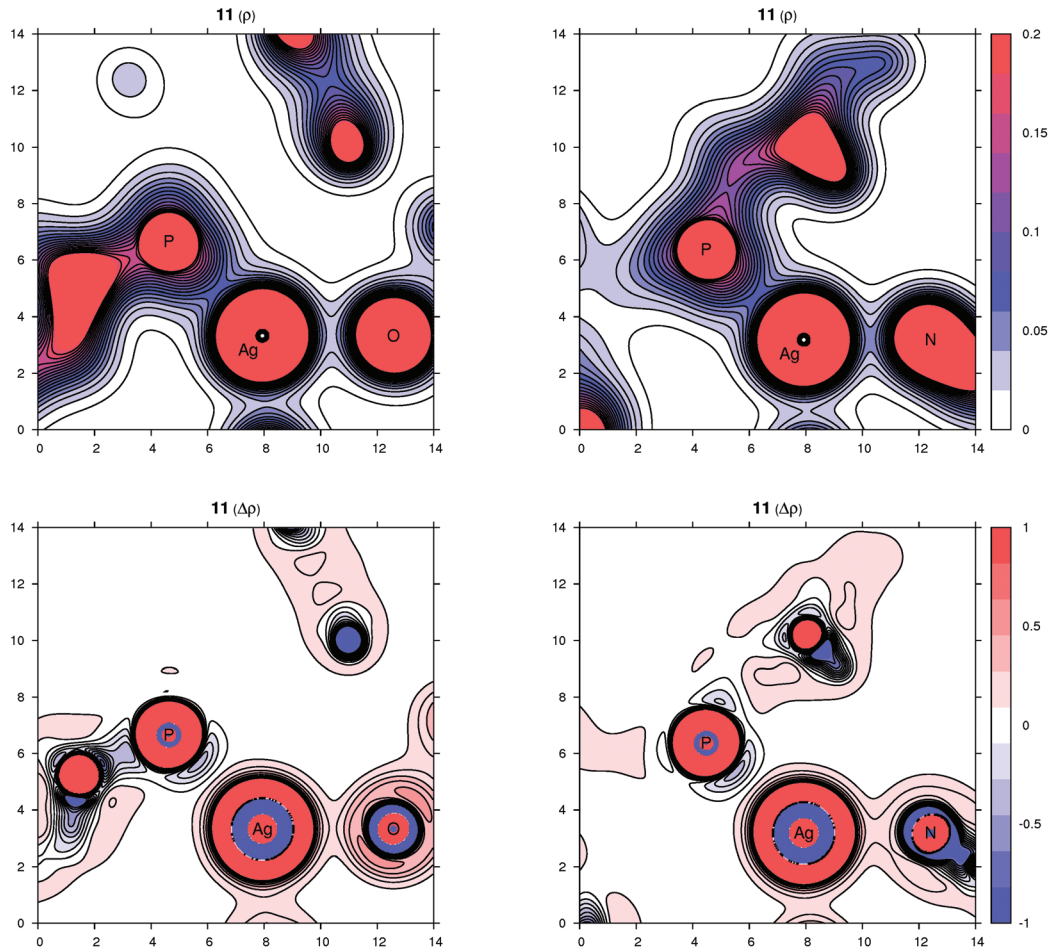


**Fig. 14** Contour plots of the electron density $\rho(r)$ (top panel) and its Laplacian $\Delta\rho(r)$ (bottom panel) for compound **11** in planes defined by three atoms whose symbols are shown (left part: P, Ag, O plane; right part: P, Ag, N plane). All values are in atomic units.

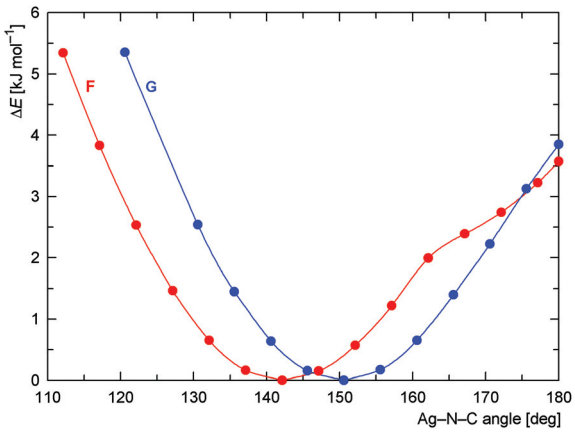


**Fig. 15** Dependence of the DFT-computed energy on the coordination angle Ag–N≡C (in the Ag–N≡$CCH_3$ fragment) with all other molecular parts relaxed for the model compounds **F** (red curve) and **G** (blue curve).

## Conclusions

Compound **1** combines two soft donor moieties of different nature and coordination properties. Its reactions with silver(I) salts containing common coordinating counter anions affords crystalline mixed-donor silver(I) complexes in which the phosphinonitrile ligand coordinates as a simple phosphine donor. The role of the supporting anions in the coordination of Ag(I) depends on their ligating ability, reaction stoichiometry and the solubility of the species present in the system. Thus, reactions with silver(I) halides and pseudohalides with a limited amount of **1** (*i.e.*, at a Ag : **1** ratio of 1 : 1) produce complexes featuring multiply bridging anions such as the heterocubanes **2**, **4**, **5** and **7** or the polymeric complex **6** built up from alternating $Ag(CN)_2^-$ and $Ag(\mathbf{1}\text{-}\kappa P)_2^+$ units. Increasing the amount of the phosphinonitrile ligand results in a preferential formation of compounds wherein the $\{Ag(\mathbf{1}\text{-}\kappa P)_2\}^+$ moieties are bridged by the same anions, but in a simple $\mu_2$-fashion (such in **3**, **8** and **10**). DFT computations indicate covalent interactions between the Ag(I) ion and phosphine phosphorus for these complexes (*i.e.*, the formation of P→Ag dative bonds), while the interactions between silver and the anionic ligands are largely electrostatic, which in turn corresponds with an easy disintegration (or at least fluxional behavior) of these compounds in a solution.

In contrast, reactions with Ag(I) salts possessing relatively weaker coordinating anions at a 1 : 1 metal-to-**1** ratio give rise to $[Ag_2(\mu(P,N)\text{-}\mathbf{1})_2]^{2+}$ cations in which the ligand's nitrile group completes the linear coordination environment of the Ag(I) ion. Counter anions with a higher propensity to coordinate form supportive weak interactions with the silver(I) ion (in the solid state), being replaceable by other donors including solvents. The "coordination" of both the nitrile moiety and the anionic ligands in these species has a prevalently electrostatic nature. Although rather counterintuitive, this bonding feature reflects the hard–soft nature of the Ag–N, Ag–O and Ag–F interactions and is also in agreement with the results of the previous theoretical studies.

The results collected in this study indicate that the soft phosphine moiety can be regarded as the primary coordination site in Ag(I) complexes with ligand **1**, forming strong covalent bonds toward the Ag(I) centers. On the other hand, the coordination of the nitrile group (as well as the counter-anions) probably has a supportive character, being predominantly electrostatic and thus less directional. Consequently, the particular combination of donor moieties and structural flexibility of **1** renders this metalloligand capable of "improvising" in the silver(I) complexes depending on the roles played by other partners (ligands), mainly recruiting from the counter anions, that further increase the overall structural diversity of the resulting compounds.

## Acknowledgements

The results reported in this paper were obtained with financial support from the Czech Science Foundation (project no. 13-08890S).

## Notes and references

1 In the absolute hardness scale, the Ag(I) ion is the hardest among the univalent group 11 metal ions: R. G. Pearson, *Inorg. Chem.*, 1988, **27**, 734.

2 R. J. Lancashire, in *Comprehensive Coordination Chemistry*, ed. G. Wilkinson, R. D. Gillard and J. A. McCleverty, Pergamon Press, New York, NY, 1987, ch. 54, vol. 5, p. 775.

3 R. Meijboom, R. J. Bowen and S. J. Bernes-Price, *Coord. Chem. Rev.*, 2009, **253**, 325.

4 (*a*) K.-S. Gan and T. S. A. Hor, in *Ferrocenes: Homogeneous Catalysis, Organic Synthesis, Materials Science*, ed. A. Togni and T. Hayashi, Wiley-VCH, Weinheim, 1995, ch. 1, p. 3; (*b*) S. W. Chien and T. S. A. Hor, in *Ferrocenes: Ligands, Materials and Biomolecules*, ed. P. Štěpnička, Wiley, Chichester, 2008, ch. 2, p. 33; (*c*) G. Bandoli and A. Dolmella, *Coord. Chem. Rev.*, 2000, **209**, 161; (*d*) D. J. Young, S. W. Chien and T. S. A. Hor, *Dalton Trans.*, 2012, **41**, 12655.

5 (*a*) T. S. A. Hor, S. P. Neo, C. S. Tan, T. C. W. Mak, K. W. P. Leung and R.-J. Wang, *Inorg. Chem.*, 1992, **31**, 4510; (*b*) S.-P. Neo, T. S. A. Hor, Z.-Y. Zhou and T. C. W. Mak, *J. Organomet. Chem.*, 1994, **464**, 113; (*c*) M. C. Gimeno, P. G. Jones, A. Laguna and C. Sarroca, *J. Chem. Soc., Dalton Trans.*, 1995, 1473; (*d*) Effendy, G. G. Lobbia, M. Pellei, C. Pettinari, C. Santini, B. W. Skelton and A. H. White, *Inorg. Chim. Acta*, 2001, **315**, 153; (*e*) X. L. Lu, W. K. Leong, T. S. A. Hor and L. Y. Goh, *J. Organomet. Chem.*, 2004, **689**, 1746; (*f*) X. L. Lu, W. K. Leong, L. Y. Goh and T. S. A. Hor, *Eur. J. Inorg. Chem.*, 2004, 2504; (*g*) Effendy, J. V. Hanna, F. Marchetti, D. Martini, C. Pettinari, R. Pettinari, B. W. Skelton and A. H. White, *Inorg. Chim. Acta*, 2004, **357**, 1523; (*h*) G. G. Lobbia, M. Pellei, C. Pettinari, C. Santini, B. W. Skelton and A. H. White, *Polyhedron*, 2005, **24**, 181;

 

(*i*) C. Di Nicola, Effendy, C. Pettinari, B. W. Skelton, N. Somers and A. H. White, *Inorg. Chim. Acta*, 2005, **358**, 695; (*j*) A. Cingolani, Effendy, C. Pettinari, B. W. Skelton and A. H. White, *Inorg. Chim. Acta*, 2006, **359**, 2170; (*k*) P. Teo, L. L. Koh and T. S. A. Hor, *Inorg. Chim. Acta*, 2006, **359**, 3435; (*l*) P. Teo, L. L. Koh and T. S. A. Hor, *Chem. Commun.*, 2007, 4221; (*m*) P. Teo, L. L. Koh and T. S. A. Hor, *Inorg. Chem.*, 2008, **47**, 9561; (*n*) C. Pettinari, J. Ngoune, A. Marinelli, B. W. Skelton and A. H. White, *Inorg. Chim. Acta*, 2009, **362**, 3225; (*o*) J. Vincente, P. González-Herrero, Y. García-Sánchez and P. G. Jones, *Inorg. Chem.*, 2009, **48**, 2060; (*p*) X. Yang, I. Isaac, C. Persau, R. Ahlrichs, O. Fuhr and D. Fenske, *Inorg. Chim. Acta*, 2014, **421**, 233.

6 For a structural study on complexes resulting from AgCN and dppf, 1,1′-bis(di-*tert*-butylphosphino)ferrocene or 1,1′-bis(dicyclohexylphosphino)ferrocene, see: M. Trivedi, Bhaskaran, G. Singh, A. Kumar and N. P. Rath, *J. Organomet. Chem.*, 2014, **758**, 9.

7 Selected examples: (*a*) I. D. Salter, S. A. Williams and T. Adatia, *Polyhedron*, 1995, **14**, 2803; (*b*) I. D. Salter, V. Šik, S. A. Williams and T. Adatia, *J. Chem. Soc., Dalton Trans.*, 1996, 643; (*c*) D. Imhof, U. Burckhardt, K.-H. Dahmen, F. Joho and R. Nesper, *Inorg. Chem.*, 1997, **36**, 1813; (*d*) K.-T. Youm, Y. Kim, Y. Do and M.-J. Jun, *Inorg. Chim. Acta*, 2000, **310**, 203; (*e*) Y. C. Neo, J. J. Vittal and T. S. A. Hor, *J. Chem. Soc., Dalton Trans.*, 2002, 337; (*f*) W.-Y. Wong, G.-L. Lu and K.-H. Choi, *J. Organomet. Chem.*, 2002, **659**, 107; (*g*) J. Lu, C.-C. Zhu, D.-C. Li and J.-M. Dou, *J. Cluster Sci.*, 2012, **23**, 545.

8 E. M. Barranco, O. Crespo, M. C. Gimeno, A. Laguna, P. G. Jones and B. Ahrens, *Inorg. Chem.*, 2000, **39**, 680.

9 M. C. Gimeno, P. G. Jones, A. Laguna and C. Sarroca, *Polyhedron*, 1998, **17**, 3681.

10 T. Mizuta, T. Aotani, Y. Imamura, K. Kubo and K. Miyoshi, *Organometallics*, 2008, **27**, 2457.

11 M. A. Fard, A. R. Kenaree, P. D. Boyle, P. J. Ragogna, J. B. Gilroy and J. F. Corrigan, *Dalton Trans.*, 2016, **45**, 2868.

12 P. Štěpnička, in *Ferrocenes: Ligands, Materials and Biomolecules*, ed. P. Štěpnička, 2008, Wiley, Chichester, ch. 5, p. 177.

13 (*a*) N. J. Long, J. Martin, G. Opromolla, A. J. P. White, D. J. Williams and P. Zanello, *J. Chem. Soc., Dalton Trans.*, 1999, 1981; (*b*) J. E. Aguado, S. Canales, M. C. Gimeno, P. G. Jones, A. Laguna and M. D. Villacampa, *Dalton Trans.*, 2005, 3005.

14 U. Siemeling, T. Klemann, C. Bruhn, J. Schulz and P. Štěpnička, *Z. Anorg. Allg. Chem.*, 2011, **637**, 1824.

15 J. Kühnert, M. Lamač, T. Rüffer, B. Walfort, P. Štěpnička and H. Lang, *J. Organomet. Chem.*, 2007, **692**, 4303.

16 K. Škoch, I. Císařová and P. Štěpnička, *Inorg. Chem.*, 2014, **53**, 568.

17 K. Škoch, I. Císařová and P. Štěpnička, *Chem. – Eur. J.*, 2015, **21**, 15998.

18 According to a search in the Cambridge Structural Database, version 5.36 of November 2014 with updates from November 2014, February 2015 and May 2015.

19 C. W. Liu, H. Pan, J. P. Fackler Jr., G. Wu, R. E. Wasylishen and M. Shang, *J. Chem. Soc., Dalton Trans.*, 1995, 3691.

20 Two types of the complex cations are found in the crystal structure of $[Ag(\mu\text{-}L)_2(MeCN)_2][SbF_6]$, differing by the distribution of the MeCN ligands, *viz.* $[(MeCN)Ag(\mu\text{-}L)_2Ag(MeCN)]^{2+}$ and $[Ag(\mu\text{-}L)_2Ag(MeCN)_2]^{2+}$: P. W. Miller, M. Nieuwenhuyzen, J. P. H. Charmant and S. L. James, *Inorg. Chem.*, 2008, **47**, 8367.

21 (*a*) E. L. Muetterties and C. W. Alegranti, *J. Am. Chem. Soc.*, 1970, **92**, 4114; (*b*) E. L. Muetterties and C. W. Alegranti, *J. Am. Chem. Soc.*, 1972, **94**, 6386.

22 NMR analysis of the crystallized products was often complicated by their very low solubility.

23 R. G. Goel and P. Pilon, *Inorg. Chem.*, 1978, **17**, 2876.

24 The cell parameters determined for unsolvated **2** are as follows: triclinic, space group $P\bar{1}$, $a$ = 13.8254(3) Å, $b$ = 17.5121(4) Å, $c$ = 20.7672(5) Å; $\alpha$ = 74.567(1)°, $\beta$ = 76.281(1)°, $\gamma$ = 69.615(1)°.

25 P. Schwerdtfeger, R. P. Krawczyk, A. Hammerl and R. Brown, *Inorg. Chem.*, 2004, **43**, 6707.

26 This can be demonstrated by the structures of other $[AgX(L)]_4$ clusters, where X = Cl, Br and I, and L = $PPh_3$: (*a*) B.-K. Teo and J. C. Calabrese, *Inorg. Chem.*, 1976, **15**, 2467; (*b*) B.-K. Teo and J. C. Calabrese, *Inorg. Chem.*, 1976, **15**, 2474; (*c*) B.-K. Teo and J. C. Calabrese, *J. Chem. Soc., Chem. Commun.*, 1976, 185; L = $PEt_3$: (*d*) M. R. Churchill and B. G. DeBoer, *Inorg. Chem.*, 1975, **14**, 2502; (*e*) M. R. Churchill, J. Donahue and F. J. Rotella, *Inorg. Chem.*, 1976, **15**, 2752; and L = $Ph_2PBu$: (*f*) R. J. Bowen, D. Camp, Effendy, P. C. Healy, B. W. Skelton and A. H. White, *Aust. J. Chem.*, 1994, **47**, 693.

27 B. Cordero, V. Gómez, A. E. Platero-Prats, M. Revés, J. Echeverría, E. Cremades, F. Barragán and S. Alvarez, *Dalton Trans.*, 2008, 2832.

28 G. A. Bowmaker, Effendy, J. V. Hanna, P. C. Healy, B. W. Skelton and A. H. White, *J. Chem. Soc., Dalton Trans.*, 1993, 1387.

29 C(118–123)···C(318–323) interactions with centroid···centroid distance = 3.775(2) Å and dihedral angle = 2.1(1)°, and C(218–223)···C(418–423) contacts with centroid···centroid distance = 3.757(2) Å and dihedral angle = 5.1(1)°.

30 The presence of two different cyanide groups is clearly manifested in the IR spectrum, displaying two bands at 2227 $cm^{-1}$ (ligand **1**) and at 2149 $cm^{-1}$ ($Ag(CN)_2^-$). In an aqueous solution, the IR absorption of the $[Ag(CN)_2]^-$ anion was observed at 2135 $cm^{-1}$: L. H. Jones and R. A. Penneman, *J. Chem. Phys.*, 1954, **22**, 965.

31 The stability constants determined for $[Ag(CN)_2]^-$ in water (1 M $NaClO_4$) and in nitromethane are $\log \beta_2$ = 20.14(5) and >34, respectively. (*a*) A. O. Gübeli and P. A. Côté, *Can. J. Chem.*, 1972, **50**, 1144; (*b*) J. Badoz-Lambling and J.-C. Bardin, *C. R. Acad. Sci., Sect. C., Chim.*, 1968, **266**, 95.

32 (*a*) G. A. Bowmaker, Effendy, J. C. Reid, C. E. F. Rickard, B. W. Skelton and A. H. White, *J. Chem. Soc., Dalton Trans.*, 1998, 2139; (*b*) M. Ghazzali, M. H. Jaafar, S. Akerboom,

A. Alsalme, K. Al-Farhan and J. Reedijk, *Inorg. Chem. Commun.*, 2013, **36**, 18.
33 For the crystal structures of $[(Cy_3P)AgNCAgCN]_n$ and $[(Cy_3P)_2AgNCAgCN]$ in which linear ($Ag(CN)_2$) and trigonal ($Ag(NC)_2(PCy_3)$) silver(I) centers coexist, see: Y.-Y. Lin, S.-W. Lai, C.-M. Che, Wen-Fu, Z.-Y. Zhou and N. Zhu, *Inorg. Chem.*, 2005, **44**, 1511.
34 (*a*) 1-Ethyl-3-methylimidazolium dicyanoargentate(1−), Ag–C = 2.06(2) Å: Y. Yoshida, K. Muroi, A. Otsuka, G. Saito, M. Takahashi and T. Yoko, *Inorg. Chem.*, 2004, **43**, 1458; (*b*) Bis(triphenylphospine)iminium dicyanoargentate(1−), Ag–C = 2.03(2) and 2.05(2) Å: M. Carcelli, C. Ferrari, C. Pelizzi, G. Pelizzi, G. Predieri and C. Solinas, *J. Chem. Soc., Dalton Trans.*, 1992, 2127.
35 G. A. Bowmaker, C. Di Nicola, Effendy, J. V. Hanna, P. C. Healy, S. P. King, F. Marchetti, C. Pettinari, W. T. Robinson, B. W. Skelton, A. N. Sobolev, A. Tăbăcaru and A. H. White, *Dalton Trans.*, 2013, **42**, 277.
36 Compare the following non-bonding distances: Ag1···Ag2 = 5.6450(6) Å, S10···S20 = 5.553(2) Å; Ag3···Ag4 = 5.6247(6), S30···S40 = 5.535(2) Å.
37 J. Howatson and B. Morosin, *Cryst. Struct. Commun.*, 1973, **2**, 51 (*SciFinder Scholar*, AN = 1973:89664).
38 (*a*) G. J. S. Venter, R. Meijboom and A. Roodt, *Acta Crystallogr., Sect. E: Struct. Rep. Online*, 2007, **63**, m3076; (*b*) N. M. Khumalo, R. Meijboom, A. Muller and B. Omondi, *Acta Crystallogr., Sect. E: Struct. Rep. Online*, 2010, **66**, m451.
39 B. Omondi and R. Meijboom, *Acta Crystallogr., Sect. B: Struct. Sci.*, 2010, **66**, 69.
40 (*a*) Effendy, C. Di Nicola, M. Fianchini, C. Pettinari, B. W. Skelton, N. Somers and A. H. White, *Inorg. Chim. Acta*, 2005, **358**, 763; (*b*) L. Yang, C. Zhu and D. Li, *Acta Crystallogr., Sect. E: Struct. Rep. Online*, 2011, **67**, m2.
41 The $(SCN)_2$ plane is defined by the atoms S3, N3, C3, S3′, N3′and C3′. These atoms are coplanar within *ca*. 0.001 Å.
42 Selected crystallographic data: triclinic, $P\bar{1}$, $a$ = 14.755(1), $b$ = 16.940(2), $c$ = 18.684(2) Å, $\alpha$ = 116.939(3)°, $\beta$ = 90.455(4)°, $\gamma$ = 104.733(4)° at $T$ = 150(2) K.
43 The $Cl^-/HF_2^-$-bridged complex was isolated even when the samples were prepared and crystallized in halogen-free solvents.
44 R. B. Johannesen, F. E. Brinckman and T. D. Coyle, *J. Phys. Chem.*, 1968, **72**, 660.
45 Compare the observed Si–F bond lengths with those determined for $M_2[SiF_6]$, where M = Na (av. 1.69 Å) and $Me_3NCH_2CO_2H$ (1.6627(9) and 1.6794(7) Å): (*a*) G. F. Schäfer, *Z. Kristallogr.*, 1986, **175**, 269; (*b*) M. Fleck, V. V. Ghazaryan and A. M. Petrosyan, *Z. Kristallogr., Cryst. Mater.*, 2013, **228**, 240.
46 C. D. Wyss, B. K. Tate, J. Bacsa, M. Wieliczko and J. P. Sadighi, *Polyhedron*, 2014, **84**, 87.
47 T. M. Klapötke, B. Krumm and M. Scherr, *Acta Crystallogr., Sect. E: Struct. Rep. Online*, 2006, **62**, m2634.
48 J. P. Foster and F. Weinhold, *J. Am. Chem. Soc.*, 1980, **102**, 7211.
49 V. Jonas, G. Frenking and M. T. Reetz, *J. Am. Chem. Soc.*, 1994, **116**, 8741.
50 R. F. W. Bader, *Acc. Chem. Res.*, 1985, **18**, 9.
51 S. H. Strauss, *Chem. Rev.*, 1993, **93**, 927.
52 M. L. Kuznetsov, *Russ. Chem. Rev.*, 2002, **71**, 265.
53 Complexes **11** and **12** were crystallized from acetone/hexane and chloroform/hexane, respectively, with a small amount of MeCN added for better solubility.
54 National Institute of Advanced Industrial Science and Technology. Spectral Database for Organic Compounds: SDBS; http://sdbs.db.aist.go.jp/sdbs/cgi-bin/cre_index.cgi, No. 889 (ethyl acetate) (accessed February 12, 2016).
55 The angles between the vectors of the C6–P and C1–C11 bonds are 93.7(2)° in **11** and 95.7(1)° in **12**.
56 The vectors of the Ag–P bonds intersect the C(6–10) planes at 19.4(1)° in **11** and 18.91(8)° in **12**.
57 P. F. Barron, J. C. Dyason, P. C. Healy, L. M. Engelhardt, B. W. Skelton and A. H. White, *J. Chem. Soc., Dalton Trans.*, 1986, 1965.
58 The P–Ag bond intersects the C(6–10) plane at an angle of 20.9(1)°, which falls between those in **11** and **12** (see ref. 56) and **13** (21.2(2)°).
59 Notably, analogous reactions with $AgClO_4$ (Ag : **1** = 1 : 2) afforded only complex **11** (after crystallization), while no defined solid product could be isolated from an analogous experiment with $Ag[SbF_6]$.
60 Complexes with bridging phosphinonitrile donors have been postulated, *e.g.*, in: (*a*) P. Braunstein, D. Matt, Y. Dusausoy, J. Fischer, A. Mitschler and L. Ricard, *J. Am. Chem. Soc.*, 1981, **103**, 5115; (*b*) D. S. Barratt, A. Hosseiny, C. A. McAuliffe and C. Stacey, *J. Chem. Soc., Dalton Trans.*, 1985, 135. However, the only structurally characterized compounds of this type are several Cu(I) complexes with ligand **1** (see ref. 16).
61 (*a*) An Ag(I) complex with a macrocyclic $N_3O_2$ donor and coordinated cyanoethyl pendant arm completing an [5 + 1] pseudooctahedral coordination around the Ag center (Ag–N≡C of 86°m Ag–N ≈ 2.68 Å): Z. Ma, H. Shi, X. Deng, M. F. C. G. da Silva, L. M. D. R. S. Martins and A. J. L. Pombeiro, *Dalton Trans.*, 2015, **44**, 1388; (*b*) A cationic Ag–Fe complex with a pyridine-dipyrrinato ligand and solvating MeCN (Ag–N≡C of 105°): S. R. Halper, L. Do, J. R. Stork and S. M. Cohen, *J. Am. Chem. Soc.*, 2006, **128**, 15255; (*c*) $[(Ph_2PPy\text{-}\kappa P)_2Ag(\mu\text{-}Cl)_2Ag(MeCN)(Ph_2PPy\text{-}\kappa P)]$ (Ag–N≡C = 106°; this angle is associated with a very long Ag–N distance, *ca*. 3.21 Å): A. Cingolani, Effendy, D. Martini, C. Pettinari, B. W. Skelton and A. H. White, *Inorg. Chim. Acta*, 2006, **359**, 2183; (*d*) $Ag(MeCN)_3^+$ cation in the structure of a complicated polyoxometalate (Ag–N≡C = 109°): J. T. Rhule, W. A. Neiwert, K. I. Hardcastle, B. Do and C. L. Hill, *J. Am. Chem. Soc.*, 2001, **123**, 12101; (*e*) $[Ag(L)(MeCN)]_n(ClO_4)_n$, $(H_2O)_n$ (L = 2,6-diamino-3,5-dicyano-4-(3-quinolinyl)-2,5-heptadiene; Ag–N≡C = 110°): C.-W. Yeh, C.-H. Tsou, F.-C. Huang, A. Jong and M.-C. Suen, *Polyhedron*, 2014, **81**, 273.

 

62 For representative examples, see: (*a*) T. C. Wright, G. Wilkinson, M. Motevalli and M. B. Hursthouse, *J. Chem. Soc., Dalton Trans.*, 1986, 2017. (*d*(Mo–N)–*d*(Mo–C) ≈ 0.10 Å); (*b*) P. A. Chetcuti, C. B. Knobler and M. F. Hawthorne, *Organometallics*, 1988, **7**, 650. (*d*(Ir–N)–*d*(Ir–C) = 0.07 and 0.15 Å); (*c*) J. Barrera, M. Sabat and W. D. Harman, *Organometallics*, 1993, **12**, 4381. (*d*(W–N)–*d*(W–C) = 0.01 and 0.03 Å); (*d*) J. J. Garcia, N. M. Brunkan and W. D. Jones, *J. Am. Chem. Soc.*, 2002, **124**, 9547. (*d*(Ni–N)–*d*(Ni–C) = 0.07 Å).

63 M. L. Kuznetsov, E. A. Klestova-Nadeeva and A. I. Dement'ev, *J. Mol. Struct. (THEOCHEM)*, 2004, **671**, 229.

# Appendix 4

Karel Škoch, Ivana Císařová, Petr Štěpnička: „Synthesis and Catalytic Use of Gold(I) Complexes Containing a Hemilabile Phosphanylferrocene Nitrile Donor“. *Chem. Eur. J.* **2015**, *21*, 15998.

ChemPubSoc Europe

DOI: 10.1002/chem.201502968

CHEMISTRY A European Journal Full Paper

Homogeneous Catalysis | *Hot Paper*

# Synthesis and Catalytic Use of Gold(I) Complexes Containing a Hemilabile Phosphanylferrocene Nitrile Donor

Karel Škoch, Ivana Císařová, and Petr Štěpnička*[a]

**Abstract:** Removal of the chloride ligand from [AuCl(**1**-κ*P*)] (**2**) containing a P-monodentate 1′-(diphenylphosphanyl)-1-cyanoferrocene ligand (**1**), by using silver(I) salts affords cationic complexes of the type [Au(**1**)]X, which exist either as cyclic dimers $[Au(\mathbf{1})]_2X_2$ (**3a**, X = $SbF_6$; **3c**, X = $NTf_2$) or linear coordination polymers $[Au(\mathbf{1})]_nX_n$ (**3a′**, X = $SbF_6$; **3b′**, X = $ClO_4$), depending on anion X and the isolation procedure. As demonstrated for **3a′**, the polymers can be readily cleaved by the addition of donors, such as $Cl^-$, tetrahydrothiophene (tht) or **1**, giving rise to the parent compound **2**, [Au(tht)(**1**-κ*P*)][$SbF_6$] (**5a**) or [Au(**1**-κ*P*)$_2$][$SbF_6$] (**4a**), respectively, of which the last two compounds can also be prepared by stepwise replacement of tht in [Au(**1**-κ*P*)$_2$][$SbF_6$]. The particular combination of a firmly coordinated (phosphane) and a dissociable (nitrile) donor moieties renders complexes **3**/**3′** attractive for catalysis because they can serve as shelf-stable precursors of coordinatively unsaturated $Au^I$ fragments, analogous to those that result from the widely used [Au($PR_3$)(RCN)]X catalysts. The catalytic properties of the Au-**1** complexes were evaluated in model annulation reactions, such as the synthesis of 2,3-dimethylfuran from (*Z*)-3-methylpent-2-en-4-yn-1-ol and oxidative cyclisation of alkynes with nitriles to produce 2,5-disubstituted 1,3-oxazoles. Of the compounds tested (**2**, **3a′**, **3b′**, **3a**, **4a** and **5a**), the best results were consistently achieved with dimer **3c**, which has good solubility in organic solvents and only one firmly bound donor at the gold atom. This compound was advantageously used in the key steps of annuloline and rosefuran syntheses.

## Introduction

Interest in the coordination chemistry[1] of gold has been recently revived, primarily because of rapid developments in the field of homogeneous gold-catalysed reactions.[2] Compounds that are typically employed as catalysts (or catalyst precursors) in gold catalysis are simple $Au^{I/III}$ salts,[2,3] gold–carbene complexes[2,4] and, mainly, stable $Au^I$ phosphane complexes of the type [AuCl($PR_3$)], which are typically activated in situ by the removal of the metal-bound halide with $Ag^I$ salts.[2] However, the latter approach can result in the formation of Au–Ag bimetallic systems, the reactivity of which may differ from that of the corresponding Au-only catalyst. This so-called silver effect in gold catalysis has stirred up a vigorous debate[5] and has also prompted a search for defined, silver-free $Au^I$ catalysts.[6] In addition to the very popular use of the solubilizing $NTf_2^-$ counterion,[7] the most successful of these newly introduced compounds appear to be cationic complexes of the type $[Au(PR_3)(RCN)]^+$ with easily dissociated nitrile ligands (e.g., compounds **A** and **B** in Scheme 1),[8,9] which presumably serve as precursors for the catalytically active $(R_3P)Au^+$ species.

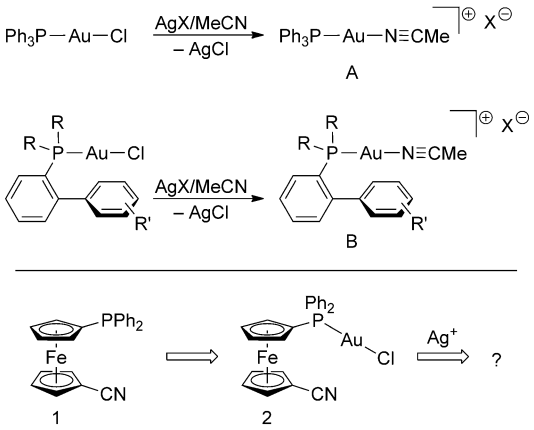


**Scheme 1.**

Recently, we synthesised 1′-(diphenylphosphanyl)-1-cyanoferrocene (**1** in Scheme 1),[10] which can be regarded as a donor-asymmetric[11] analogue of the ubiquitous 1,1′-bis(diphenylphosphanyl)ferrocene (dppf).[12] In view of the unexpectedly versatile coordination behaviour of **1** towards $Cu^I$,[10] we decided to study the interactions of this ligand with $Au^I$, the softest Group 11 metal ion.[13] Herein, we describe the synthesis of structurally unique $Au^I$-**1** complexes (Scheme 1, bottom) and report on their catalytic applications in selected $Au^I$-mediated organic reactions.

[a] *K. Škoch, Dr. I. Císařová, Prof. Dr. P. Štěpnička*
*Department of Inorganic Chemistry*
*Faculty of Science, Charles University in Prague*
*Hlavova 2030, 12840 Prague (Czech Republic)*
*E-mail: stepnic@natur.cuni.cz*

*Supporting information for this article is available on the WWW under http://dx.doi.org/10.1002/chem.201502968.*

## Results and Discussion

### Synthesis of the Au$^{I}$ complexes with ligand 1

The syntheses and mutual interconversions of Au$^{I}$ complexes with phosphanylnitrile **1** as a ligand are illustrated in Scheme 2. Ligand **1** reacts cleanly and rapidly with [AuCl(tht)]

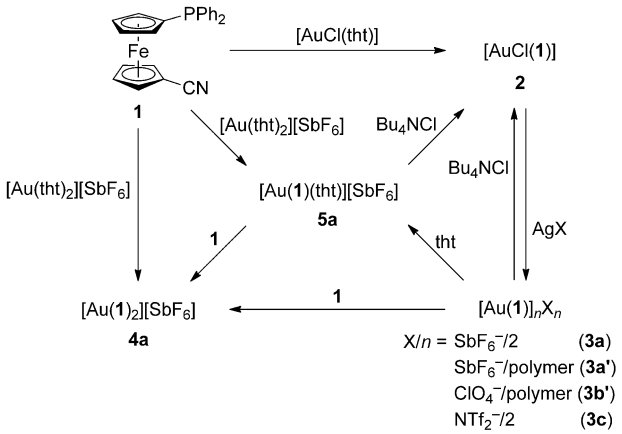


**Scheme 2.** Synthesis and mutual conversions of Au$^{I}$ complexes with phosphanylnitrile **1** (tht = tetrahydrothiophene).

(tht = tetrahydrothiophene) to afford the expected phosphane complex [AuCl(**1**-κ*P*)] (**2**).[14] In the $^{1}$H and $^{13}$C NMR spectra of **2**, there are characteristic signals assigned to the phosphanylferrocene ligand, whereas the $^{31}$P NMR spectrum displays a resonance at $\delta_P = +28.1$ ppm. The crystal structure of **2** (Figure 1) reveals the typical linear coordination around the Au$^{I}$ centre.[15] The ferrocene cyclopentadienyls in P-coordinated **1** are negligibly tilted (the dihedral angle of the cyclopentadienyl planes

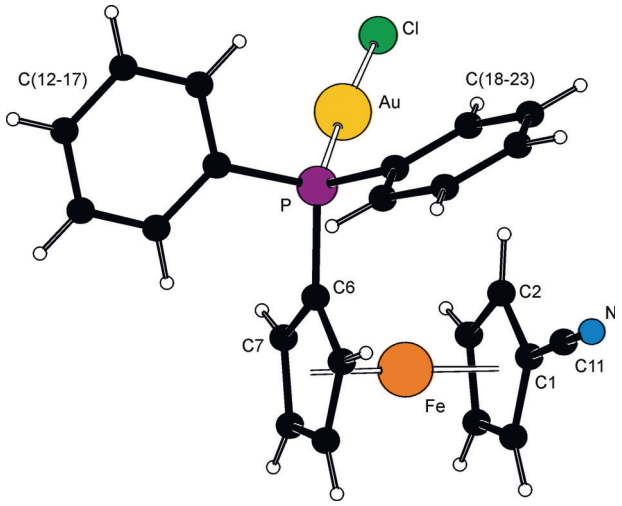


**Figure 1.** View of the molecular structure of chlorogold(I) complex **2**. Selected bond lengths [Å] and angles [°]: Au–P 2.2287(6), Au–Cl 2.2891(7), C11–N 1.144(4), Fe–Cg1 1.639(1), Fe–Cg2 1.637(1), P-Au-Cl 176.25(2), C1-C11-N 178.8(3).

is only 1.0(2)°) and assume a synclinal eclipsed conformation with a torsion angle of 71.3(2)° for C1-Cg1-Cg2-C6 ($\tau$; see Ref. [12a]; note that Cg1 and Cg2 are the centroids of the cyclopentadienyl rings C(1–5) and C(6–10), respectively). No interactions between the gold atom and the nitrile groups[16] or aurophilic contacts[17] were detected in the solid-state structure of **2**.

Complex **2** reacts smoothly with silver(I) salts to give the corresponding cationic complexes with the general formula [Au(**1**)]$_n$X$_n$ (Scheme 2).[18] Depending on anion X and the isolation procedure (additives) used, these compounds are isolated either as symmetric dimers, in which the phosphanylnitrile connects two gold centres as a P,N-bridge (**3**), or as coordination polymers, in which the ligands play a similar role albeit in an linearly propagating chain (**3′**). For example, the reaction of **2** with Ag[SbF$_6$] gives polymeric [Au(**1**)]$_n$[SbF$_6$]$_n$ (**3a′**). Analogous perchlorate salt **3b′**, obtained in a similar manner, is rather unstable and cannot be crystallised because it readily decomposes. However, the insolubility of **3b′** in common solvents attests to a similar polymeric structure. In contrast, the reaction between **2** and AgNTf$_2$ reproducibly affords the reasonably soluble dimer [Au(**1**)]$_2$(NTf$_2$)$_2$ (**3c**).

The preferred formation of only one type of product under analogous conditions appears to be controlled by an interplay of the relative solubility of the hypothetical Au(**1**)X fragments (as such or solvated) and their overall crystallisation properties. The distinct influence of the synthesis conditions on the aggregation state of the [Au(**1**)]$_n^{n+}$ species can be further highlighted by the serendipitous isolation of complex **3a**,[19] an isomer to **3a′**, in which the structure of the dimeric [Au$_2$(**1**)$_2$]$^{2+}$ motif is associated with two [SbF$_6$]$^-$ anions.[20]

Importantly, the reaction that leads to compounds **3** can be easily reversed by the addition of [Bu$_4$N]Cl as a chloride source (as demonstrated for **3a′**, see Scheme 2). The cleavage of the multi-gold assemblies can be also achieved by the addition of other donors, such as **1**, tht or even a donor solvent (e.g., MeCN). Thus, polymer **3a′** readily dissolves upon the addition of **1** to afford the monogold(I) species [Au(**1**-κ*P*)$_2$][SbF$_6$] (**4a**), in which the two phosphanylnitrile ligands coordinate as equivalent P-monodentate donors.[21] The same product can be prepared directly by the treatment of [Au(tht)$_2$][SbF$_6$] with two equivalents of **1**. A similar reaction at the Au/**1** molar ratio of 1:1 provides a product with an intermediate level of substitution, [Au(**1**-κ*P*)(tht)]SbF$_6$ (**5a**), which can be converted to **4a** by the addition of another equivalent of **1**. Complex **5a** also results from cleavage of polymer **3a′** with tht and can be transformed back to the parent complex **2** upon treatment with [Bu$_4$N]Cl (Scheme 2).

The crystal structures of **3a, 3a′**·Me$_2$CO,[22] **3c** and **4a** were determined by using X-ray diffraction analysis and are presented in Figure 2 and in the Supporting Information.[23,49] Selected geometric parameters are given in Table 1. The Au–P bond lengths in these compounds do not differ greatly from those of parent complex **2**. A slight yet statistically significant elongation of the Au–P bonds in **4a** (compared with complexes **3**/**3′**) can be attributed to steric repulsion of the proximal phosphane moieties. The variation in the lengths of the C≡N bonds

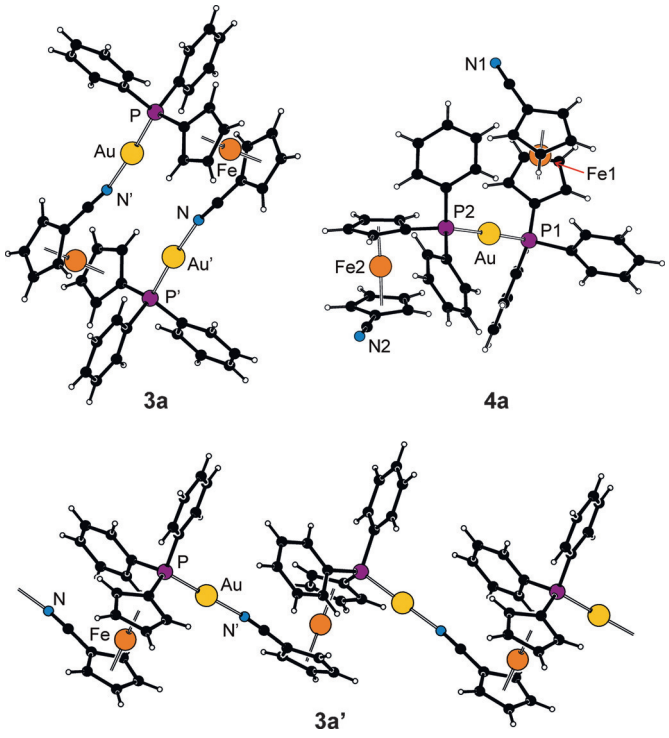


**Figure 2.** View of the cations in the crystal structures of **3a**, **3a**′·$Me_2CO$ and **4a**. For the conventional displacement ellipsoid plots and structural drawing of **3c**, see the Supporting Information.

**Table 1.** Comparison of the pertinent geometric parameters of **3a**, **3a**′·$Me_2CO$, **3c** and **4a**.[a]

| | 3a | 3a′·$Me_2CO$ | 3c | 4a[b] |
|---|---|---|---|---|
| bond lengths [Å] | | | | |
| Au–P | 2.225(2) | 2.2246(9) | 2.232(1) | 2.3104(8)/2.3140(8) |
| Au–N | 2.035(4) | 2.028(3) | 2.035(3) | – |
| N≡C | 1.139(8) | 1.143(5) | 1.142(5) | 1.148(4)/1.136(6) |
| Fe–Cg1 | 1.645(3) | 1.651(2) | 1.645(2) | 1.649(1)/1.645(2) |
| Fe–Cg2 | 1.642(3) | 1.644(2) | 1.650(2) | 1.648(2)/1.643(1) |
| angles [°] | | | | |
| P–Au–N | 175.1(1) | 179.4(1) | 173.4(1) | 175.43(2)[c] |
| Au–N≡C | 168.2(5) | 173.9(3) | 168.0(4) | – |
| tilt | 2.9(4) | 3.3(2) | 3.4(3) | 3.6(2)/4.3(2) |
| $\tau$ | −60.6(5) | −66.8(3) | −78.2(3) | −142.0(2)/75.5(2) |

[a] Cg1 and Cg2 are the centroids of cyclopentadienyl rings C1–5 and C6–10, respectively; tilt is the dihedral angle of the cyclopentadienyl planes; $\tau$ is the torsion angle of C1-Cg1-Cg2-C6. [b] Data for ligand **1** (Fe1)/ligand **2** (Fe2). [c] P1-Au-P2 angle.

is only marginal (both in the series and with respect to uncoordinated **1**[10]), which indicates that the bonding and back-bonding components of the Au–NC dative bond counteract each other, and thus result in marginal changes in the bond order. This corresponds to a decrease in the ratio between the π-acceptor and σ-donor abilities of the nitrile donors with respect to, for example, the isonitrile and CO ligands.[24] Overall, the Au–donor separations and the interligand angles in compounds **3** and **3**′ are similar to those reported previously for $[Ph_3PAu(NCMe)][SbF_6]$[25] and similar complexes with 2-phosphanylbiphenyl ligands (type **B** in Scheme 1),[25,26] while the Au–P bonds in **4a** compare well with the data determined for complexes $[Au(PR_3)_2]X$, in which R/X = Me/$PF_6$,[27] Ph/$NTf_2$,[28] Ph/$NO_3$[29] and $FcCH_2PPh_2/ClO_4$ (Fc = ferrocenyl).[30]

The conformations of the ferrocene units in complexes **3**/**3**′ are all nearly synclinal eclipsed (ideal value: 72°). One of the two structurally independent molecules of ligand **1** in the structure of **4a** has a similarly compact conformation (Fe2), whereas the other ligand molecule adopts an anticlinal eclipsed conformation, which renders the donor substituents at the ferrocene unit more distant (Fe1).

## Catalytic evaluation of the Au-1 complexes

The mutual interconversions of the $Au^I$ complexes with ligand **2** described above clearly demonstrate the hemilabile nature[11] of the cationic Au-**1** species, which results from different strengths of the Au–donor bonds. Apparently, the phosphane donor moiety acts as a firmly bound pivot in these compounds, whereas the CN–Au bond can be readily cleaved by neutral and anionic donors. Such a facile splitting of the parent structure to provide coordinatively unsaturated fragments, and their possible reassembly to allow for self-stabilisation of these intermediates, renders these compounds attractive for use in catalysis.

Catalytic properties of the Au-**1** complexes were evaluated with some known ring-forming reactions;[31] first, in the cyclisation of (*Z*)-3-methylpent-2-en-4-yn-1-ol ((*Z*)-**6**) to 2,3-dimethylfuran (**7** in Scheme 3). In general, this reaction and similar

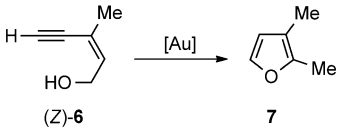


**Scheme 3.** Gold-catalysed cycloisomerisation of (*Z*)-**6** to 2,3-dimethyl-furan (**7**).

transformations represent an attractive route to furan derivatives, and although a vast number of transition-metal compounds have been tested in this area,[32] applications of $Au^I$ catalysts to this particular cyclisation of 2-en-4-yn-1-ols still remain quite rare.[33,34]

The results obtained with the $Au^I$-**1** complexes (Table 2) indicate a superior performance of the **3**-type compounds, which achieve full conversions of (*Z*)-**6** to **7** at catalyst loadings as low as 0.01 %. Even at this scale, the reactions quickly reach completion (being typically complete within less than 5 min) and are strongly exothermic, which becomes evident when the experiments are performed without any solvent and on a larger scale. The best results were obtained with complex **3c**, the solubility of which ensures rapid and complete dissolution of the catalyst in the reaction mixture. However, compounds with two strongly coordinated ligands (phosphane and chloride in **2** and **4a**), and **5a**, proved to be less efficient, which became particularly evident at low metal loadings.[35]

**Table 2.** Summary of the catalysis results achieved with Au$^{I}$-**1** complexes in the cyclisation of (*Z*)-3-methylpent-2-en-4-yn-1-ol.[a]

| Catalyst | Au loading [%] | Yield [%][b] |
|---|---|---|
| [AuCl(tht)] | 0.1 | 82 |
| **2** | 0.1 | 65 |
| **3a′** | 0.1 | quant. |
| **3a′** | 0.01 | 45 |
| **3b′** | 0.1 | quant. |
| **3b′** | 0.01 | 22 |
| **3c** | 0.1 | 98 |
| **3c** | 0.01 | quant. |
| **4a** | 0.1 | 0 |
| **5a** | 0.1 | quant. |
| **5a** | 0.01 | 17 |
| none | 0 | 0 |

[a] Conditions: reaction in $CHCl_3$ at RT for 30 min. The yields are the average of two independent runs and are given relative to the major (*Z*)-isomer of the starting enynol ((*Z*)/(*E*) ≈90:10). [b] Yield determined by using NMR spectroscopy.

These promising results led us to demonstrate the usefulness of the Au-**1** catalysts under practically relevant conditions. When the cyclisation reaction was carried out with **3c** (0.01 mol%) in the absence of any solvent at a 50 mmol scale (under ambient conditions for 30 min[36]), it afforded furan **7** in an isolated yield of 92% after simple distillation.[37] The turnover frequency (TOF) for catalyst **3c** used in this reaction was as high as $2\times10^5$ h$^{-1}$.[38] Unfortunately, a further reduction of the catalyst loading to 0.001 mol% markedly decreased the conversion (only ≈35% **7** was formed at 80 °C over 72 h).

A similar annulation of (*Z*)-3,7-dimethyl-2,6-octadien-4-yn-1-ol (**8**) to give 3-methyl-2-(3-methylbut-2-en-1-yl)furan or rosefuran (**9** in Scheme 4),[39] which is a constituent of natural essential oils,[40] required more forcing conditions, most likely because of the lower reactivity of the internal triple bond present in the substrate. For example, no cyclisation product was detected when neat enynol **8** was treated with **3c** (0.1 mol%) at room temperature for 20 h, whereas heating the reaction mixture to 80 °C for 40 h resulted in only a 4% conversion. On increasing the catalyst amount to 0.5 mol%, however, the reaction proceeded with complete conversion within 2 h at 60 °C and gave pure rosefuran in 91% yield after column chromatography.

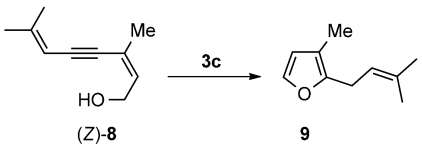


(*Z*)-**8** **9**

**Scheme 4.** Gold-catalysed cycloisomerisation of **8** to rosefuran (**9**).

In a continuation of our catalytic tests, we turned to the synthesis of 1,3-oxazoles[41] by an Au-mediated oxidative cyclisation of alkynes with nitriles in the presence of *N*-heterocyclic *N*-oxides,[42] which offers an attractive alternative to conventional synthetic approaches.[43] The initial screening experiments were carried out with the reaction between acetonitrile and phenylethyne to provide 2-methyl-5-phenyl-1,3-oxazole (**12a** in Scheme 5; the crystal structure of **12a** is presented in the Supporting Information).

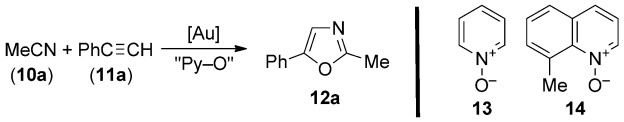


**Scheme 5.** The model Au-catalysed oxidative cyclisation of terminal alkynes with nitriles to give 1,3-oxazoles and structures of the *N*-oxides employed in this reaction.

The results (Table 3) clearly differentiated the catalysts. Whereas the coordinatively saturated complexes **2**, **4a** and **5a**, as well the precursor [AuCl(tht)], provided **12a** with only poor yields, compounds **3** performed much better. Similar to the previous tests, the best results were obtained with dimer **3c**, which afforded **12a** in an isolated yield of 78%. A further increase in the yield, though not for all of the complexes (see also the results for practically insoluble **3b′** in Table 3), could be achieved by replacing *N*-oxide **13** with its more bulky counterpart **14**.[42]

**Table 3.** Summary of catalysis results obtained with various Au$^{I}$ catalysts in the model reaction to give oxazole **12a**.[a]

| Catalyst | Yield with *N*-oxide **13** [%] | Yield with *N*-oxide **14** [%] |
|---|---|---|
| [AuCl(tht)] | 7 | n.a. |
| **2** | ≈1.5 | n.a. |
| **3a′** | 50 | 83 |
| **3b′** | 33 | 33 |
| **3c** | 78 | 88 |
| **4a** | 12 | n.a. |
| **5a** | 44 | n.a. |

[a] Conditions: phenyl acetylene (0.250 mmol) and *N*-oxide (0.325 mmol, 1.3 equiv) were reacted in the presence of the Au catalyst (5 mol%) in acetonitrile (2.5 mL) at 60 °C for 24 h. The isolated yields are given as the average of two independent runs; n.a. = not available.

The reactions performed next with different substrates (Scheme 6, data in Table 4) demonstrated that the cyclisation of ring-substituted phenylacetylenes with **3c** and **14** in acetonitrile gives the respective 2-methyloxazoles in very good isolated yields. A similar result was attained with propionitrile, but

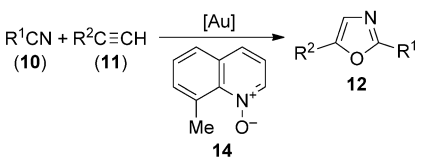


**Scheme 6.** Au-catalysed synthesis of 2,5-disubstituted 1,3-oxazoles.

**Table 4.** The substrate scope tests for the reaction to give oxazoles **12**.[a]

| Nitrile | Alkyne | Product | Yield [%] |
|---|---|---|---|
| MeCN (**10a**) | $C_6H_5C{\equiv}CH$ (**11a**) | **12a** | 88 |
| **10a** | 4-$MeC_6H_4C{\equiv}CH$ (**11b**) | **12b** | 92 |
| **10a** | 4-$MeOC_6H_4C{\equiv}CH$ (**11c**) | **12c** | 92 |
| **10a** | 4-$CF_3C_6H_4C{\equiv}CH$ (**11d**) | **12d** | 72 |
| **10a** | 4-$BrC_6H_4C{\equiv}CH$ (**11e**) | **12e** | 82 |
| EtCN (**10f**) | **11a** | **12f** | 85 |
| $CH_2{=}CHCN$ (**10g**) | **11a** | **12g** | 46 |
| PhCN (**10h**)[b] | **11a** | **12h** | 73 |

[a] Conditions: alkyne, catalyst **3c** (5 mol%) and **14** (1.3 equiv) were reacted in neat nitrile at 60 °C for 24 h unless specified otherwise. The isolated yields are given as the average of two independents experiments. Note: The first entry is repeated from Table 3 for a comparison. [b] Reaction with the nitrile (6 equiv) in chlorobenzene (2 mL).

the reaction with the generally more reactive acrylonitrile furnished **12g** in only 46% yield.

Encouraged by the successful screening experiments, we set out to employ this [2+2+1] annulation in the preparation of a naturally occurring oxazole alkaloid annuloline (**15**; Scheme 7).[44,45] The nitrile required for this cyclisation, (2*E*)-3-(3,4-dimethoxyphenyl)-2-propenenitrile (**18**), was obtained in

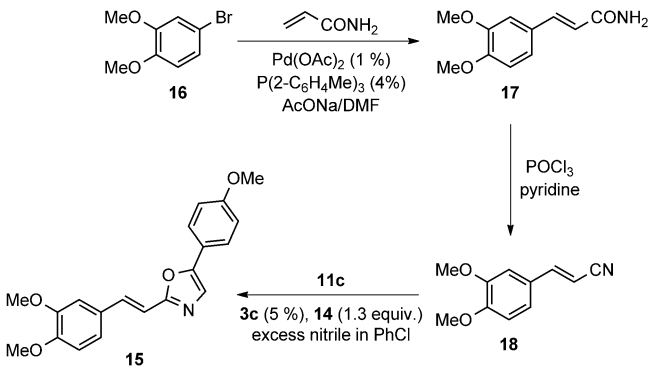


**Scheme 7.** Synthesis of annuloline **15** by Pd-catalysed cross-coupling and Au-mediated cyclisation.

two steps through a Pd-catalysed Heck coupling of 4-bromoveratrole (**16**) with acrylonitrile and subsequent dehydration of formed amide (*E*)-**17**. The dehydration was associated with a partial isomerisation at the double bond, which led to an approximately 90:10 mixture of the (*E*) and (*Z*) isomers; however, the latter isomer could be easily removed by a single recrystallisation from ethyl acetate/heptane. It is notable that the Heck coupling of **16** with acrylonitrile, which could be suggested as a direct route to nitrile **18**, proved to be less practical due to its lower selectivity (a ≈2:1 mixture of (*E*)- and (*Z*)-**18** was obtained under otherwise similar conditions).

The subsequent cyclisation of **18** with **11c** and *N*-oxide **14** was performed in chlorobenzene with three molar equivalents of the nitrile with respect to **11c** and 5 mol% of **3c** as the catalyst. Gratifyingly, the reaction proceeded smoothly (at 60 °C for 24 h) and provided analytically pure **15** in 63% yield after column chromatography, during which the majority of the unreacted nitrile could also be recovered (2.1 equiv of **18** was isolated). On the whole, this four-step synthesis represents a high-yield and convergent approach towards annuloline (≈34% with respect to **16**) that obviates the use of advanced and/or expensive starting materials and reagents and tedious experimentation, and even avoids unwanted isomerisation at the double bond in the styryl moiety. As such, it represents a practical alternative to the methods reported earlier.[45b,c,46]

In addition to the cyclisation route presented above, another approach to **15** has been investigated based on the Heck coupling of the respective 2-vinyl-1,3-oxazole and **16**.[47d] In a pilot experiment, oxazole **12f** was employed as a model substrate and was treated with **16** in the presence of a Pd catalyst under conventional Heck conditions. However, the reaction did not proceed to any appreciable extent, leading instead to a complete decomposition of the oxazole, whereas **16** remained unchanged.[47]

## Conclusion

Abstraction of the chloride ligand from [AuCl(**1**-κ*P*)] (**2**) gives rise to structurally remarkable cationic complexes $[Au(\mathbf{1})]_nX_n$, the degree of association (*n*) of which in the solid state (dimer vs. polymer) can be controlled by the counterion X, presumeably through modulation of the solubility and crystallisation properties of plausible "Au(**1**)X" intermediates. In these compounds, the structurally flexible 1′-(diphenylphosphanyl)-1-cyanoferrocene (**1**) behaves as a bridging hemilabile donor, which makes use of both of its donor moieties.[48] However, the relatively weaker coordination of the nitrile groups allows for an easy disaggregation of these multinuclear compounds upon the addition of donors and thus makes them an attractive and practical source of coordinatively unsaturated $Au^I$ species that are potentially capable of self-stabilisation through equilibria between the mononuclear (solvated) fragments and their aggregated form. The fact that the $[Au(\mathbf{1})]_nX_n$ complexes can indeed serve as a reservoir of catalytically active, low-nuclear gold species was established for selected organic transformations. The catalytic experiments revealed a consistently superior performance of the most soluble derivative, **3c**, in which the dimeric motif $\{Au_2(\mathbf{1})_2\}^{2+}$ pairs with the $NTf_2^-$ anions. This compound, in particular, emerges as an attractive (shelf-stable and well-defined) catalyst for gold-mediated organic reactions, which still rely predominantly on ill-defined species generated in situ from chlorogold(I) complexes with various supporting ligands and silver(I) salts or on the relatively unstable cationic **B**-type complexes.

## Acknowledgements

The results presented in this paper were obtained with financial support from the Czech Science Foundation (project no. 13-08890S) and the Grant Agency of Charles University in Prague (project no. 108213).

**Keywords:** gold · homogeneous catalysis · metallocenes · phosphane ligands · structure elucidation

[1] a) R. J. Puddephatt, in *Comprehensive Coordination Chemistry, Vol. 2* (Eds.: G. Wilkinson, R. D. Gillard, J. A. McCleverty), Pergamon, Oxford, **1987**, Chapter 55, pp. 861 – 923; b) M. C. Gimeno, A. Laguna, in *Comprehensive Coordination Chemistry II, Vol. 6* (Ed.: J. A. McCleverty, T. J. Meyer), Elsevier, Amsterdam, **2004**, Chapter 6.7, pp. 911 – 1145.

[2] For recent reviews, see: a) A. S. K. Hashmi, *Angew. Chem. Int. Ed.* **2005**, *44*, 6990 – 6993; *Angew. Chem.* **2005**, *117*, 7150 – 7154; b) A. S. K. Hashmi, G. J. Hutchings, *Angew. Chem. Int. Ed.* **2006**, *45*, 7896 – 7936; *Angew. Chem.* **2006**, *118*, 8064 – 8105; c) A. S. K. Hashmi, *Chem. Rev.* **2007**, *107*, 3180 – 3211; d) Z. Li, C. Brouwer, C. He, *Chem. Rev.* **2008**, *108*, 3239 – 3265; e) A. Arcadi, *Chem. Rev.* **2008**, *108*, 3266 – 3325; f) E. Jiménez-Núñez, A. M. Echavarren, *Chem. Rev.* **2008**, *108*, 3326 – 3350; g) D. J. Gorin, B. D. Sherry, F. D. Toste, *Chem. Rev.* **2008**, *108*, 3351 – 3378; h) N. T. Patil, Y. Yamamoto, *Chem. Rev.* **2008**, *108*, 3395 – 3442; i) M. Rudolph, A. S. K. Hashmi, *Chem. Soc. Rev.* **2012**, *41*, 2448 – 2462; j) Y.-M. Wang, A. D. Lackner, F. D. Toste, *Acc. Chem. Res.* **2014**, *47*, 889 – 901; k) R. Dorel, A. M. Echevarren, *Chem. Rev.* **2015**, *115*, 9028 – 9072.

[3] For a few representative examples, see: a) A. S. K. Hashmi, T. M. Frost, J. W. Bats, *J. Am. Chem. Soc.* **2000**, *122*, 11553 – 11554; b) B. Alcaide, P. Almendros, *Beil. J. Org. Chem.* **2011**, *7*, 622 – 630; c) M. S. Reddy, Y. K. Kumar, N. Thirupathi, *Org. Lett.* **2012**, *14*, 824 – 827; d) S. Basceken, M. Balci, *J. Org. Chem.* **2015**, *80*, 3806 – 3814.

[4] For examples of reactions leading to gold-carbene complexes, see: a) A. S. K. Hashmi, C. Lothschütz, C. Böhling, T. Hengst, C. Hubbert, F. Rominger, *Adv. Synth. Catal.* **2010**, *352*, 3001 – 3012; b) A. S. K. Hashmi, D. Riedel, M. Rudolph, F. Rominger, T. Oeser, *Chem. Eur. J.* **2012**, *18*, 3827 – 3830; c) D. Riedel, T. Wurm, K. Graf, M. Rudolph, F. Rominger, A. S. K. Hashmi, *Adv. Synth. Catal.* **2015**, *357*, 1515 – 1523.

[5] a) D. Weber, M. R. Gagné, *Org. Lett.* **2009**, *11*, 4962 – 4965; b) D. Wang, R. Cai, S. Sharma, J. Jirak, S. K. Thummanapelli, N. G. Akhmedov, H. Zhang, X. Liu, J. L. Petersen, X. Shi, *J. Am. Chem. Soc.* **2012**, *134*, 9012 – 9019; c) A. Homs, I. Escofet, A. M. Echavarren, *Org. Lett.* **2013**, *15*, 5782 – 5785; d) Y. Zhu, C. S. Day, L. Zhang, K. J. Hauser, A. C. Jones, *Chem. Eur. J.* **2013**, *19*, 12264 – 12271.

[6] H. Schmidbaur, A. Schier, *Z. Naturforsch. b* **2011**, *66*, 329 – 350.

[7] a) N. Mézailles, L. Ricard, F. Gagosz, *Org. Lett.* **2005**, *7*, 4133 – 4136; for an application of this approach, see: b) A. S. K. Hashmi, A. Loos, A. Littmann, I. Braun, J. Knight, S. Doherty, F. Rominger, *Adv. Synth. Catal.* **2009**, *351*, 576 – 582.

[8] C. Nieto-Oberhuber, S. López, A. M. Echavarren, *J. Am. Chem. Soc.* **2005**, *127*, 6178 – 6179.

[9] Examples of the numerous applications of the **A**- and **B**-type complexes can be found in the review articles cited in Ref. [2].

[10] K. Škoch, I. Císařová, P. Štěpnička, *Inorg. Chem.* **2014**, *53*, 568 – 577.

[11] Although both donor moieties present in **1** are classified as soft according to the HSAB concept, their different natures can be expected to result in hemilabile coordination, which is typical for hybrid donors, see: a) A. Bader, E. Lindner, *Coord. Chem. Rev.* **1991**, *108*, 27 – 110; b) C. S. Slone, D. A. Weinberger, C. A. Mirkin, *Progr. Inorg. Chem.* **1999**, *48*, 233 – 350; c) P. Braunstein, F. Naud, *Angew. Chem. Int. Ed.* **2001**, *40*, 680 – 699; *Angew. Chem.* **2001**, *113*, 702 – 722.

[12] a) K.-S. Gan, T. S. A. Hor, in *Ferrocenes: Homogeneous Catalysis, Organic Synthesis Materials Science* (Eds.: A. Togni, T. Hayashi), Wiley-VCH, Weinheim, **1995**, Chapter 1, pp. 3 – 104; b) S. W. Chien, T. S. A. Hor, in *Ferrocenes: Ligands, Materials and Biomolecules* (Ed.: P. Štěpnička), Wiley, Hoboken, **2008**, Chapter 2, pp. 33 – 116; c) G. Bandoli, A. Dolmella, *Coord. Chem. Rev.* **2000**, *209*, 161 – 196; d) D. J. Young, S. W. Chien, T. S. A. Hor, *Dalton Trans.* **2012**, *41*, 12655 – 12665.

[13] R. G. Pearson, *J. Am. Chem. Soc.* **1963**, *85*, 3533 – 3539.

[14] Similar [AuCl(L)] complex, where L is (diphenylphosphanyl)acetonitrile, has been reported in: P. Braunstein, D. Matt, F. Mathey, D. Thavard, *J. Chem. Res. Synop.* **1978**, 232 – 233.

[15] The geometry around the gold atom in **1** is similar to that in [AuCl(FcPPh$_2$)] (Fc = ferrocenyl), see: K. Rößler, T. Rüffer, B. Walfort, R. Packheiser, R. Holze, M. Zharnikov, H. Lang, *J. Organomet. Chem.* **2007**, *692*, 1530 – 1545.

[16] The shortest intermolecular Au···N distance in the structure of **1** of 3.323(2) Å is found for molecules related by elemental translation along the crystallographic *a* axis.

[17] Selected reviews: a) H. Schmidbaur, A. Schier, *Chem. Soc. Rev.* **2012**, *41*, 370 – 412; b) H. Schmidbaur, A. Schier, *Chem. Soc. Rev.* **2008**, *37*, 1931 – 1951; c) H. Schmidbaur, *Gold Bull.* **2000**, *33*, 3 – 10; d) P. Pyykkö, *Angew. Chem. Int. Ed.* **2004**, *43*, 4412 – 4456; *Angew. Chem.* **2004**, *116*, 4512 – 4557.

[18] Compounds **3** are best isolated by diluting the crude reaction mixture (acetonitrile/dichloromethane) with ethyl acetate and hexane and subsequent evaporation under vacuum. In this case, the products are isolated as microcrystalline solids. Other isolation procedures (e.g., direct precipitation) typically afford glassy solids that adhere to the walls of the reaction vessel.

[19] Crystals of dimer **3a** formed during the attempted preparation of an asymmetric diphosphane complex (an analogue of **4a**) by the reaction of **3a** with tricyclohexylphosphane and crystallisation from chloroform/diethyl ether.

[20] If the role of the counterion and solid-state effects were negligible, formation of the dimers would be favoured for entropy reasons because the bonds in both compound types ($[Au_2(\mathbf{2})_2]^{2+}$ and $[Au_n(\mathbf{2})_n]^{n+}$) are identical and, thus, no significant contribution from the reaction enthalpy to the overall energy balance would be expected.

[21] The conversion of **2** into **4a** can also be effected through a one-pot reaction by successive addition of **1** and then Ag[SbF$_6$] to a solution of **2**. In this case, however, the product is contaminated by an Ag-**1** complex even when the reaction stoichiometry is strictly maintained.

[22] Crystals of **3a′**·Me$_2$CO suitable for X-ray diffraction analysis were grown by recrystallization from acetone/hexane. However, this solvate partly loses the solvent of crystallization upon drying and prolonged storage.

[23] To complete the series of structurally characterised compounds, we also attempted to determine the crystal structure of **5a**. Unfortunately, the crystal structure data revealed extensive disorder of the tht ligand that could not be reliably described.

[24] M. L. Kuznetsov, *Russ. Chem. Rev.* **2002**, *71*, 265 – 282.

[25] E. Herrero-Gómez, C. Nieto-Oberhuber, S. López, J. Benet-Buchholz, A. M. Echavarren, *Angew. Chem. Int. Ed.* **2006**, *45*, 5455 – 5459; *Angew. Chem.* **2006**, *118*, 5581 – 5585.

[26] V. M. Lau, C. F. Gorin, M. W. Kanan, *Chem. Sci.* **2014**, *5*, 4975 – 4979.

[27] U. E. I. Horvath, H. G. Raubenheimer, *Acta Crystallogr. Sect. E* **2007**, *63*, m567.

[28] G. Seidel, C. W. Lehmann, A. Fürstner, *Angew. Chem. Int. Ed.* **2010**, *49*, 8466 – 8470; *Angew. Chem.* **2010**, *122*, 8644 – 8648.

[29] R. J. Staples, C. King, M. N. I. Khan, R. E. P. Winpenny, J. P. Fackler, Jr., *Acta Crystallogr. Sect. C* **1993**, *49*, 472 – 475.

[30] E. M. Barranco, O. Crespo, M. C. Gimeno, A. Laguna, P. G. Jones, B. Ahrens, *Inorg. Chem.* **2000**, *39*, 680 – 687.

[31] With another series of experiments, we attempted to perform a gold-catalysed addition of diphenylmethanol across acetonitrile with the Au-**1** complexes. However, under the conditions described in the literature (5 mol% of **3c**, reaction in MeCN at 75 °C for 22 h), this reaction produced none of the desired *N*-(diphenylmethyl)acetamide but only bis-(diphenylmethyl)ether. For a reference, see: N. Ibrahim, A. S. K. Hashmi, F. Rominger, *Adv. Synth. Catal.* **2011**, *353*, 461 – 468.

[32] A. V. Gulevich, A. S. Dudnik, N. Chernyak, V. Gevorgyan, *Chem. Rev.* **2013**, *113*, 3084 – 3213.

[33] Reviews: a) P. Belmont, E. Parker, *Eur. J. Org. Chem.* **2009**, 6075 – 6089; b) M. Hoffmann, S. Miaskiewicz, J.-M. Weibel, P. Pale, A. Blanc, *Beilstein J. Org. Chem.* **2013**, *9*, 1774 – 1780. Relevant examples:c) Y. Liu, F. Song, Z. Song, M. Liu, B. Yan, *Org. Lett.* **2005**, *7*, 5409 – 5412; d) X. Du, F. Song, Y. Lu, H. Chen, Y. Liu, *Tetrahedron* **2009**, *65*, 1839 – 1845; e) X. Zhang, Z. Lu, C. Fu, S. Ma, *J. Org. Chem.* **2010**, *75*, 2589 – 2598.

[34] To the best of our knowledge, no Au-catalysed route to **7** has been reported in the literature. For the first report, dealing with the use of Au catalyst in this type of cyclization, see: A. S. K. Hashmi, L. Schwarz, J.-H. Choi, T. M. Frost, *Angew. Chem. Int. Ed.* **2000**, *39*, 2285 – 2288; *Angew. Chem.* **2000**, *112*, 2382 – 2385.

[35] It should be noted that our catalysts proved to be inactive in the hydrative cyclisation of 1,3-diphenylbutadiyne to 2,5-diphenylfurane: S. Kramer, J. L. H. Madsen, M. Rottländer, T. Skrydstrup, *Org. Lett.* **2010**, *12*, 2758 – 2761.

[36] The reaction flask was cooled in a water bath to avoid overheating.
[37] The distillation removes unreacted (*E*)-**6** that was present as a minor isomer in the starting alcohol, as well as the catalyst.
[38] For examples of reactions with TOFs in the range of $10^6\,h^{-1}$, see: a) M. C. Blanco Jaimes, C. R. N. Böhling, J. M. Serrano-Becerra, A. S. K. Hashmi, *Angew. Chem. Int. Ed.* **2013**, *52*, 7963 – 7966; *Angew. Chem.* **2013**, *125*, 8121 – 8124; b) M. C. Blanco Jaimes, F. Rominger, M. M. Pereira, R. M. B. Carrilho, S. A. C. Carabineiro, A. S. K. Hashmi, *Chem. Commun.* **2014**, *50*, 4937 – 4940.
[39] For an analogous, Pd-mediated preparation of **9**, see: a) B. Gabriele, G. Salerno, *Chem. Commun.* **1997**, 1083 – 1084; b) B. Gabriele, G. Salerno, E. Lauria, *J. Org. Chem.* **1999**, *64*, 7687 – 7692. This method required 1 mol% of a $PdI_2$/KI catalyst and heating to 100 °C for 24 h (GC yield: 85%).
[40] a) B. S. Rao, K. S. Subramaniam, *Proc. Indian Acad. Sci.* **1936**, *3*, 31 – 37; b) G. S. R. S. Rao, B. Ravindranath, V. P. S. Kumar, *Phytochemistry* **1984**, *23*, 399 – 401; c) G. Ohloff, E. Demole, *J. Chromatogr.* **1987**, *406*, 181 – 183; d) E. Kováts, *J. Chromatogr.* **1987**, *406*, 185 – 222; e) L. N. Misra, A. Husain, *Planta Med.* **1987**, *53*, 379 – 380; f) A. O. Tucker, M. J. Maciarello, *J. Essent. Oil Res.* **1995**, *7*, 653 – 655.
[41] The 1,3-oxazole motif represents an essential component of various natural and biologically active compounds. For selected reviews, see: a) X.-M. Peng, G.-X. Cai, C.-H. Zhou, *Curr. Top. Med. Chem.* **2013**, *13*, 1963 – 2010; b) V. S. C. Yeh, *Tetrahedron* **2004**, *60*, 11995 – 12042; c) D. Davyt, G. Serra, *Mar. Drugs* **2010**, *8*, 2755 – 2780; d) Z. Jin, *Nat. Prod. Rep.* **2013**, *30*, 869 – 915.
[42] W. He, C. Li, L. Zhang, *J. Am. Chem. Soc.* **2011**, *133*, 8482 – 8485.
[43] a) D. C. Palmer, S. Venkatraman, in *Chemistry of Hererocyclic Compounds Vol. 60* (Ed.: D. C. Palmer), Wiley, Hoboken, **2004**, Part A, Chapter 1, p. 1; b) G. V. Boyd, in *Science of Synthesis (Houben-Weyl), Vol. 11* (Ed.: E. Schaumann), Thieme, Stuttgart, **2002**, Chapter 11.12, p. 383; c) I. J. Turchi, M. J. S. Dewar, *Chem. Rev.* **1975**, *75*, 389 – 437.
[44] Annuloline was the first isolated and characterised natural compound that contained an oxazole motif in its structure.
[45] a) B. Axelrod, J. Belzile, *J. Org. Chem.* **1958**, *23*, 919 – 920; b) R. S. Karimoto, B. Axelrod, J. Wolinsky, E. D. Schall, *Tetrahedron Lett.* **1962**, *3*, 83 – 85; c) R. S. Karimoto, B. Axelrod, J. Wolinsky, E. D. Schall, *Phytochemistry* **1964**, *3*, 349 – 355.
[46] a) A. Brossi, E. Wenis, *J. Heterocycl. Chem.* **1965**, *2*, 310 – 312; b) M. P. Doyle, W. E. Buhro, J. G. Davidson, R. C. Elliott, J. W. Hoekstra, M. Oppenhuizen, *J. Org. Chem.* **1980**, *45*, 3657 – 3664; c) P. Molina, P. M. Fresneda, P. Almendros, *Heterocycles* **1993**, *36*, 2255 – 2258; d) F. Besselièvre, S. Piguel, F. Mahuteau-Betzer, D. S. Grierson, *Org. Lett.* **2008**, *10*, 4029 – 4032; e) C. Wan, L. Gao, Q. Wang, J. Zhang, Z. Wang, *Org. Lett.* **2010**, *12*, 3902 – 3905; f) C. W. Cheung, S. L. Buchwald, *J. Org. Chem.* **2012**, *77*, 7526 – 7537; g) D. Kumar, N. M. Kumar, M. P. Tantak, *Chem. Biol. Interface* **2012**, *2*, 331 – 338; h) W.-C. Lee, T.-H. Wang, T.-G. Ong, *Chem. Commun.* **2014**, *50*, 3671 – 3673.
[47] Bromoveratrole **16** (1.05 equiv) and **12 f** were reacted in the presence of as much as 5 mol% $Pd(OAc)_2$ and 20 mol% $P(C_6H_4Me\text{-}2)_3$ in *N*,*N*-dimethylformamide at 120 °C for 24 h. An analysis of the crude reaction mixture by using NMR spectroscopy revealed only the presence of unreacted **16** and no signals due to protons at the C=C double bond of either **12 f** or any other 1,2-disubstituted alkene.
[48] For examples of $Au^I$ complexes with P,N-donors and their catalytic use, see: C. Khin, A. S. K. Hashmi, F. Rominger, *Eur. J. Inorg. Chem.* **2010**, 1063 – 1069.
[49] CCDC 1412074 (2), 1412075 (**3 a**), 1412076 (**3 a**′·$Me_2CO$), 1412077 (**3 c**), 1412078 (**4 a**), 1412079 (**12 a**), 1412080 (**17**), 1412081 (**18**), contain the supplementary crystallographic data. These data can be obtained free of charge by The Cambridge Crystallographic Data Centre.

Received: July 29, 2015
Published online on September 23, 2015

 